Università degli Studi di Padova

Dipartimento Territorio e Sistemi Agro-Forestali (TeSAF)

Scuola di dottorato di ricerca in Territorio, Ambiente, Risorse e Salute

Indirizzo in Medicina Ambientale: Nutrizione e Inquinamento

XXIII CICLO

HUMAN CELL RESPONSE TO IONIZING RADIATION IN GROUND GRAVITY AND MICROGRAVITY CONDITION

Direttore della Scuola: Ch.mo Prof. Mario Aristide Lenzi

Coordinatore d'indirizzo: Ch.mo Prof. Bruno Saia

Supervisore: Ch.ma Prof.ssa Lucia Celotti

Dottorando: Cristina Girardi

DECLARATION OF AUTHENTICITY

I hereby declare that I have authored this thesis independently and that it contains no material which has been accepted for the award of any other degree or diploma in any University. To the best of my knowledge and belief, this thesis contains no material previously published or written by another person, except where due references or acknowledgements have been made.

Padua, 31st January, 2010 Cristina Girardi

Acknowledgements

I gratefully acknowledge Prof. Lucia Celotti (Dep. of Biology), which has been the main supervisor and tutor during my PhD training, Maddalena Mognato that supervised the IR-cell response study, and all members of Prof. Lanfranchi's laboratory (C.R.I.B.I), in particular: Cristiano De Pittà, for his important support in the Microarray data analysis and Silvia Casara, for her RT-qPCR technical assistance. The computational approach in the study of miRNAs has been possible thanks to the laboratory of Chiara Romualdi where Gabriele Sales performed the integrating-predictive data analysis and Paolo Martini dealt with data normalization and statistical assistance.

From the "*Institute for Cancer Genetics*" (Columbia University, New York), Prof. Riccardo Dalla-Favera and Katia Basso for the opportunity and the important knowledge they gave me, Christof Schneider who followed me during all my training period and all members of Prof. Dalla-Favera's laboratory. Finally, thanks to Vito Barbieri (Dep. of Oncological and Surgical Sciences) for cell irradiation.

This research work has been supported by grants from University of Padua and Italian Space Agency (ASI, XMAB-from Molecules to Man 2006–2009), my PhD was supported by a fellowship of the University of Padua.

CONTENTS

LIST OF FIGURES

ABBREVIATIONS

1g = ground gravity

3'UTR = 3'-Untraslated Region

γ-H2AX = phosphorylated histone H2AX

A.I = Apoptotic Index

DAVID = Database for Annotation, Visualization and Integrated Discovery

DDR = DNA Damage Response

DSB = Double Strand Breaks

FDR = False Discovery Rate

FR = Fraction of DNA Released

GO = Gene Ontology

HR = Homologous Recombination

IR = Ionizing Radiation

IRIF = Ionizing Radiation-Induced Foci

MAGIA = MiRNA And Genes Integrated Analysis

miRNA = microRNA

MMG = Modeled Microgravity

NHEJ = NonHomologous End-Joining

OD = Optical Density

PBL = Peripheral Blood Lymphocytes

PFGE = Pulsed-Field Gel Electrophoresis

RISC = RNA-Induced Silencing Complex

RT-qPCR = Reverse Transcription-quantitative Polymerase Chain Reaction

RWV = Rotating Wall Vessel bioreactor

SAM = Significance Analysis of Microarrays

ABSTRACT

In eukaryotic cells, ionizing radiation (IR) induces damages to proteins, lipids and DNA, directly or indirectly, as a result of free radical formation. Among the numerous types of DNA lesions, the double-strand breaks (DSBs) are particularly important, since an inefficient or inaccurate repair may lead to cell death or genomic instability. The presence of DSBs leads to a complex DNA damage response, consisting in a cascade of cellular events, which involve sensing the damage, signal transduction to the effectors of DNA repair, cell cycle arrest and apoptosis induction. In mammals, a very early step in the cellular response to DSBs is the phosphorylation of the histone H2AX (γ-H2AX) at the sites of DNA damage by members of the phosphatidylinositol-3-OH kinase (ATM, DNA-PK and ATR). This event plays a critical role in the recruitment of signaling–repair proteins (i.e 53BP1, Mre11, Rad50, Nbs1) to the sites of damage to form the ionizing radiation-induced foci (IRIF), which contain hundreds to thousands of proteins. DNA damage and repair can be quantified in individual cells by monitoring the kinetics of formation and disappearance of IRIF that accumulate at sites of DSBs; in particular, the rate of loss of γ-H2AX foci correlates with the progression of DSB repair.

Cell signaling events in response to ionising radiation depend on environmental conditions occurring during DNA repair, besides genetic and physiological features of the biological systems. For this reason we have studied and compared the human cell response to IR in different gravity conditions, normal gravity as on Earth and reduced gravity as in space environment where exposure to cosmic radiation during space missions is associated to the reduction of gravitational force, which is approximately 10^{-4}-10^{-6}g. Indeed, space environment is characterized by the presence of ionizing radiation in the form of charged atomic particles travelling at close to the speed of light, which represents the most significant factor limiting humans' ability to participate in long-duration space missions, and also by a condition of weightlessness called microgravity. As reported in literature, microgravity effects on astronauts include: immune cell function suppression, skeletal muscle atrophy, cardiovascular problems and loss of calcium and minerals from bone. In-flight cell cultures and ground models of microgravity showed inhibition of lymphocyte proliferation, suppression or alteration in cytokine secretion, modifications of cytoskeleton, and also increase of chromosome aberrations and apoptosis. The question whether radiation effects are influenced by microgravity is still open and it is an important point in the risk estimation of space missions.

In our experiments, microgravity condition was obtained in laboratory using of the bioreactor "*Rotating Wall Vessel*" (Synthecon, Inc., Houston, Texas), which simulates the weightlessness, an aspect of spaceflights. This condition is called "modeled microgravity" (MMG).

In the first part of this project, DSB rejoining was investigated in human PBL irradiated with γ-rays and incubated in 1g or MMG during repair time. Formation and disappearance of γ-H2AX foci were monitored at various times after irradiation by *in situ* immunofluorescence; in the same samples the apoptotic index and the DNA fragmentation were determined, the last one was measured by pulsed-field gel electrophoresis (PFGE) and the fraction of DNA released in the gel (FR) was considered as a measure of DSBs. Results obtained provided evidences that MMG incubation during repair time affected cell survival, apoptosis and delayed DSB rejoining, increasing the genotoxic effects of ionising radiation. On the base of these evidences, we investigated if ionizing radiation and modeled microgravity could have an effect on cells focusing on the expression profile of microRNAs: negative regulators of gene expression.

MicroRNAs (miRNAs) are a recently discovered class of small (~22nt) endogenously expressed translational-repressor RNAs that play a key role in many cellular pathways. In animal cells, these molecules bind to complementary sequences in the 3'-untraslated region (3'UTR) of the target messenger RNAs (mRNAs) of protein-coding genes, to direct their translational repression. For this reason, miRNAs have been implicated in numerous biological processes including developmental timing, cell fate decisions, cell death and proliferation, stem cell function, tumorigenesis and disease.

Aim:

The aims of this project were: *i)* to analyze the efficiency of DNA repair occurring in modeled microgravity culture conditions focusing on DSBs repair kinetics; *ii)* to investigate if ionizing radiation and modeled microgravity could have a synergistic action on human cells by comparing radio-responsive miRNA in ground gravity and MMG.

Activity carried out:

The presence of nuclear γ-H2AX foci and the apoptotic index were monitored by *in situ* immunofluorescence and western blot in not- and γ-irradiated Peripheral Blood Lymphocytes (PBL), at 0.5, 2, 6 and 24h from irradiation, in 1g and MMG. In the same samples was studied the DSBs repair analyzing the fraction of DNA released (FR) after Pulsed-field gel electrophoresis (PFGE), this value was calculated either by measuring

optical density of DNA migrating in the gel and by quantity of DNA (ng) retained in the plug/wells.

MiRNA expression profile of human PBL, irradiated with γ-rays (0.2-2Gy) and incubated in MMG and in parallel 1g condition, was examined through "*Human miRNA microarray Kit V2*" (Agilent) and quantitative real-time PCR (RT-qPCR). In addition, we used "*Whole Human Genome Oligo Microarray*" (Agilent) to determine the gene expression profile, in the same PBL analysed for miRNA profiling, with the aim to identify the most likely miRNA targets by integration of miRNA and mRNA expression data in an anti-correlation analysis. Finally, to identify biological pathways most involved in radiation cell response we performed a Gene Ontology (GO) analysis, on significant anti-correlated target genes identifying biological pathways significantly enriched ($P<0.05$).

Results and conclusions:

Results obtained in the study of nuclear γ-H2AX foci in irradiated PBL showed that the mean number of foci/nucleus during a short-repair time was comparable in 1g and MMG. At later times the decrease of foci number was significantly different; indeed, PBL incubated in 1g at 24h after irradiation showed 2 foci/nucleus, instead those incubated in MMG showed a mean of 6.4 foci/nucleus at the same time-points. To verify whether the disappearance of γ-H2AX foci correlated with the rejoining of double strand breaks, we subjected irradiated PBL, incubated in 1g or MMG, to PFGE assay. We found that in cells incubated in MMG, FR was higher than in 1g (77% vs. 33% at 2 h and 50% vs. 17% at 6 h, respectively). Summarizing, MMG probably affects the chromatin structure modulation that occurs after DSB formation, decreasing the efficiency of DNA repair. Thus, DSB rejoining that is almost completed in few hours in normal culture conditions, could take more time in MMG. In second part of the project we focused on miRNA expression profile analysis of γ- irradiated PBL incubated in 1g and MMG. Our results showed that radiation affected miRNA expression profile according to the dose and the time after irradiation, in both gravity conditions. Exposure to γ-rays in 1g altered miRNA expression profile at early and late time points (4h and 24h), with more responsive miRNAs at 24h after high irradiation dose (2Gy). In particular, the 20 radio-responsive miRNAs common to 0.2Gy and 2Gy of treatment showed a time dependent expression pattern, with a general down-regulation at 4h and up-regulation at 24h after irradiation. Human PBL incubated in MMG after γ-irradiation showed miRNA expression profile alteration higher at 24h than at 4h, in both irradiation doses. Interestingly, in non-irradiated PBL, 24h of MMG incubation altered the expression profile of 42 miRNA species respect to 1g. At the end, comparing the miRNA

expression profiles of γ-irradiated PBL incubated 24h in the two different gravity conditions, we individuated miRNAs specifically expressed during repair time in MMG; these miRNA species were probably altered by the combined action of IR and MMG in a way that is dose dependent. In order to figure out the mechanism by which miRNAs can modulate a certain biological function in response to IR, gene expression profiles were analysed on the same PBL samples used to assess miRNA expression levels, in 1g and MMG. The anti-correlation analysis was performed between differentially expressed mRNAs and deregulated miRNAs to investigate the putative miRNA target genes. Finally, Gene Ontology analysis was conducted on significant anti-correlated target genes with the aim of identifying the biological categories which they belong to. From our results it arose that few genes were activated in irradiated PBL incubated 24h either in 1g or MMG and most of them were gravity-specific. In 2Gy PBL incubated in 1g a great number of deregulated genes belonged to the DNA Damage Response (DDR) categories: apoptosis, response to wounding and response to DNA damage. These categories were not found in 2Gy PBL incubated in MMG, where instead were altered biological processes involved in regulation of development, cell differentiation/activation, immune system, cytokine production and hemopoiesis; they were all characterized by a general gene down-regulation. In addition, we focused on significantly anti-correlated genes of DDR pathway, activated in the two gravity conditions, to highlight the differences between 1g and MMG. We hypothesize that the smaller number of radio-responsive miRNAs in MMG can operate an unscheduled regulation of the expression level of transcripts usually not targeted. The scenario proposed in this work is that modeled microgravity incubation, following ionizing radiation exposure (simulated space environment), could affect the appropriate radiation cell response of human lymphocytes reducing the efficiency of DNA repair.

To better investigate miRNA biological functions in the simulated space environment, it has been necessary to focus our studies on miRNA target validation and functional analysis. For this reason, the PhD program was carried out for seven months in the laboratory of Prof. Riccardo Dalla-Favera at "*Institute for Cancer Genetics*", Columbia University (New York, USA), to acquire some expertise in molecular biology techniques and their applications to the study of microRNAs.

ABSTRACT (italian version)

Le radiazioni ionizzanti (IR), colpendo le cellule degli organismi eucarioti è in grado di provocare danni a proteine, lipidi e molecole di DNA, in modo diretto o indiretto come risultato della formazione di radicali liberi. Tra i numerosi tipi di danno al DNA, le rotture a doppio filamento o double-strand breaks (DSBs) rappresentano il tipo di lesione più grave, dal momento che una riparazione inefficiente o non accurata può portare a morte cellulare o instabilità genomica. La presenza di DSBs induce una complessa risposta al danno al DNA che vede coinvolti una serie di eventi cellulari quali: la rilevazione del danno, la trasduzione del segnale agli effettori della riparazione, l'arresto del ciclo cellulare e l'induzione di apoptosi. Nei mammiferi, una delle risposte cellulari più precoci dopo l'induzione di una doppia rottura è la fosforilazione dell'istone H2AX (γ-H2AX) in corrispondenza del sito di danno, che avviene per opera delle fosfatidilinositolol-3-OH-chinasi (ATM, DNA-PK and ATR). Questo evento sembra essere importante nel reclutamento di fattori di segnalazione del danno e di proteine coinvolte nella riparazione delle DSBs nei siti danneggiati (i.e 53BP1, Mre11, Rad50, Nbs1), dando origine a ionizing radiation-induced foci (IRIF), che possono essere costituiti da migliaia di queste molecole proteiche. Monitorando la cinetica di formazione e scomparsa degli IRIF, che si accumulano nei siti danneggiati, è possibile analizzare il danno al DNA e la sua riparazione; in particolare, è stato osservato che la diminuzione dei foci di γ-H2AX correla con la progressione della riparazione delle DSBs. Gli eventi di segnalazione attivati in risposta alle radiazioni ionizzanti dipendono, oltre che dalle caratteristiche genetiche e fisiologiche del sistema biologico osservato, anche dalle condizioni ambientali presenti durante la riparazione del DNA. Per questa ragione abbiamo analizzato e confrontato la risposta cellulare umana alle IR in condizioni diverse di gravità, normale come sulla Terra (1g) e ridotta come nell'ambiente spaziale; in quest'ultimo l'esposizione ai raggi cosmici a cui l'uomo è soggetto durante le missioni spaziali e associata alla riduzione della forza di gravità. L'ambiente spaziale è caratterizzato dalla presenza di radiazioni ionizzanti, nella forma di particelle atomiche cariche che rappresentano il più importante fattore limitante la lunga permanenza dell'uomo nello spazio, ma anche dalla condizione di assenza di peso, che prende il nome di microgravità (10^{-4}–10^{-6}g). In letteratura sono stati riportati alcuni effetti della microgravità osservati in astronauti di ritorno dai voli spaziali, questi riguardano: la soppressione del sistema immunitario, l'atrofia muscolare, problemi cardiovascolari e la demineralizzazione e decalcificazione ossea. Cellule mantenute in coltura durante le missione spaziali e modelli a

terra della microgravità mostrano inibizione della proliferazione dei linfociti, soppressione o alterazione della secrezione di citochine, modificazioni del citoscheletro e anche incremento delle aberrazioni cromosomiche e apoptosi. Pertanto, capire se gli effetti della radiazione ionizzante possano essere influenzati dalla microgravità rimane un punto di rilevante importanza nella valutazione dei rischi durante le missioni spaziali.

In questo lavoro, la microgravità è stata simulata in laboratorio usando il bioreattore *"Rotating Wall Vessel"* (Synthecon) messo a punto nei laboratori della NASA a Houston; questo strumento permette di riprodurre un aspetto dei voli spaziali che è l'assenza di peso, condizione che prende il nome di "modeled microgravity" (MMG). Nella prima parte di questo progetto è stata studiata la riparazione delle DSBs in linfociti umani irradiati con raggi gamma e mantenuti durante il tempo di riparazione in 1g o MMG. La formazione e la scomparsa dei foci dell'istone γ-H2AX è stata monitorata a diversi tempi dall'irradiazione mediante immunofluorescenza; nei medesimi campioni è stato anche analizzato l'indice apoptotico e la frammentazione del DNA, quest'ultimo con la tecnica della pulsed-field gel electrophoresis (PFGE) in cui la frazione di DNA rilasciata nel gel (FR) è considerata una misura delle DSBs. I risultati ottenuti confermano che l'incubazione in MMG durante il tempo di riparazione influenza la sopravvivenza cellulare, l'apoptosi e ritarda la riparazione delle DSBs, incrementando l'effetto genotossico delle radiazioni ionizzanti. Sulla base delle osservazioni fatte, si è passati a studiare se la IR e la MMG possono avere un'azione sinergica sulle cellule analizzando i profili di espressione dei microRNAs: regolatori negativi dell'espressione genica. I microRNAs (miRNAs) sono una classe di corti RNA (~22nt) endogeni, che svolgono un ruolo chiave in molti processi cellulari poiché reprimono l'espressione dei mRNA target. Nelle cellule animali, queste molecole vanno a reprimere la traduzione dei geni codificanti proteine legandosi a sequenze complementari nelle regioni non tradotte al 3' terminale (3'UTR) dei mRNA. Per questo motivo i miRNAs sono coinvolti in numerosi processi biologici come: lo sviluppo, la proliferazione cellulare, l'apoptosi, la funzionalità delle cellule staminali e la tumorigenesi.

Scopo:

Questo progetto si proponeva di: *i)* analizzare l'efficienza di riparazione del DNA in condizione di microgravità simulata (MMG), puntando l'attenzione alla cinetica di riparazione delle DSBs; *ii)* capire se la radiazione ionizzante e la microgravità simulata possono avere un'azione sinergica in cellule umane, confrontando i miRNA radio-responsivi nelle due condizioni di gravità (1g e MMG)

Attività svolta:

La presenza di foci nucleari dell'istone γ-H2AX e l'indice apoptotico sono stati monitorati in linfociti umani irradiati con raggi γ e non, incubati in 1g e MMG. Negli stessi campioni è stata studiata la riparazione delle DSBs analizzando la frazione di DNA rilasciata (FR) dopo Pulsed-field gel electrophoresis (PFGE). In seguito, usando l'approccio dei microarray con "*Human miRNA microarray Kit V2*" (Agilent) e della real-time qPCR, sono stati analizzati i profili di espressione dei miRNAs in linfociti umani irradiati con raggi γ e incubati in 1g e MMG. Impiegando poi i microarrays "*Whole Human Genome Oligo Microarray*" (Agilent) per gli stessi campioni di cellule, è stato possibile determinare i profili di espressione genica; allo scopo di identificare i probabili mRNA target dei miRNA radio-responsivi i dati di espressione dei miRNA e dei mRNA sono stati integrati in un'analisi di anticorrelazione. Infine, per studiare i processi biologici maggiormente coinvolti nella risposta cellulare alle radiazioni ionizzanti è stata eseguita una Gene Ontology analysis (GO) applicata ai miRNA-mRNA target significativamente anti-correlati.

Risultati e conclusioni:

I risultati ottenuti dallo studio dei foci dell'istone γ-H2AX in PBL irradiati mostrano che il numero medio di foci/nucleo a tempi brevi di riparazione nelle due condizioni di gravità è comparabile. Al contrario, per tempi lunghi, la diminuzione del numero di foci è significativamente differente; infatti, a 24h dall'irradiazione i PBL incubati in 1g presentano 2 foci/nucleo, mentre quelli in MMG 6.4 foci/nucleo. Per verificare che la scomparsa dei foci di γ-H2AX fosse correlata con la riparazione delle DSBs è stata utilizzata la tecnica della PFGE. La cinetica di riparazione delle DSBs è stata analizzata in PBL irradiati e incubati in 1g e MMG; nelle cellule incubate in MMG il contenuto di DNA frammentato era maggiore rispetto alla 1g (FR 77% vs. 33% a 2 h e FR 50% vs. 17% a 6 h, rispettivamente). Probabilmente la MMG influisce sulle modificazioni strutturali della cromatina che avvengono in risposta alla DSBs, diminuendo l'efficienza di riparazione; pertanto, la riparazione delle DSBs che in 1g avviene in poche ore, richiede più tempo in MMG.

Nella seconda parte del progetto sono stati analizzati i profili di espressione di miRNA in PBL irradiati con raggi γ e incubati in 1g e MMG. Dai risultati ottenuti è emerso che la radiazione altera i profili di espressione dei miRNA in modo dose e tempo dipendente, in entrambe le condizioni di gravità. L'esposizione ai raggi gamma in 1g altera i profili di espressione dei miRNA, sia a tempi brevi che lunghi, con maggior numero di miRNA radio-responsivi a 24h dopo esposizione alla dose maggiore (2Gy). Dal confronto dei profili di espressione di miRNA in PBL irradiati e mantenuti 24h nelle due condizioni di gravità

vengono individuati miRNAs espressi in modo specifico durante l'incubazione in MMG; questi miRNAs vengono probabilmente alterati dall'azione combinata della IR con la MMG con effetto dose-dipendente. Anche le cellule non irradiate ma mantenute 24h in MMG presentano 42 miRNA deregolati rispetto alla 1g. Per far luce sul meccanismo col quale i miRNAs possono modulare alcuni processi biologici in risposta alle radiazioni ionizzanti, sono stati analizzati i profili di espressione di mRNAs negli stessi campioni per i quali sono stati ricavati i profili dei miRNAs. L'analisi di anti-correlazione tra i miRNA e i mRNA differenzialmente espressi e l'analisi computazionale con PITA hanno permesso di predire geni target dei miRNA. Infine, è stata eseguita la Gene Ontology analisi su geni target significativamente anti-correlati, allo scopo di identificare le categorie biologiche di appartenenza. Dai nostri risultati è emerso che alcuni geni sono attivati in PBL irradiati e incubati 24h sia in 1g che MMG, molti di loro sono gravità-specifici. In cellule irradiate con 2Gy e incubate in 1g un grande numero di mRNAs alterati appartiene alle categorie della risposta al danno al DNA (DDR): apoptosi, risposta allo stress, risposta al danno al DNA. Queste categorie non sono risultanti dall'analisi dei PBL irradiati e mantenuti in MMG, dove invece sono alterati processi coinvolti nel differenziamento e attivazione cellulare, sistema immunitario, produzione di citochine ed emopoiesi; tutte caratterizzate da una sostanziale down-regolazione genica. Questo studio fornisce prove che la MMG associata alla radiazione ionizzante porta ad una non appropriata risposta al danno al DNA in linfociti umani, dovuta probabilmente alla perdita di miRNAs radio-responsivi coinvolti nella DDR.

Per meglio studiare le funzioni biologiche dei miRNAs in condizione di microgravità simulata è stato necessario puntare l'attenzione sulla validazione dei messageri target predetti e sull'analisi funzionale. Per questa ragione il programma finale di dottorato è stato svolto presso il laboratorio del Prof. Riccardo Dalla-Favera all'"*Institute for Cancer Genetics*" (Columbia University, New York, USA), per un periodo di sette mesi, allo scopo di acquisire competenze di biologia molecolare che vengono applicate allo studio dei microRNAs.

1. BACKGROUND

1.1 INTRODUCTION

Eukaryotic cells are under continuous assault by environmental agents such as: ultraviolet light, ionizing radiation, chemical compounds and reactive oxygen species exogenously or endogenously produced. It has been already demonstrate that ionizing radiation induces a wide variety of cellular damages, among which the DNA double-strand breaks are the most dangerous ones because an inability to properly repair them may lead to genomic instability and promote carcinogenesis [1,2]. For this reason, mammalian cells have mechanisms for quickly sensing and transmitting the damage signal to the cell cycle arrest machineries, in order to repair the DNA or induce apoptosis when the situation is un-repairable; both of these processes are considered as effective barriers to tumorigenesis. On the base of fact that cell signaling events in response to ionizing radiation depend on environmental conditions occurring during DNA repair, we have studied and compared the human cell response in different gravity conditions: normal gravity as on earth and reduced gravity as in space environment; indeed, space environment is characterized by the presence of cosmic radiation associated to the reduction of gravitational force called microgravity (10^{-4}–10^{-6}g). In the coming International Space Station era the most critical point limiting the ability of astronauts to participate in long-duration space missions is represented not only by radiation exposure, but also by microgravity, which affects human health and may influence radiation response. For these reasons, the investigation on human cell response to IR in microgravity condition could be an important point in risk estimation of space missions.

The work carried on during my PhD training was partially funded by Italian Space Agency (ASI) within the XMAB project, with the aim of investigating human cell response to ionizing radiation (IR) and the role of microgravity in the modulation of this biological process. In this project were compared the efficiency of DNA double-strand breaks repair in normal gravity and in modeled microgravity culture conditions; then, to better understand if ionizing radiation and microgravity could have a synergistic action on human cells, the study was focused on microRNAs: post-transcriptional regulators of gene expression [3].

1.2 IONIZING RADIATION AND BIOLOGICAL EFFECTS

Ionizing radiation (IR) consists of particles or electromagnetic waves with enough energy to interact and remove electrons from atoms or molecules of target substrate, producing ions. Particularly important is the interaction with biological substrates, which could be direct or indirect as a result of intracellular free radicals formation; it induces cellular damages to proteins, lipids, RNA molecules and the most deleterious DNA lesions (base damage, single- and double-strand breaks).

The main types of ionizing radiation are:

- Alpha- and beta-particles: directly ionizing because they carry a charge and are able to interact with atomic electrons through coulomb forces. They can be stopped by a piece of paper or a sheet of aluminium, respectively.
- Neutrons: indirectly ionizing particles because they don't carry an electrical charge, the ionization is caused by charged particles produced during collisions with atomic nuclei.
- Gamma- and X-rays: electromagnetic indirectly ionizing radiation because they are electrically neutral and do not interact with atomic electrons through coulomb forces. A thicker shielding is required for protection.

The amount of damage induced by ionizing radiation on living tissue is more related to the amount of energy deposited rather than the charge; this is called "Absorbed Dose" and is expressed in *Gray* (Gy), which represents the amount of radiation required to deposit 1 joule of energy in 1 kilogram of matter (J/kg). Equal doses of different types of radiation cause different amounts of damage on living tissue; thus, the "Equivalent Dose" was defined to give an approximate measure of the biological effect of radiation. This is the dose of a given type of radiation in Gy that has the same biological effect on a human as 1Gy of X- or γ-rays and it is indicated with the unit *Sievert* (Sv) [4].

On Earth, all living organisms are constantly exposed to a natural ionizing radiation background: terrestrial sources, radon, solar and cosmic radiation, and to human-made sources resulting from radioactive materials in power generation, military and industrial applications, nuclear medicine and particle accelerators. Also during spaceflights humans are exposed to ionizing radiation (galactic cosmic radiation and solar proton events), which might lead to acute radiation poisoning for unprotected astronauts [5]. The most biologically significant genotoxic lesion induced by ionizing radiation is the DNA double-strand break (DSB), which usually leads to a cascade of cellular events: the DNA damage

response; this involves sensing DNA damage and signal transduction to different cellular pathways such as: cell cycle checkpoints, DNA repair, stress response and apoptosis. Failure in the DNA damage response affects the level of cell survival and increases the frequency of gene mutation or chromosomal instability, which are the main mechanisms of carcinogenesis [6].

1.3 DNA DOUBLE-STRAND BREAK SIGNALING AND REPAIR

DNA double-strand break (DSB) is the result of two opposed single strand breaks within 10-20 base pairs on DNA backbone [7] and represents the most severe type of DNA damage that occurs in mammalian cells. DSBs are mainly generated by exogenous agents such as ionizing radiation and radiomimetic drugs used for chemotherapy. Moreover, these breaks may be also induced by endogenous products of cellular metabolism (reactive oxygen species, ROS) and during programmed cellular processes such as V(D)J and meiotic recombination [8]. DSBs are particularly dangerous in proliferating cells, since incorrect DNA repair may lead to genomic instability and increase the frequency of gene mutation; therefore, when a DSB occurs, the cell cycle is arrested at checkpoint level, in order to give the cell enough time to repair the DNA or to undergo apoptosis if the damage is excessive or un-repairable [9]. For this reason all living organisms are able to detect the presence of DSBs and relay this information to the cell cycle.

In eukaryotes, two important protein kinases are involved in sensing and signaling the DNA damage: ataxia telangiectasia mutated (ATM) and ataxia telangiectasia mutated and rad3-related (ATR) [10]. Finally, DSBs may be repaired through two distinct and complementary mechanisms: non homologous end-joining (NHEJ) and homologous recombination (HR).

• Signal transduction of DNA damage

Under genotoxic stress the majority of DSB recruited proteins become activated through phosphorylation catalyzed by phosphoinositide 3-kinase (PI3-K)-like kinase proteins: ATM, ATR and DNA-PKcs, which possess a serine/threonine kinase activity. Although the PI3-K related kinases exhibit broad substrate specificity and mediate phosphate transfer to common residues present on: histone variant H2AX, breast cancer protein 1 (BRCA1), P53-binding protein 1 (53BP1), mediator of damage checkpoint protein 1 (MDC1) and tumor

protein p53, they become activated under specific stimuli [11]. In mammals, ATM responds directly to DSBs by interacting with proteins involved in DNA repair such as the Mre11-Rad50-Nbs1 (MRN) complex and Rad51 [12, 13]; in addition, it is critical for signals downstream cell cycle checkpoint regulators including p53 and Chk2 [14]. In comparison, ATR, in a complex with the ATR interacting protein (ATRIP) responds to replication stress-related DNA damage; it induces cell cycle arrest, replication restart and apoptosis by recognizing stalled replication forks and signaling to Chk1 and p53 [15]. Finally, the DNA-PKcs exhibits functional overlap with both kinases.

Exposure to ionizing radiation or other DSB-inducing agents triggers a fast increase in ATM kinase activity; the key event is the auto-phosphorylation of ATM dormant dimer at the residue Ser^{1981}, which leads to the dissociation in two catalytically active ATM monomers. Although ATM is the central signal transducer of DSB response, the Mre11-Rad50-Nbs1 (MRN) complex is an essential mediator of ATM activation and recruitment to the DSB sites [16]. The MRN complex is implicated in the initial sensing step because it binds DNA ends at sites of DNA damage and recruits ATM, which phosphorylates proximal H2AX (γ-H2AX); then, MDC1 binds to γ-H2AX and recruits more MRN–ATM (Fig. 1). The new pool of ATM phosphorylates more distal H2AX amplifying in few minutes the DSB signal [17]. Many targets of ATM are recruited to ionizing radiation-induced "foci" (IRIF) marking the site of DNA breaks.

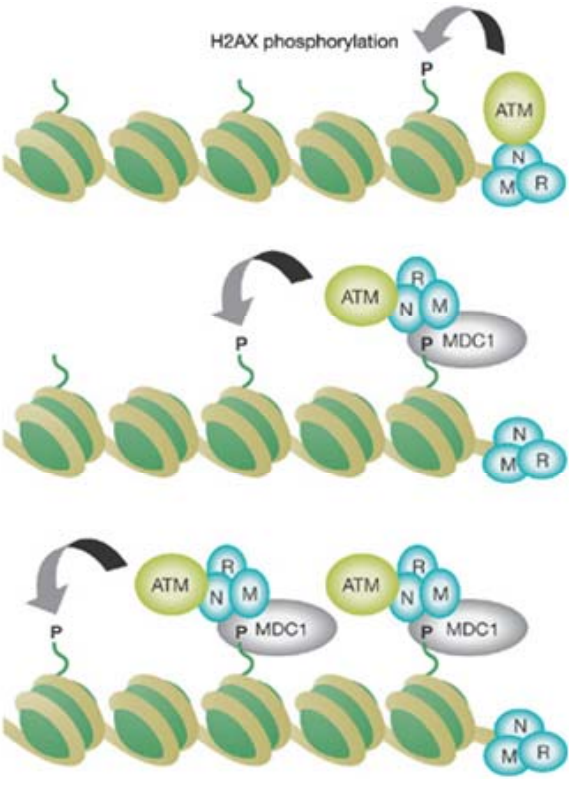

Fig. 1. Amplification of histone H2AX phosphorylation (picture adopted from [18]).

• Role of H2AX in DNA repair

The basic unit of chromatin is the nucleosome, which consists of ~146 base pairs of DNA wrapped around a central core of eight histone proteins consisting of two copies of H2A, H2B, H3 and H4 histones. The organization of DNA into chromatin is not only important for resolving problems of spatial accommodation, but it is also essential for the functional utilization of the DNA, transcriptional regulation of gene expression and in the mechanisms of DNA repair [19]. The histone H2AX is one of the most conserved H2A-variants, which is present in mammalian chromatin between 2 and 25% of the H2A pool and it has a role in DNA damage response [20, 21]. The earliest cellular response to DSBs generation is a rapid kinase-based signaling pathway activated to coordinate DNA repair through the induction of cell cycle checkpoints. The principal mediators in this pathway are the PIKK family members: ATM, ATR and DNA-PKcs, which are responsible for the phosphorylation that occurs on the conserved Ser^{139} residue at the carboxyl terminus of H2AX (termed γ-H2AX). The amount of H2AX surrounding a DSB that is γ-phosphorylated corresponds to ~2 megabases of chromatin or thousands of nucleosomes and it is known as "nuclear focus" [21]. Many factors of DNA repair and activation of cell cycle checkpoints, such as: ATM, 53BP1, Rad51, Mre11/Rad50/Nbs1 complex are recruited on the damaged sites to form IRIF, which co-localize with γ-H2AX foci [22]. These IRIF indicate the site of DNA damage and may be directly visualized through the expression of an IRIF-protein tagged to a fluorescent protein, or indirectly through immune-staining with antibodies against IRIF-proteins.

•DSBs repair pathways

In mammalian cells, DNA double-strand breaks may be repaired through two major pathways: homologous recombination (HR) and non-homologous end-joining (NHEJ). HR uses the sister chromatid as DNA template to perform an accurate or "error-free" repair, which it is more efficient in the S and G2 phases of cell cycle. On the contrary, NHEJ operates in all phases of cell cycle and in G1 phase; the two broken ends of DNA are simply pieced together, resulting in a quick but "error-prone" repair. A large number of proteins are specifically required to repair DSBs in each pathway, although some of these may be involved in both HR and NHEJ. The protein complex MRN has functional importance in telomere maintenance, cell cycle checkpoint activation and during DSBs signaling in both

repair mechanisms [23, 24]; as a matter of fact, following the induction of DSBs by irradiation, cells respond by activating the ATM signal transduction pathway, which is amplified by the MRN complex [25].

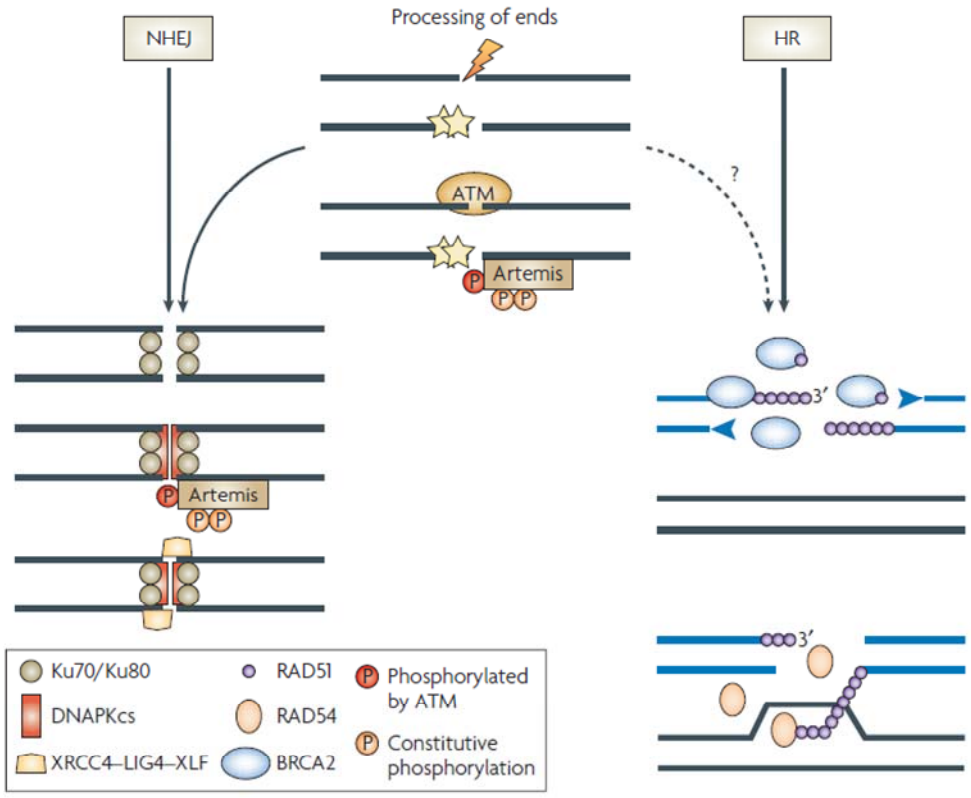

Fig. 2. DNA DSB repair pathways. Non-homologous end-joining (NHEJ) and homologous recombination (HR) (picture adopted from [26])

During NHEJ, Ku70 and Ku80 proteins form a heterodimer which recognizes the DNA breaks and holds the ends together; then, the DNA protein kinase catalytic subunit (DNA-PKcs) is attracted to the termini and stabilized, signaling the presence of the damage and activating repair proteins by phosphorylation. The coordinated assembly of Ku and DNA-PKcs is followed by processing of incompatible DNA ends operated by nuclease Artemis and recruitment of the DNA ligase IV-XRCC4 complex, which is responsible for the rejoining step [27]. Although NHEJ may disrupt coding sequences or generate errors, it contributes to the immune diversity in B and T cells. In HR, DNA ends are processed to produce 3'-single strand tails, which invade the intact homologous chromosome forming the Holliday structure; after DNA synthesis on this DNA template the structure is resolved and DNA repair is completed. Rad51 protein plays a key role in this mechanism, because it promotes the DNA strand exchange through its assembly in a nucleoprotein filament on the

processed single-strands termini, generating a joint molecule between the broken DNA and the undamaged homologous position [28] (Fig. 2).

1.4 TRANSCRIPTIONAL RESPONSE TO IONIZING RADIATION

Mammalian cells respond to genotoxic stress induced by IR and try to repair DNA damages through the activation of immediate stress response pathways. These complex molecular processes result in the modulation of numerous target genes, whose products play a role in: DNA repair, cell cycle control, signal transduction, apoptosis and oncogenesis. Since the increasing interest to develop biological markers for identifying exposed individuals in human populations, changes in the expression of IR-responsive genes have been studied extensively. Currently, in literature there are a large number of reports focused on the transcriptional alterations induced by high (>2Gy) and low (<2Gy) doses of IR. Several studies have used microarray approach to investigate the immediate transcriptional response to IR in human peripheral blood lymphocytes irradiated in vitro or in-vivo [29-33], in human lymphoblastoid cell lines [34, 35], in human fibroblasts [36], in neonatal rat cardiac fibroblasts [37], as well as in mouse spleen and thymus [38]. To mimic the conditions of peripheral blood cells irradiated during an in vivo exposure, some experiments were carried out using un-stimulated quiescent PBL obtained from human healthy donors; in some cases the IR dose used was 2Gy of γ-ray, because this corresponds to a standard radiotherapy dose used in cancer treatment [29]. On the whole, these data have led to the identification of γ-rays responsive genes modulated at different post-irradiation time points and radiation doses (Fig. 3); most of them belong to cell cycle regulation, DNA repair pathways and apoptosis.

CDKN1A is a member of the cyclin-dependent kinase family, which plays an important role in cell cycle arrest, by inhibiting cyclin-dependent kinases. MDM2 is a p53-inhibitor which controls both its transcription and degradation; it is likely that up-regulation of CDKN1A keeps the cell cycle in G0/G1-phase whereas up-regulation of MDM2 decreases p53 activity suppressing the IR induced apoptosis [33]. TNFSF9 is one of the TNF-receptor superfamily genes, which codes for a cytokine that belongs to the TNF-ligand-family; it is mainly involved in antigen presentation, co-stimulation of T-lymphocytes and induction of p53-mediated apoptosis. As reported in Turtoi et al. (2008), TNFSF9 is up-regulated

following γ-irradiation with a significant dose-response trend. Also the IFN-γ appeared to be up-regulated in response to γ-ray with a dose-dependent trend. Of the p53-pathway genes affected by IR, Barenco et al. (2006) identified the ISG20L1 gene in T-cell acute lymphoblastic leukaemia; this gene is activated through interferons and appears to be involved in apoptosis. The expression of CD69 gene was found to be up-regulated after γ-irradiation; it encodes a cell surface glycoprotein with function of signal-transmitting receptor in lymphocytes and natural killer cells. PLK2 is a serine/threonine protein kinase which has an important role in normal cell division and has been found to be up-regulated in PBL and fibroblast after irradiation with different doses of γ-rays [29, 33, 36, 39, 40]. Experiments carried out in PBL with low γ-irradiations doses showed induction of DNA ligase IV gene (LIG4), which is essential for the DSB/SSB repair, and DNAJA1 gene co-chaperone of hsc70 [36]. In fibroblast cell lines, the ATM/p53-induced response to IR involved the up-regulation of PLK3, CDKN1A and TP53INP1 leading to a massive transcriptional response of cell cycle genes. PLK3 is a member of the polo-like kinase family which appears to have key role in the cellular response to DNA damage; it is immediately phosphorylated after IR in an ATM-dependent manner and regulates cell cycle checkpoints by phosphorylating Chk2 and p53[41, 42]. TP53INP1 has been found to increase p53 transcriptional activity on p53-responsive promoters, including CDKN1A, MDM2 and BAX [42, 43]. In agreement with several studies carried out by Amudson's group and Rieger, Kies (2006) confirmed the modulation of: CDKN1A, PPM1D, TP53INP1, BBC3, IER5, PCNA and GADD45A genes in several primary fibroblast cell lines exposed to γ-irradiation. Since GADD45A and CDKN1A are targets of p53 and TP53INP1 increase its transcriptional activity, induction of CDKN1A leads to cell cycle arrest, while up-regulation of GADD45A may activate the MAPK signaling pathway resulting in apoptosis [36].

Fig. 3 (next page)**.** List of genes modulated in response to ionizing radiation. Experiments were carried out using microarray and RT-qPCR approach in peripheral blood lymphocytes (PBL), in human lymphoblastoid cells (AHH-1), in human normal primary fibroblast (VH-16) and in several primary fibroblast cell lines (termed here HPF). These data were adopted from [29, 31-33, 35, 36]

Gene symbol	Gene name	IR dose	modulation	Cell line	Reference
TP53	tumor protein p53 (Li-Fraumeni syndrome)	< 0.4Gy	↑	PBL	Sakamoto-Hojo et al. [31]
LIG4	Ligase IV, DNA, ATP-dependent		↑		
GPR30	G protein-coupled receptor 30		↓		
DNAJA1	Dna J(Hsp40) homolog, subfamily A, member 1		↑		
MAPK10	mitogen-activated protein kinase 10		↑		
MAPK8IP1	mitogen-activated protein kinase 8 interacting protein 1		↑		
KIF13A	kinesin family member 13A	0.25-0.5Gy	↑	PBL	Fachin et al. [32]
BAG4	BCL2-associated athanogene 4		↓		
MAP4K2	mitogen-activated protein kinase kinase kinase kinase 2		↑		
DDX49	DEAD (Asp-Glu-Ala-Asp) box polypeptide 58		↓		
SERPINB2	serpin peptidase inhibitor, clade B (ovalbumin), member 2		↑		
REV3L	REV3-like, catalytic subunit of DNA polymerase zeta (yeast)		↓		
CDH6	human chromodomain helicase DNA binding protein 6	0.5Gy	↑	AHH-1	Wang et al. [35]
STAT3	signal transducerand activator of trascription 3 gene		↑		
CAMKK2	calcium/calmodulin-dependent protein kinase kinase 2β		↑		
SIRT1	silent mating type information regulation 2 homolog		↑		
CREM	cAMP esponsive element modulator gene		↑		
MAPK3-K7IP2	mitogen-activated protein kinase kinase kinase 7 interacting protein 2		↑		
PHIP	pleckstrin homology-like domain interacting protein		↑		
GPR56	G protein-coupled receptor 56		↑		
MCM2	minichromosome maintenance deficient 2 (S. cerevisiae)		↓		
XRCC4	X-ray repair complementing defective repair in Chinese hamster cells 4		↓		
WASF2	WAS protein family member 2		↓		
KIF2C	kinesin family member 2C		↓		
IL1A	interleukin 1A	2 Gy	↑	PBL	Amudson et al. [29]
IL1B	interleukin 1B		↑		
IL6	interleukin 6		↑		
SCYA4	Small induced cytokine A4		↑		
XPC	xeroderma pigmentosum, complementation group C		↑		
DDB2	damage-specific DNA binding protein 2		↑		
CCNG1	cyclin G1, transcript variant 1		↑		
PCNA	proliferating cell nuclear antigen	2Gy	↑	PBL/HPF	Amudson; Kis [29,36]
TP53INP1	tumor protein p53 inducible nuclear protein 1	2Gy	↑	HPF	Kis et al. [36]
GADD45A	growth arrest and DNA-damage-inducible, alpha		↑		
IER5	immediate early response 5		↑		
PPM1D	protein phosphatase 1D magnesium-dependent, delta isoform		↑		
PRKDC	Protein kinase, DNA-activated, catalytic polypeptide (DNA-PK)	2Gy	↑	VH-16	Sakamoto-Hojo et al. [31]
TNFRSF6	Tumor necrosis factor receptor superfamily, member 6		↑		
CRADD	CASP2 and RIPK1 domain containing adaptor with death domain		↑		
CASP10	Caspase 10, apoptosis-related cysteine protease		↑		
E2F4	E2F transcription factor 4, p107/p130-binding		↑		
CDKN1A	cyclin-dependent kinase inhibitor 1A (p21, CIP1, WAF1)	1-4Gy	↑	PBL/HPF	Amudson, Turtoi,Kis [29,33, 36]
PLK2	polo-like kinase 2 (Drosophila)		↑		
MDM2	transformed 3T3 cell double minute 2, p53 binding protein (mouse)	1-4Gy	↑	PBL	Turtoi et al. [33]
TNFSF9	tumor necrosis factor (ligand) superfamily, member 9		↑		
INF-γ	Interferon-γ		↑		
ISG20L1	interferon stimulated exonuclease gene 20kDa-like 1		↑		
CD69	CD69 molecule		↑		
c-JUN	oncogene c-JUN		↑		
MUC5B	mucin 5B		↑		
STARD13	Start domain containing 13		↓		
SGK3	serum/glucocorticoid regulated kinase 3		↓		
RPL10A	ribosomal protein L10A		↓		
SERHL2	Serine hydrolase-like 2		↓		

1.5 MicroRNAs: REGULATORS OF GENE EXPRESSION

The induction of DNA double-strand breaks in eukaryotes triggers transcriptional changes and modulation of gene expression level of proteins involved in repair pathways, cell cycle checkpoints and programmed cell death; thus, cells have many regulatory factors to switch on or off these genes. Recent studies indicate that small non-protein-coding RNA molecules, termed microRNAs (miRNAs), might function as regulators of gene expression. MiRNAs are single-stranded RNAs of ~22 nucleotides encoded in the genomes of invertebrates, vertebrates and plants, which post-transcriptionally regulate gene expression through the RNA interference pathway [44, 45]. MiRNAs may originate from various genomic areas including repetitive regions, transposons and intronic sequence of coding genes, where they share regulatory elements with their host genes, or from either introns or exons of non-coding RNAs [46]. Based on the evidence that, most miRNAs derived from regions of the genome that are distinct from annotated protein-coding sequences and some miRNA encoding loci reside far from other miRNAs, it has been suggested that they form their own transcription units; others are clustered and show similar expression patterns, implying that they are transcribed as polycistronic transcripts [47-50]. In mammals, microRNAs are processed by the DICER protein and function by base pairing imperfectly with target mRNAs to inhibit protein accumulation. In humans, ~800 miRNAs are predicted to exist, and each of these is thought to have hundreds of mRNA targets [51].

• microRNAs biogenesis and maturation

In the nucleus, miRNAs are transcribed by RNA polymerase II in a primary miRNAs (pri-miRNAs), which range from hundreds to thousands of nucleotides in length [52]. As reported in figure 4, the pri-miRNA is first processed by the RNase III endonuclease Pasha-Drosha, which cleaves both strands of the stem at sites near the base of the pri-miRNA liberating a ~70-80 nt stem-loop intermediate, called miRNA precursor (pre-miRNA) [53, 49]. This pre-miRNA is then exported from the nucleus to the cytoplasm by Ran-GTP and Exportin 5, where the other end is processed by the enzyme Dicer [52, 54]; also Dicer is a RNase III endonuclease, which cleaves the hairpin releasing a miRNA-miRNA* duplex with two base overhang at both 3' ends.

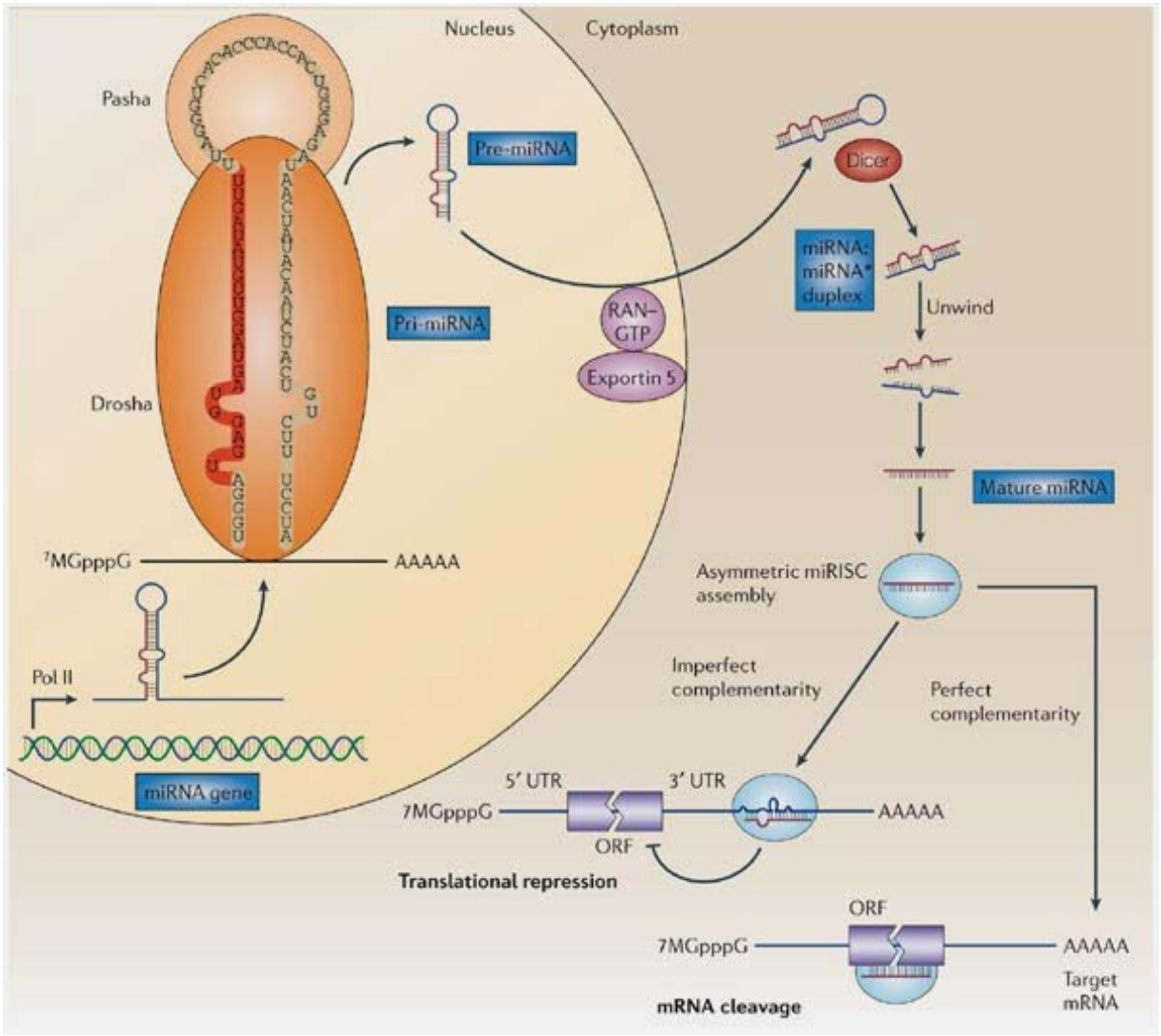

Fig. 4. microRNA biogenesis and mechanism (picture adopted from [55])

The strands of this duplex separate and a 21-25 nt mature miRNA is released; only one strand of the duplex becomes a mature miRNA, on the base of which 5' end of the duplex has less stable pairing, the other miRNA* strand is degraded [56]. At the end mature miRNA is integrated into a ribonucleoprotein complex, the RNA-induced silencing complex (RISC), and interacts with its target mRNA by base pairing [57]. In animals, miRNAs bind endogenous target messengers through sites in the 3'Untraslated Region (3'UTR); although miRNA binding sites have been identified in the Open Reading Frame (ORF) or 5' Untraslated Region (5'UTR) of mRNAs, they are less frequent and appear less effective than those in the 3'UTR [58-60].

• **RISC complex and mechanisms of microRNA function**

The core component of RNA-induced silencing complex (RISC) is a member of the Argonaute (Ago) protein family, whose members all contain a central PAZ domain and a carboxy-terminal PIWI domain. The PAZ domain binds to the 3' end of single-stranded RNAs, whereas the PIWI domain binds to small RNAs at their 5' end and closely resembles the RNase H, an enzyme that cleaves the RNA strand of an RNA-DNA hybrid [61-63]; for this reason, the Argonaute protein is considered the target-cleaving endonuclease of the RISC [64, 65].

Mature single-stranded miRNA is loaded in the RISC and directs this complex to complementary sites of mRNA target to negatively regulate gene expression in two ways, which depend on the degree of complementarity between the miRNA and its target. MiRNAs that bind to their mRNA targets with perfect (or nearly perfect) complementarity induce target-mRNA cleavage; on the contrary, when miRNAs bind with imperfect complementarity the expression of target gene is blocked at the level of protein translation or the mRNA stability is affected [57]. In animals the latter mechanism is prevalent and the complementarity between miRNAs and their targets is usually restricted to the 5' region of the miRNA (nucleotides 2-8 or 2-7), which has been called "seed region". Since the seed region is so short, miRNAs are predicted to regulate a large number of genes in a sequence-specific manner and are involved in various processes such as cellular differentiation, proliferation, apoptosis and they may affect an individual predisposition to malignancy [66-69].

• **microRNA annotation**

Since 1993, when the first members of miRNA class, lin-4 and let-7 were discovered in *Caenorhabditis elegans,* over 2000 miRNA sequences have been identified in vertebrates, flies, worms, plants, viruses and have been deposited in the mirBASE database (http://microrna.sanger.ac.uk/). This rapid rate of miRNA gene discovery has led to two basic needs for researchers: adoption of a gene naming scheme (miRBase Registry) and providing a comprehensive database of all published miRNA sequences (miRBase Sequences) [70]. A novel miRNA requires cloning or expression evidence and is submitted in miRBase only when a manuscript describing its discovery is accepted for publication; then, the official gene name is reported into the manuscript final version [71] following these miRNA nomenclature features:

1. The name of a mature microRNA contains: the "miR" prefix (the precursor hairpin is labeled "mir"), a sequential numerical identifier and an additional three- or four-letter prefix to designate the species (i.e hsa-miR-9 in *Homo sapiens*).
2. A mature miRNA sequence expressed from more than one hairpin precursor locus is denoted through further numeric suffixes (i.e dme-miR-6-1 and dme-miR-6-2 in *Drosophila melanogaster*).
3. Paralogous sequences whose mature miRNAs differ at only one or two positions are given lettered suffixes (i.e mmu-miR-10a and mmu-miR-10b in *Mus musculus*).
4. miRNAs deriving from opposite arms of the hairpin precursor are denoted using -5p and -3p prefixes; these respectively designate miRNAs from the 5' and 3' arms if both are functional, or until the data are sufficient to confirm which is predominantly expressed (i.e hsa-miR-140-3p and hsa-miR-140-5p).
5. When an arm of the precursor is determined to originate the predominantly expressed miRNA, the less predominant form is denoted with an asterisk (i.e miR-56 and miR-56*) [72, 73].

Currently, the number of mature miRNA sequences in the miRBase database is 17341 in 142 species, 1212 of which are human miRNAs (miRBase Release 16.0: September 2010), but it continues to grow rapidly thanks to the results of many microRNA discovery and profiling projects.

1.6 DIFFERENT APPROACHES IN THE STUDY OF microRNAs

MicroRNAs direct post-transcriptional repression of mRNAs through the RNA interference pathway, usually pairing on the 3'UTR of messengers. Given that the mature miRNA sequence is short and the perfect complementarity with the mRNA is not required, a large number of different mRNAs can be modulated by a single miRNA. Recent studies suggest that miRNAs may regulate up to 20%–25% of mammalian genes contributing in crucial biological processes, including development, differentiation, apoptosis, proliferation and tumorigenesis [59]. In the study of miRNAs the biggest challenge is to understand their biological function in a given cell line, tissue, developmental stage or malignancy; thus, different approaches have been used to profile miRNA expression, identify target mRNAs and demonstrate their role at cellular level.

- miRNA expression analysis: it could be done genome-wide with microarrays or focusing on a single miRNA with RT-qPCR or Northern Blot.
- miRNA target identification and validation: miRNA/target recognition is a very complex mechanism, which is not easy to study because the majority of target genes are predicted computationally. Different algorithms often predict different targets for the same miRNA and the false discovery rate in most cases is higher. For these reasons, after analysis *in-silico* of miRNA's target genes it is necessary to perform an experimental validation using 3'UTR-reporter assay.
- Functional analysis: once an interaction miRNA/target has been positively demonstrated by 3'UTR-reporter assay, the next step is miRNA silencing or over-expression in cell lines followed by the observation of changes in cell growth, cell cycle or transformation ability. This is the main approach to validate the miRNA effects on its endogenous target and to understand the role of miRNA at cellular level.
- *In vivo* models: finally, to study miRNA's function in a physiological context, animal models are used to mimic loss or gain of miRNA expression.

• miRNA microarray

MiRNAs function as regulatory molecules in post-transcriptional gene silencing, for this reason gene expression changes could result from altered or aberrant miRNA expression. Microarray technique is a genome-wide approach used in miRNA profiling, which allows to simultaneously determine the expression levels of a large number of known miRNAs in a

single experiment. A microarray consists of oligonucleotide probes, corresponding to mature sense miRNA sequences, covalently cross-linked to or *in situ*-synthesized on a solid support matrix (glass slide). Often miRNA samples are reverse-transcribed with random primers and cRNAs are labeled with a fluorophore, although recently it has been developed a method of miRNA direct labeling; then the sample is deposited on the solid matrix and let hybridize [74] (Fig. 5). Researchers use this approach to compare miRNA expression in different organs, cell lines, proliferating stages or pathological conditions with significant advantages over the other methods, including higher sensitivity, high throughput and higher comparative capabilities [75].

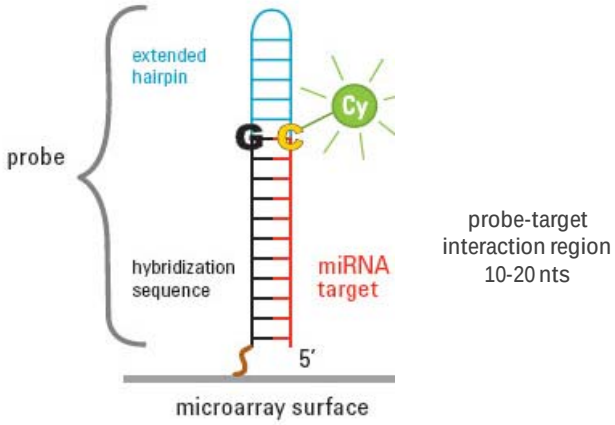

Fig. 5. Microarray approach scheme. Oligonucleotide probes are anchored to the glass slide surface and hybridize to the complementary target miRNAs labeled with a fluorophore (picture adopted from [76])

• **Quantitative RT-PCR**

The expression of miRNAs has been studied using traditional, semi-quantitative methods such as Northern blotting, bead-based flow-cytometry and microarray technology; however the real-time quantitative PCR (RT-qPCR) is the more sensitive and reproducible gene expression quantitation technique, which is now being used to validate miRNA expression data obtained with microarrays. The first method to amplify and quantify miRNAs using real-time PCR was developed by Schmittgen in 2004. The application of fluorescence techniques to the RT-PCR, together with suitable instrumentation capable of combining amplification, detection and quantification, has led to the development of kinetic RT-PCR methodologies [77, 78]. To correct errors occurring upon systematic variables such as different amounts of starting template, poor RNA quality and altered enzymatic efficiencies, RT-qPCR data are commonly normalized to an endogenous control gene, which ideally, is stably-expressed across the test sample set [79].

• **Northern blotting**

Northern blotting is a labor-intensive, but very efficient technique to study the expression/processing of a specific miRNA. This approach consists in a poly-acrylamide gel electrophoresis to separate RNA molecules from 10 to few hundred nucleotides, transfer of RNAs on a nylon membrane and miRNA detection through complementary radio-labeled oligo-nucleotides probes. Specific 20mer-probes are end-labeled with (dATP)^{32}P and let hybridize on the nylon membrane containing the RNAs. If there is miRNA expression/processing, it is possible to observe the typical bands of pre-miRNA (60-70nt) and the mature microRNA (20-25nt) by exposing the membrane on photographic film.

• **Target prediction**

The miRNA's targets prediction is a fundamental approach to investigate physiological or pathological roles of miRNAs, because they exert their function destabilizing target messengers. In plants, miRNAs are nearly perfectly complementary to their mRNA targets [80], so computational target prediction is straightforward and powerful. In contrast, in animals, the specificity of miRNA-mRNA interaction is mainly conferred by the first eight nucleotides of miRNA sequence (seed region) and the exact complementarity is not required for silencing, therefore a large number of potential mRNA targets can be predicted. Currently, several computational algorithms are available to predict target mRNAs, such as Pita, TargetScan, miRanda, PicTar, DIANA-microT, mirWIP and RNA22; they rely on different criteria including:

- sequence alignment of the miRNA seed region to the 3'UTR sequences of candidate target genes in order to identify putative miRNA binding sites [81]
- evolutionary conservation of the binding site on mRNA-3'UTR [82]
- structural accessibility of the target binding site, which needs to be open without interactions with other sites in the mRNA to bind with the RISC-miRNA complex [83]
- location and nucleotide composition of the binding site in the 3'UTR. Binding sites have to be located within the 3'UTR, at least 15nt from the stop codon; sites residing near the two ends of long UTRs are more effective than those near the center. In addition, high local AU content increases the accessibility of a site because the mRNA secondary structure is weaker [81]
- proximity of one binding site to another within the same 3'UTR [84]

- thermodynamic stability of the miRNA: target duplex, which means that the binding of a miRNA to a mRNA is stronger when the free energy of the duplex is low (ΔG duplex <0) [85]

Since molecular bases of miRNA-target interaction are still poorly understood, miRNA target prediction tools can be based on few of these criteria leading to a reduction of their predictions specificity, which produces a large fraction of false positives; for this reason, target identification requires extensive experimental validation.

• **3'UTR Report-Assay**

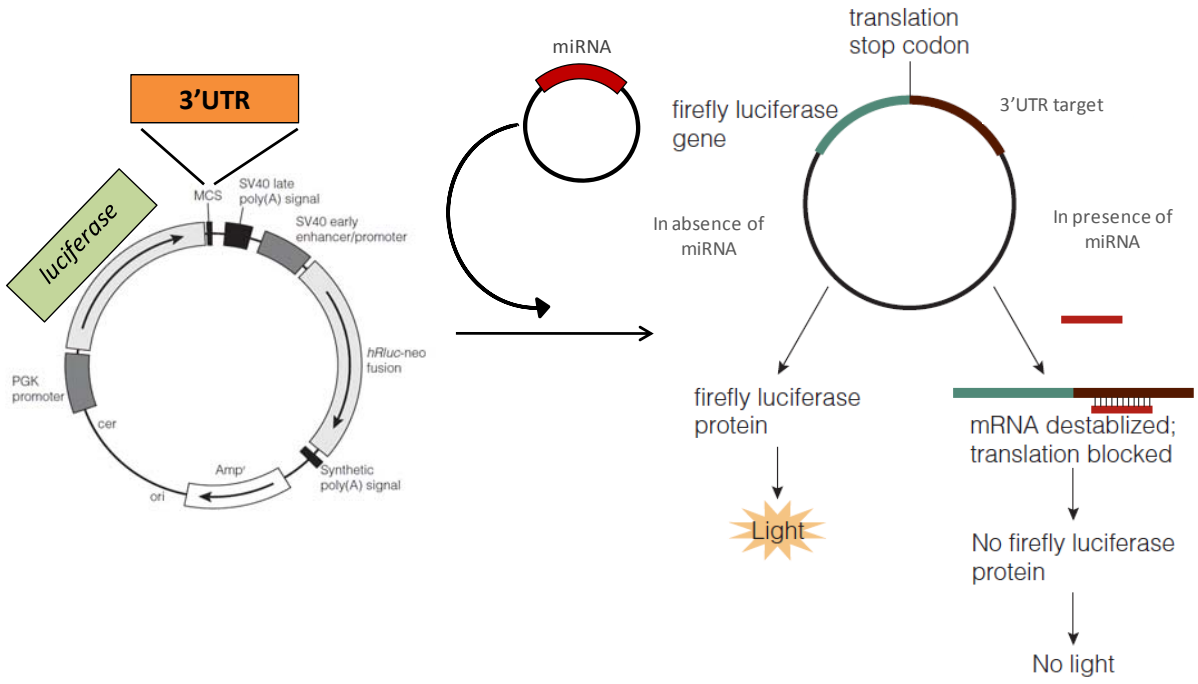

Fig. 6. 3'UTR Report-Assay approach to validate miRNA-mRNA direct interaction. 3'UTR-expression plasmid and miR-expressing vector are co-transfected in cells, a luciferase-3'UTR target sequence is transcripted. The binding of the miRNA to the 3' UTR target sequence can repress the luciferase activity.

This technique represents the first test used to validate, in cell culture, a miRNA-target interaction predicted by computational analysis. By using cloning strategies, a 3'UTR sequence of interest is inserted downstream of a reporter gene, such as Luciferase, inside a proper vector for expression in cell. After co-transfection of this 3'UTR-expression plasmid with a miR-expressing vector a chimeric mRNA (luciferase-3'UTR target sequence) is transcribed. The binding of the miRNA to the 3' UTR target sequence can affect the luciferase activity, reducing the emission of light that is quantified with a

spectrophotometric assay (Fig. 6). In general, to confirm a direct interaction miRNA-mRNA are tested not only the 3'UTR target sequences, but also the corresponding mutated versions designed to not be recognized by the miRNA. With this approach it is not possible to replicate temporal and physiological aspects of these interactions, therefore a rigorous analysis in animal models is required [86].

1.7 RADIO-RESPONSIVE microRNAs

Ionizing radiation (IR) is a potent DNA damaging and cancer inducing agent with an important role as diagnostic and treatment modality. Lymphoid and myeloid hematopoietic tissues are the main targets for radiation carcinogenesis, but the exact mechanism by which IR exposure may result in a predisposition to develop IR-induced leukemia and lymphoma remains to be determined [87-89]. In recent years, the role of epigenetic in the etiology of diseases and cancer has been increasingly studied. Epigenetic changes are stable alterations in gene expression that include DNA methylation, histone modification and small RNA-mediated effects; among the small RNA, miRNAs are the most abundant and well understood [90-92]. MiRNAs play pivotal roles in several processes such as development and differentiation, control of cell proliferation, stress response, metabolism, all of which are often perturbed in cancer. Recent reports on oncogenic or tumor-suppressive miRNAs have demonstrated that let-7 family may repress oncogenes, including RAS family members, thereby inhibiting tumor growth [93]. Cimmino and coworkers (2005) described a mechanism of regulation of BCL2 expression in hematopoietic cancer cells consisting in a post-transcriptional down-regulation mediated by miR-15 and miR-16; the important functional consequence of this interaction is the activation of the intrinsic apoptosis pathway [94]. Increased expression of miR-21 gene has been implicated in various processes involved carcinogenesis, including inhibition of apoptosis, promotion of cell proliferation and stimulation of tumor growth [95-97]. The study carried on by Lu (2008) demonstrates that the translation of the tumor suppressor gene Programmed Cell Death 4 (PDCD4) is negatively regulated by miR-21 in tumor cell lines (HEK-293T, MCF-7 and JB6); thus, miR-21 gene functions as an oncogene to promote cell transformation [98]. Other oncogenic miRNAs include the miR-17-92 and the miR-106a-363 polycistronic clusters; they contain 18 members with a seed region homology that in the work of Ivanovska (2008) were indicated to belong to the miR-106b family. Several members of this family correlated with cell cycle-related transcripts; in particular, miR-106b, miR-106a, miR-93, miR-17-5p and miR-20 regulate genes involved in DNA replication, cell cycle progression in G1 and S phases, and mitosis. Interestingly, this study provides evidences that the miR-106b family promotes the G1-to-S transition and targets the CDK inhibitor p21 (CDKN1A) [99]. In another similar study has been demonstrated that the cyclin-dependent kinase inhibitor $p27^{Kip1}$ is regulated by miR-221 and miR-222 [100, 101]. Although miRNAs have been recognized as important post-transcriptional

regulators, which are involved in various biological processes, it is not well exanimate if they could play a role in the cellular response to ionizing radiation. A Recent study demonstrates that, in IM9 human B lymphoblast cell line irradiated with 1Gy and 10Gy of γ-ray, radio-responsive miRNAs to both IR doses (let-7c, miR-202, -134, -520b, -557, -560, -575, -583, -630, -638, -663) are predicted to target several genes related to apoptosis, cell cycle and DNA damage signaling/repair; interestingly, some of these miRNAs showed dose-dependent expression profiles. Since cell responded differently to each dose, cell cycle arrest in response to 1Gy and apoptosis after 10Gy, the scenario suggested was that different miRNA expression profiles reflect different functional outputs which contribute to the major cellular response to each dose [102]. To test the hypothesis that miRNA are involved in the cellular response to IR, the same research group performed microarray experiments in A549 human lung carcinoma cell line irradiated with 20Gy and 40Gy of γ-ray. They found that the fraction of strongly up- and down-regulated miRNAs differed between the two radiation doses; Eight miRNAs, showing expression changes with both IR doses, were characterized by the same expression change direction but not magnitude (i.e miR-16-2*, -106a, -127-3p, -206, -345, -516a-5p, -548c-3p, -885-3p). Computational analysis was carried out to determine potential targets genes of the radio-responsive miRNAs and results showed that more of the predicted targets had functions related to apoptosis compared to cell cycle control and DNA repair. This observation supports the hypothesis that the modulation of miRNA expression contribute to the major cellular response to IR [103]. Among the radio-responsive miRNAs with potential roles in ionizing radiation cell response, miR-34a is the best characterized; it is directly trans-activated by p53 and is involved in the regulation of apoptosis, cell cycle arrest and senescence-like growth arrest by targeting many genes including SIRT1, CCND1, CDK6 and by the modulation of (AR)-dependent p53-induced apoptosis and the E2F pathways [104-108].

• Transactivation of miRNAs by p53

Ionizing radiation causes DNA DSBs that are the main stress signal activating the p53 pathway. The DNA damage is followed by the phosphorylation and stabilization of p53 by protein kinase ATM, then the activated p53 selectively induces cell cycle arrest or apoptosis; for this reason p53 is considered a key transcriptional factor that controls gene expression in response to stress signals. Currently, there are several reports describing a p53-signaling pathway involving miRNAs; cellular stress stabilizes p53 that regulates the

expression of a set of miRNAs, which in turn may control apoptosis and senescence. Among these miRNAs, the miR-34a has been suggested to be sufficient to induce apoptosis through p53-dependent and independent mechanisms; interestingly, loss of the genomic region harboring mir-34a (1p36 locus) is common in diverse human cancers [104, 105, 108, 109]. Yamakuchi's group used *in silico* analysis to screen candidate miR-34a target genes and found that the 3'UTR of SIRT1 (Silent Information Regulator 1) has a miR-34a responsive element. SIRT1 is a NAD-dependent deacetylase which plays an important role in protecting cells from cellular oxidative and genotoxic stress; once SIRT1 is activated, it deacetilates a variety of histone and non-histone proteins such as p53, decreasing p53-mediated transcriptional activation of p21 and PUMA (Fig. 7). The target prediction data were experimentally validated using different approaches and results suggested that over-expression of miR-34a decreases SIRT1 mRNA translation leading to an increase in acetylated p53 levels and also p53 targets, p21 and PUMA; therefore, miR-34a activates apoptosis in a p53-dependent pathway [104]. In a recent work of Shin (2009) were identified miRNAs affected by p53 in human colon carcinoma cell lines (HCT116, p53wt) irradiated with 10Gy of γ-ray; among these miRNAs, miR-34a, -34b, -202, -330, -516-5p, -548c were modulated by the combined action of p53 and IR [110].

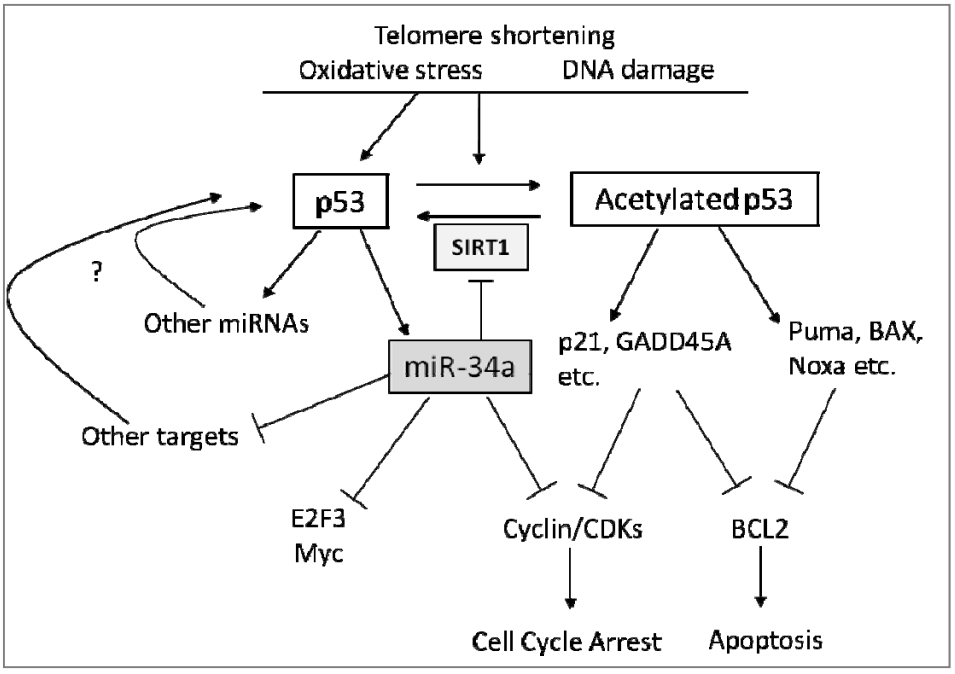

Fig. 7. Schematic representation of p53-miR-34a feedback loop. p53 induces miR-34a expression, which increases p53 acetylation by suppressing SIRT1 expression. Resultant increase of p53 activity prolongs miR-34a expression. MiR-34a induces apoptosis, cell growth arrest and senescence (picture B adopted from [111])

1.8 SPACE ENVIRONMENT AND MODELED MICROGRAVITY

During space missions astronauts are exposed to a radiation environment that is totally different, as to composition and intensity, from our biosphere; indeed, the natural radiation encountered in orbit is a complex mixture of charged particles of galactic and solar origin and particles trapped by the geomagnetic field. Galactic cosmic radiation derived from matter that has been selected by its ionization potential and then accelerated to high energies, whereas elements from hydrogen to iron are generated during normal stellar processes or supernova explosions; then, this accelerated material propagates through space. In addition, secondary radiations are produced by interaction of cosmic ray with the space craft shield and the astronaut's body itself. The Earth's magnetic field acts as a natural protective barrier against charged particles which impact on the magnetosphere [112], but spacecrafts operate above the shield provided by the Earth and are subjected to the full intensity of the cosmic radiation transmitted through the geomagnetic field; for this reason, the radiation dose received by astronauts during space flight is carefully monitored. The radiation dose codes utilized by NASA predict the radiation exposure due to cosmic radiation; for example, US space shuttle flights in 28° inclination orbits receive between 42 to 62 Gy per day (depending on the cosmic ray spectrum). In a 51° inclination orbit, such as the MIR space station and the international space station, the radiation dose varies from 90 to 150 Gy per day [113]. Therefore, the possibility of experiencing a significant radiation exposure during space flights continues to be a potential operational limit that must be taken in consideration by mission planners. For example, since the opacification of the ocular lens is an important effect of exposure to ionizing radiation, a study has been initiated to examine the astronauts' ocular lenses to detect signs of radiation-induced cataracts; the aim of this project was to provide further essential data upon which the assessment of radiation-induced risk associated with long space missions can be based [114, 115].

Another important source of potentially detrimental effects, inevitably present during space flights, is the reduction of gravitational force (10^{-4}-10^{-6} g), which remain one of the main obstacles in long term space missions. In human exposed to microgravity were commonly observed alterations in the number and function of mature blood cells in the peripheral blood. These alterations are characterized by reduced red blood cell mass, inhibition of lymphocyte proliferation and suppressed or altered cytokine secretion, increased number of neutrophils and monocytes. Other space flight-related effects include

changes in fluid volume and distribution, loss of calcium and minerals from bones, decreased skeletal muscle mass and hormonal dysregulation [116-118]. In addition, analysis performed on astronauts, during or early after space mission, revealed several impaired cellular functions, such as apoptosis induction, cytoskeletal alteration, cell growth inhibition and increased frequency of chromosome aberrations [118-125].

Since there are severe limits to the number and type of experiments that can be performed during space flight, microgravity can be achieved with a number of technologies, each depending upon the act of free fall. Drop towers and drop tubes, aircraft performing parabolic flights and small rockets can be used to establish several minutes of microgravity environment; to conduct longer term experiments (days, weeks, months, and years) it is necessary to travel into space with orbiting spacecraft [126] or use bioreactors able to simulate weightlessness condition on Earth. Several ground-based simulators of microgravity have been developed; these include different types of rotating culture systems, such as the Fast-Rotating Clinostat (FRC), the Rotating Wall Vessel bioreactor (RWV) and the Random Positioning Machine (RPM or 3D-Clinostat) [127]. The culture condition obtained through these methods is termed simulated or modeled microgravity. In particular, to carry on this research work modeled microgravity (MMG) was obtained in laboratory through the RWV bioreactor (Synthecon), which is a device developed at the NASA Johnson Space Center in Houston (Fig. 8). It is used to simulate an aspect of space flight that is the weightlessness condition, by balancing the force of gravity with equal and opposite forces; in this way, the direction of gravity vector is randomized, thus the constant reorientation nullifies cumulative sedimentation of particles producing a gravitational reduction to 10^{-2}g [128]. Qualitatively, the results obtained from experiments documenting reduced function, activation, proliferation and locomotion of hematopoietic cells in MMG were very similar to the results obtained with space flight-cell cultures [129]. Risin and Pellis (2001) used the RWV to investigate the possibility that MMG affects apoptosis process in lymphocytes, contributing through this mechanism to the impairment of the immunity. Their results showed inhibition of apoptotic cell death in human lymphocytes maintained in microgravity condition, although no expression changes of Bcl-2, BAX, FasL proteins were involved; thus, the scenario proposed was that MMG impairs membrane-bound Fas and FAsL interaction, altering receptor affinity, interfering with receptor distribution or minimizing the area of cell-cell interaction [130]. Plett and coworkes (2004) described an inhibitory effect of MMG on in vitro migration potential and alteration of normal hematopoietic differentiation in primitive human hematopoietic progenitor cells

(BM CD34+), most likely via altered cytoskeletal organization and cell cycling factors [131]. cDNA expression array approach was used in human fibroblast cells cultured 24h in the 3D-Clinostat; results showed alteration of genes involved in cell cycle progression, apoptosis, stress response and differentiation, such as Cdc-like kinase-1 (CLK1), Tumor Necrosis Factor (TNF), X-ray Repair Cross Complementing (XRCC), p38 mitogen activated protein kinase (p38 MAPK) and Cdk-interacting protein 1 (CDKN1A) [132]. Finally, since microgravity leads to a 10-15% loss of bone mass in astronauts during space flight, a recent study has been performed applying microarray approach in osteoclast progenitor cells (OCL RAW 264.7), maintained in modeled microgravity condition through the RWV. Microarray analysis revealed significantly increased expression of critical molecules such as cytokines, growth factors, proteases and signaling proteins, which play an important role in enhanced OCL differentiation and function [133].

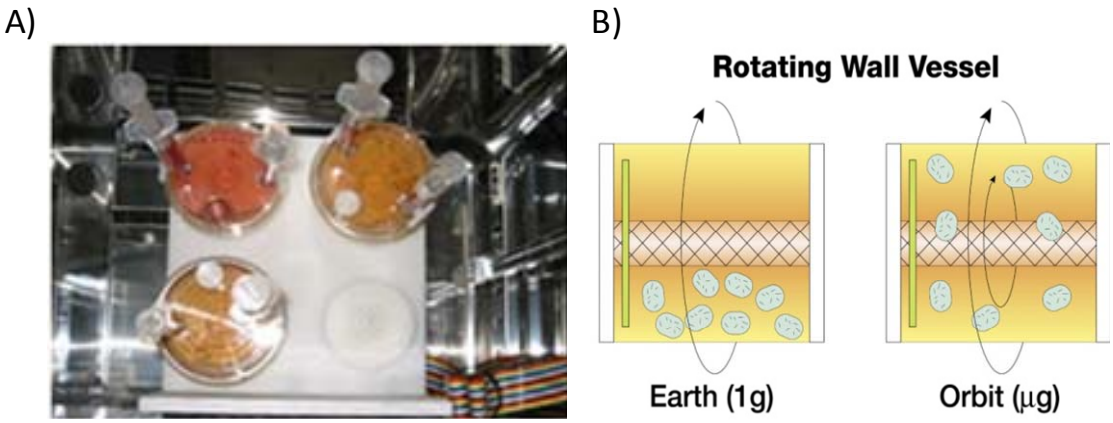

Fig. 8. Ground-based simulator of microgravity. A) The Rotating Wall Vessel bioreactor (NASA Johnson Space Center, Houston). B) Simulation of weightlessness condition through RWV (picture adopted from www.nasaimages.org).

• Study of the interaction radiation-microgravity

To assess the risks for humans in space, it is necessary to consider the combined influence of different stressors, especially those acting over extended periods of time, such as radiation and microgravity [134]. It was observed that, human resting lymphocytes exposed to 1.5Gy of X-ray presented incidence of chromosome-type aberrations (dicentrics, rings and fragments) significantly higher in MMG culture condition (clinostat) compared to parallel "ground" condition; probably because MMG synergistically influences the outcome of X-ray-induced chromosome aberration or, chromatin structure could be modified by

MMG, generating different qualities and quantities of DNA lesions [123]. To investigate the possibility that a reduced gravitational force impairs the efficiency of DNA damage repair, increasing the risk of IR exposure during spaceflights, several experiments were performed in human lymphocytes and lymphoblastoid cells (TK6) irradiated with γ-ray and incubated in "ground" (1g) and MMG conditions. Results indicated that MMG incubation after irradiation affects cell response to ionizing radiation, reducing the level of radiation-induced apoptosis and increasing the frequency of damaged cells that survive after irradiation; indeed, the frequency of HPRT mutants and micronucleated cells, were higher in cultures incubated in MMG than in 1g [135, 136].

2. AIM OF THE WORK

On Earth we are constantly exposed to low levels of ionizing radiation (IR), moreover professional or accidental exposures may occur, thus producing serious risks to human health. Among the numerous types of DNA lesions, DNA double-strand breaks (DSBs) represent the most severe form of IR-induced damages, since an inefficient or inaccurate repair may lead to cell death or genomic instability [1, 2]. Whereas the surface of the Earth is largely spared from cosmic radiation, the natural radiation encountered above the geomagnetic shield is a complex mixture of charged particles of galactic and solar origin and this represents the main risk for astronauts [113]. To estimate the health risks for humans during space missions, it is necessary to take into consideration the interaction between different stressors, such as radiation and microgravity. Since cells of the immune system are among the most radiosensitive in the body, this study was carried out using human lymphocytes obtained from healthy donors and maintained in normal gravity and in condition simulating reduced gravity (modeled microgravity, MMG) [118, 119, 123].

The aim of my research is to study human cell response to ionizing radiation in normal gravity and microgravity. In the first part, the efficiency of DNA repair occurring in modeled microgravity (MMG) was compared to ground gravity (1g) culture conditions; DSB repair kinetic was screened by immune-fluorescence of damage-induced foci of phosphorylated histone H2AX (γH2AX), Pulsed-field gel electrophoresis and Western blotting of DNA damage signaling/repair proteins. In eukaryotic cells, ionizing radiation induces transcriptional changes and modulation of the expression levels of a variety of genes, which are involved in multiple cellular pathways, such as DNA repair, cell cycle control, signal transduction, apoptosis and tumorigenesis. In order to figure out quantitative and qualitative changes in gene expression patterns induced by ionizing radiation, in the second part of this work, microarray approach was used to identify radiation responsive miRNA and mRNA. An anti-correlation analysis was performed between significantly deregulated miRNA and mRNA to identify direct miRNA-mRNA interactions elucidating the mechanism of ionizing radiation cell response. Finally, miRNA, mRNA and biological pathways modulated in response to ionizing radiation were compared in ground gravity and MMG, to investigate if ionizing radiation and modeled microgravity could have a synergistic action on human cells.

3. RESULTS AND DISCUSSION

3.1 KINETICS OF γ-H2AX

In mammals, the DSBs induction leads to a cascade of cellular events which are early activated through the phosphorylation of the histone H2AX (γ-H2AX) at the sites damage; DNA damage and repair can be quantified in individual cells by monitoring the kinetics of formation and disappearance of γ-H2AX foci (IRIF) at sites of DSBs. For this reason, to figure out if the efficiency of DNA repair is impaired when it occurs in modeled microgravity culture conditions, IRIF quantification at different repair time points were performed in human lymphocytes (PBL) irradiated with 5Gy of γ rays.

• Immunofluorescence analysis of γ-H2AX foci

The *in situ* immunofluorescence of nuclear γ-H2AX foci was performed in irradiated PBL during a repair time of 24h in 1g and MMG. Results shown that the fraction of γ-H2AX foci-positive cells (mean values) was significantly higher in MMG than in 1g at 6 and 24h ($p < 0.01$, t-test) (Fig. 9).

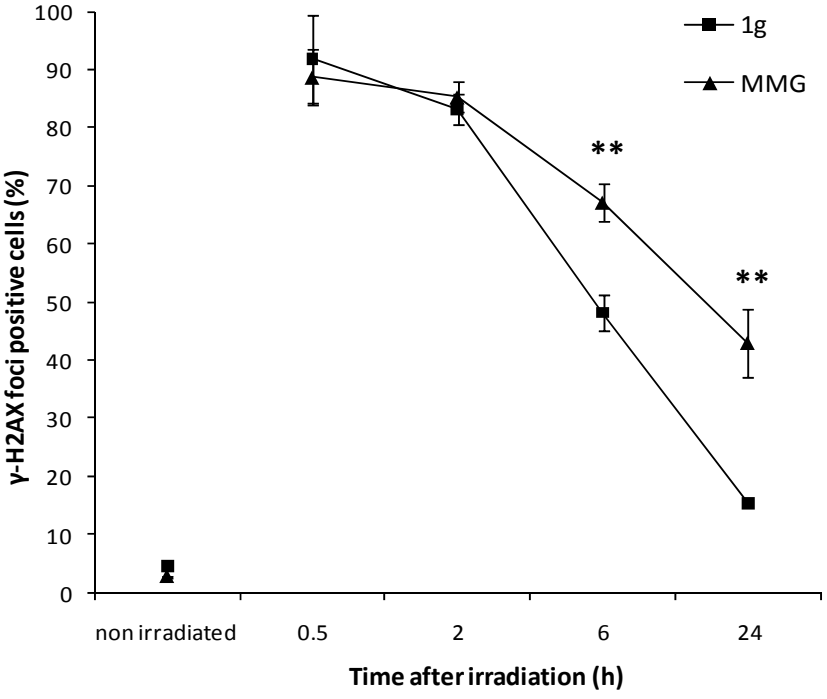

Fig. 9. Kinetics of γ-H2AX foci in PBL irradiated with 5Gy of γ-rays and incubated in 1g or in MMG during repair time. It is represented by the fraction of γ-H2AX foci positive cells determined by counting 300–500 cells for each experimental time-point. Results represent the mean of 3–4 independent experiments ±S.E (**$p < 0.01$, t-test).

In accordance with these data, the mean number of foci/nucleus in 1g was 16 and 12 from 30min to 2h, respectively, comparable with the foci number in MMG. At later times the foci number in sample maintained in the two culture conditions was significantly different. Indeed, PBL incubated in 1g had a mean of 4foci/nucleus at 6h and 2foci/nucleus at 24h after irradiation; on the contrary, those incubated in MMG showed a mean of 7.5foci/nucleus and 6.4foci/nucleus at the same time points (*** $p < 0.001$) (Fig. 10).

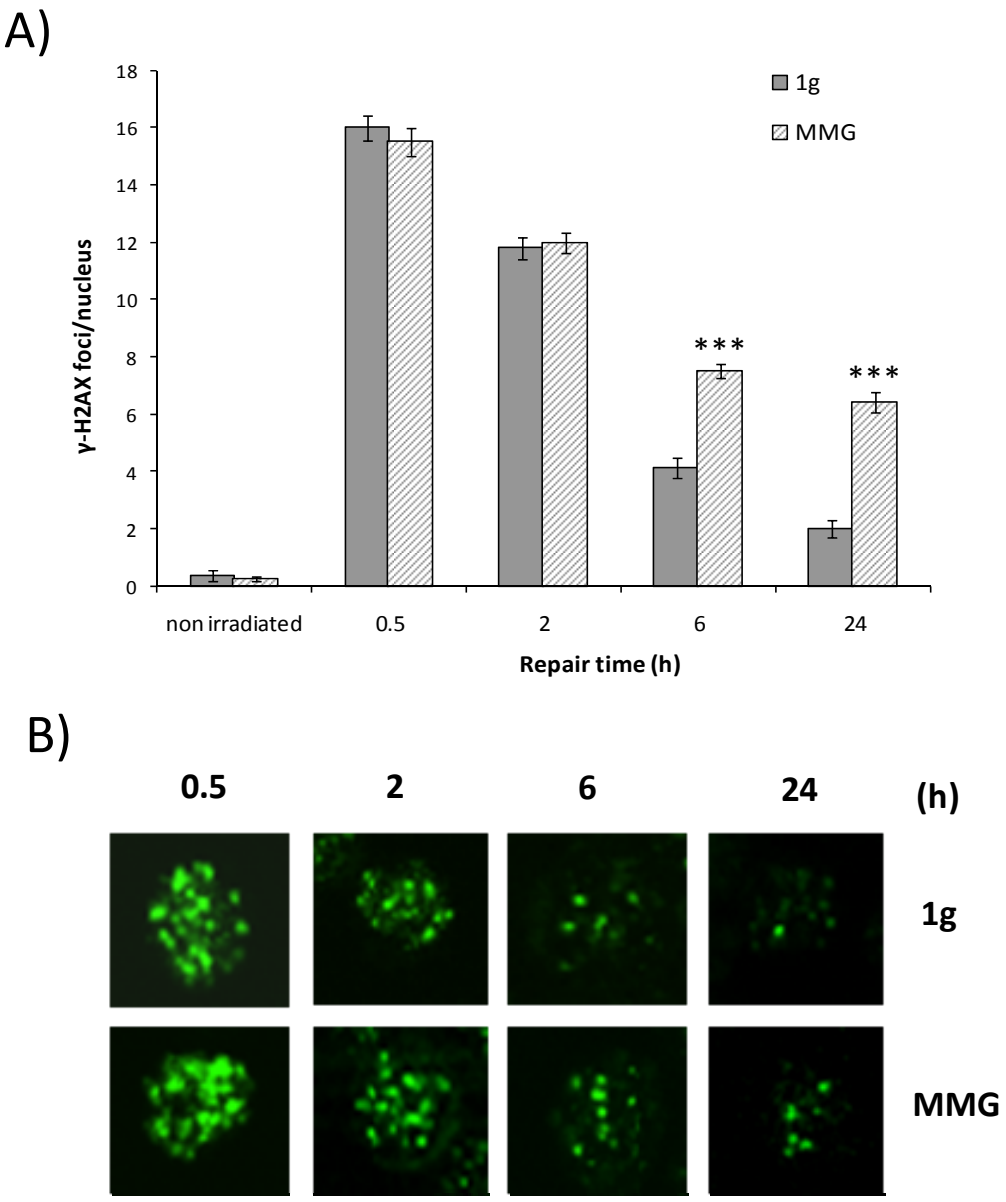

Fig. 10. Kinetics of γ-H2AX foci in PBL irradiated with 5Gy of γ-rays and incubated in 1g or in MMG during repair time. (A) Mean number of γ-H2AX foci per nucleus; at least 100cells/time-points were scored for foci. (B) Immunofluorescence of γ-H2AX foci at 0.5, 2, 6 and 24 h after irradiation. Results represent the mean of 3–4 independent experiments ±S.E. (***$p < 0.001$, t-test).

Finally, by grouping the cells in different categories based on the number of γ-H2AX foci/nucleus (0, 1–4, 5–9, 10–20 or more foci/nucleus), the different kinetic of γ-H2AX foci disappearance in the two culture conditions was more evident. In 1g, PBL with 10–20 or more foci/nucleus were absent from 6h after irradiation, whereas in MMG they were still present up to 24h after irradiation (Fig. 11).

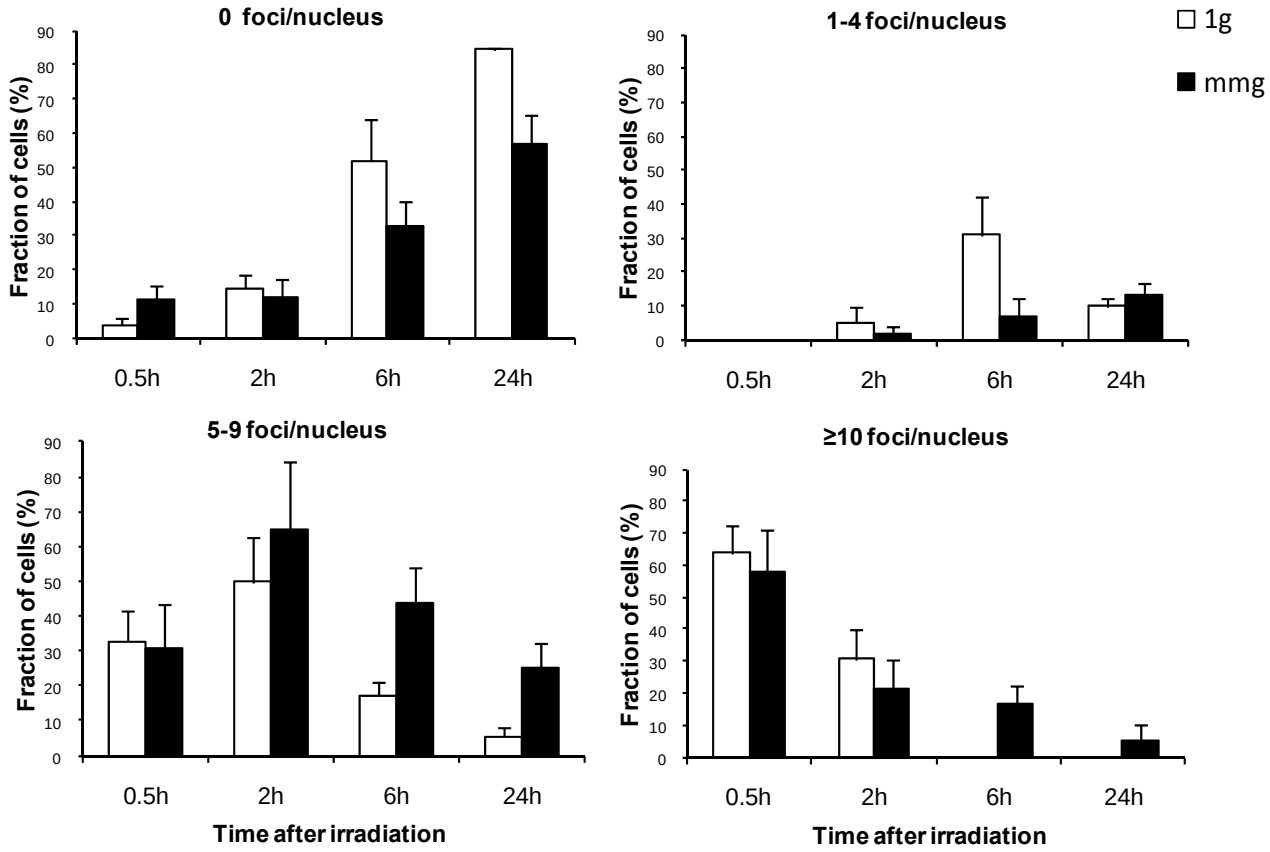

Fig. 11. Fraction of PBL (%±S.D.) with 0, 1–4, 5–9, ≥10 γ-H2AX foci/nucleus.

• **Flow cytometry for γ-H2AX**

The level of phosphorylated H2AX was assessed by flow cytometry in non-irradiated and γ-irradiated PBL, maintained in 1g and MMG condition during the repair time; values of γ-H2AX fluorescence were estimated by excluding debris and apoptotic bodies. In the bar chart (Fig. 12) are reported the mean values of γ-H2AX-fluorescence measured by FACs; it shows that γ-H2AX was induced at 30min after irradiation with similar fluorescence intensity in both gravity conditions. At 2h after irradiation the fluorescence intensity

slightly decreased in samples incubated in 1g, whereas no significant changes were observed in MMG.

At 6h after irradiation γ-H2AX fluorescence further decreased, more in 1g than in MMG, persisting with the same values at 24h.

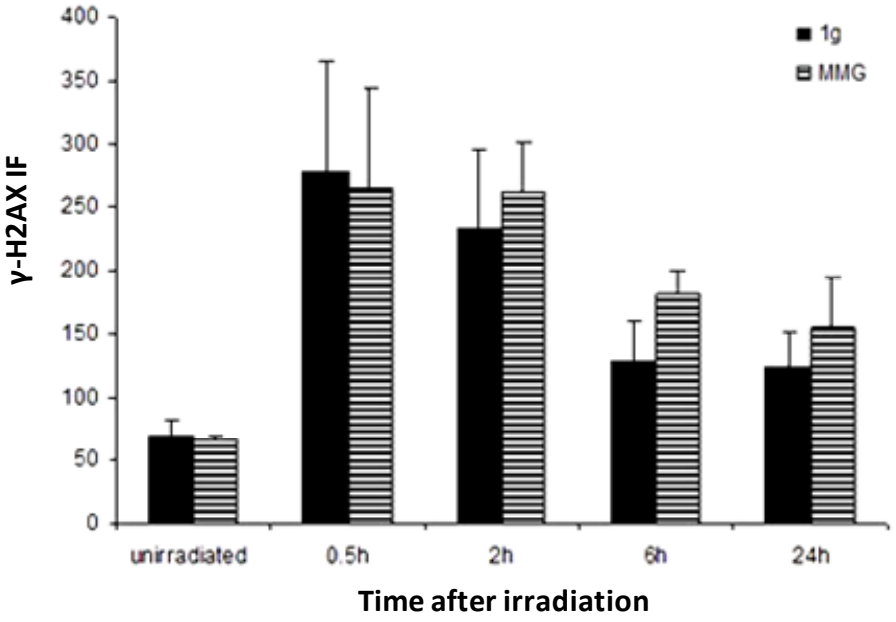

Fig. 12. Nuclear level of γ-H2AX assessed through flow cytometry in γ-irradiated PBL (5Gy) incubated in 1g or MMG and harvested at indicated time-points after irradiation.

By using Western blotting method these data were partially confirmed, most likely because this technique is less sensitive compared to flow cytometry and cannot discriminate apoptotic cells and debris. Indeed, no differences in γ-H2AX immunoreactivity were observed at 6h and 24h in both gravity conditions; therefore, this high amount of γ-H2AXwhich persisted at long times could reflect an increasing level of apoptotic induction.

3.2 INDUCTION OF APOPTOSIS

The apoptotic index (A.I) and the Caspase activity were determined in γ-irradiated human cells in order to investigate the MMG incubation effect on IR-induced apoptosis; A.I was analyzed through nuclear staining with DAPI and Caspase3-activation with a fluorimetric assay. The presence of fragmented nuclei and apoptotic bodies were evaluated in non-irradiated and irradiated PBL (5Gy) incubated in 1g and MMG conditions. As

reported in Fig. 13A, the A.I. value increased with time after irradiation and at 24h it was significantly higher in PBL incubated in MMG compared to those in 1g (19.3% vs. 13.7% respectively, $p<0.001$). Since DSBs can be induced also by DNA fragmentation during early apoptosis, caspase-3 activation was measured at the same time-points. Caspase-3 activation increased during repair incubation: at 2 h it was ~2-fold higher than non-irradiated cells in both gravity conditions, at 6 h it was 2.4- and 2.6-fold in 1g and MMG, respectively, and at 24h caspase-3 activation increased 3- and 3.5-fold, respectively (Fig. 13B). These values were slightly higher in MMG than in 1g, in contrast to the high persistence of foci-positive cells ($p<0.01$) and foci number/nucleus ($p<0.001$) in PBL incubated in MMG; probably the level of γ-H2AX was principally correlated to a delayed DSB rejoining rather than apoptosis induction.

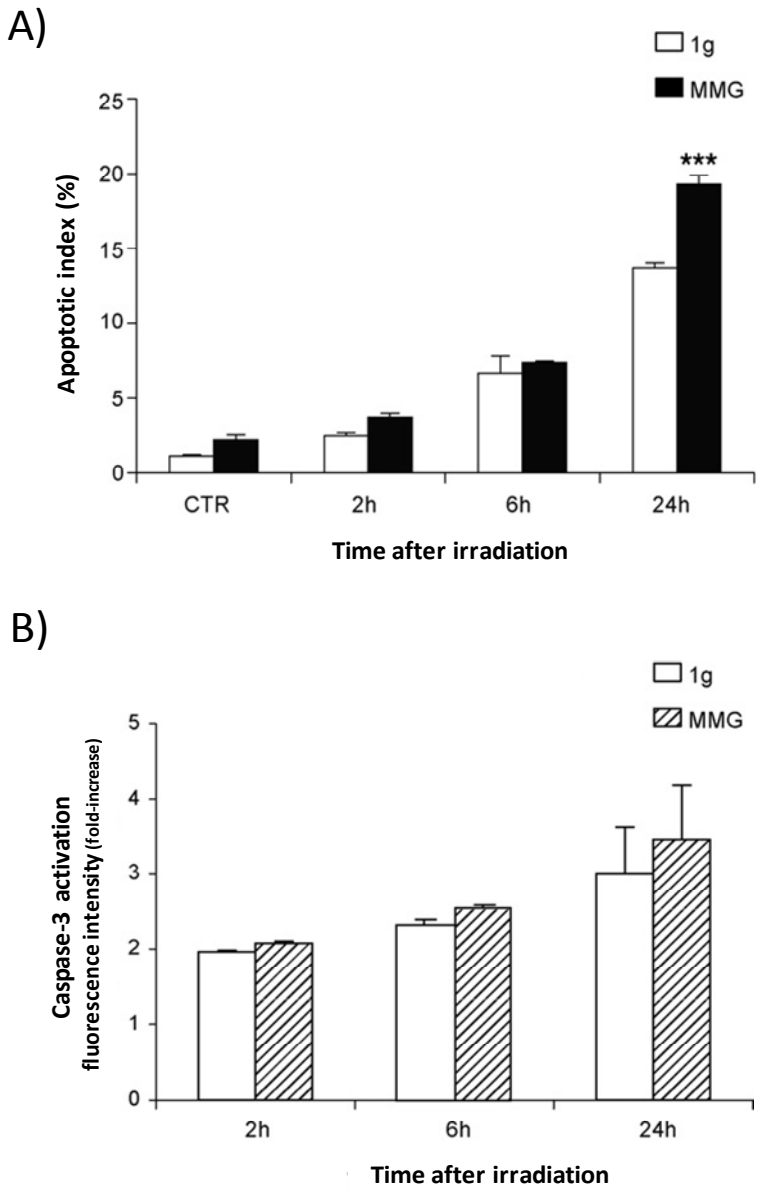

Fig. 13. Apoptotic index (A) and caspase-3 activation (B) in PBL irradiated with 5Gy of γ-rays and incubated for 2, 6 and 24 h in 1g or MMG. Results represent the mean of 3–4 independent experiments±S.D. (***$p< 0.001$, t-test).

3.3. RECRUITMENT OF SIGNALING PROTEINS TO DSB SITES

The induction of DSBs recruits many factors of DNA damage signaling/repair and cell cycle checkpoints on the damaged sites, to form ionizing radiation-induced foci (IRIF) which co-localize with γ-H2AX foci. *In situ* immunofluorescence and Western blotting methods were used to investigate the possibility that MMG incubation affects DNA damage response by altering the recruitment of signaling proteins such as 53BP1, NBS1^{-p343} and ATM^{-p1981} to DSB sites; these experiments were performed in the same samples analyzed for γ-H2AX foci: PBL irradiated with 5Gy of γ-rays and incubated in 1g or MMG during a repair time of 24h.

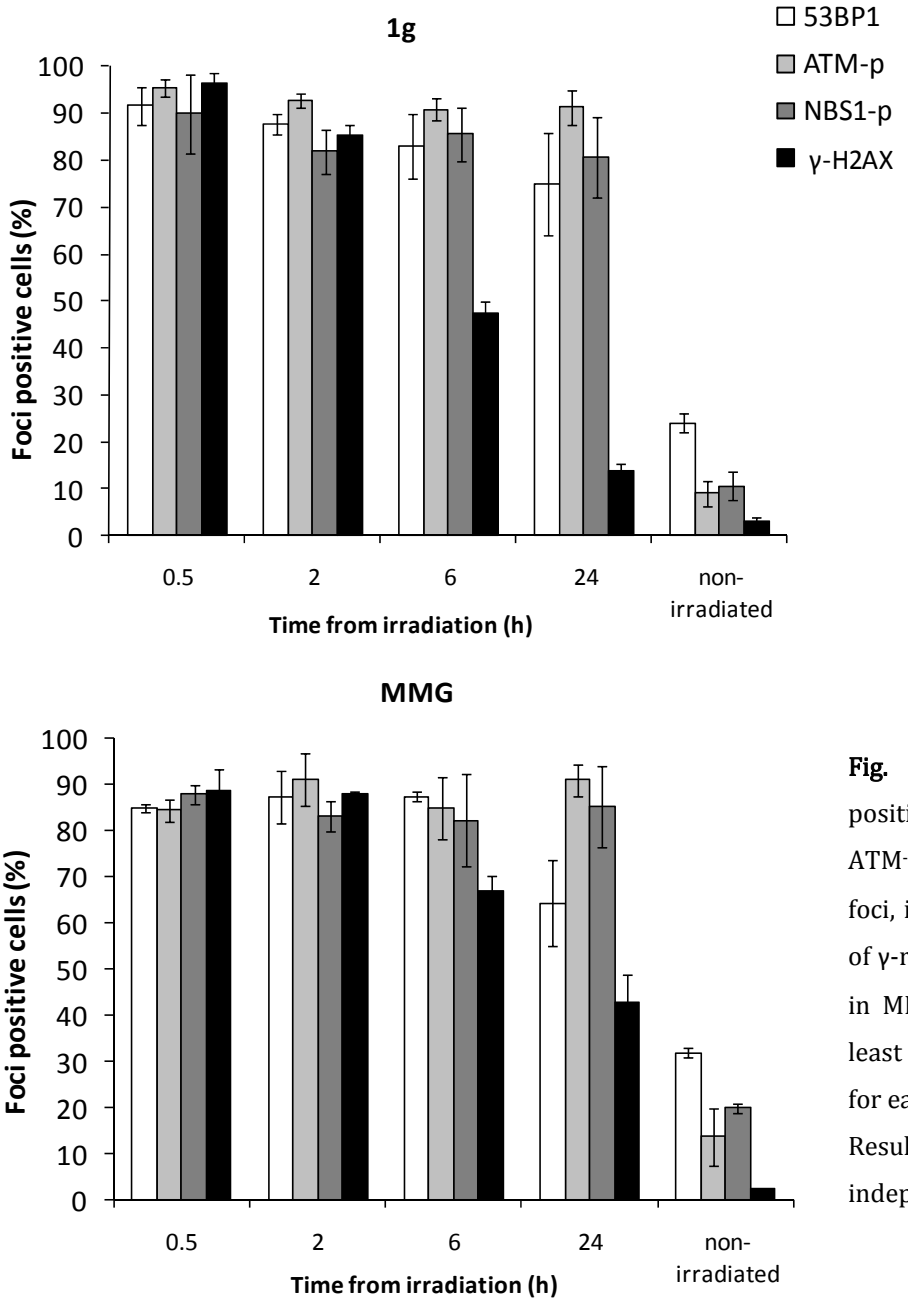

Fig. 14. Percentage of foci-positive cells for 53BP1, ATM^{-p1981}, NBS1^{-p343} and γ-H2AX foci, in PBL irradiated with 5Gy of γ-rays and incubated in 1g or in MMG during repair time; at least 400–500 cells were scored for each time-point.
Results represent the mean of 3 independent experiments±S.E.

Results showed that after irradiation ~90% of cells became foci-positive for the three proteins in both gravity conditions. In contrast to γ-H2AX, the fraction of foci-positive cells persisted high up to 24h after irradiation in 1g and no differences between the two culture conditions were detected (Fig. 14).

As reported in the panel in figure 15, the number of foci/nucleus decreased during post-irradiation incubation from 14–16 foci/nucleus at 30min to 4–5 foci/nucleus at 24h, without differences between samples in 1g and MMG; interestingly, a time-dependent size increase of 53BP1, NBS1^{-p343} and ATM^{-p1981} foci was observed during repair time. The discrepancies with the kinetics of γ-H2AX foci suggest that these proteins could represent the remaining scaffold structure used for DSB repair that persisted after the repair has been completed.

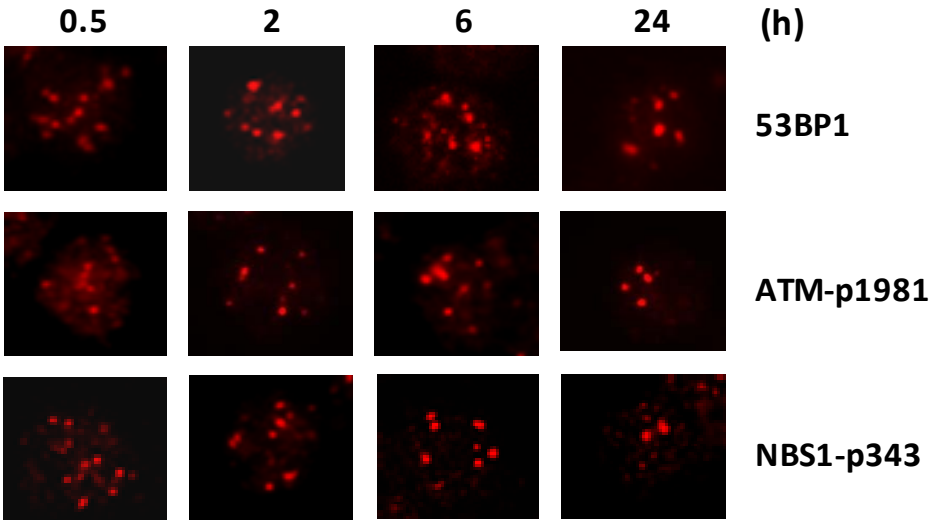

Fig. 15. Recruitment kinetic of signaling proteins to DSB sites. Immunofluorescence results of 53BP1, ATM^{-p1981} and NBS1^{-p343} signaling proteins, in γ-irradiated PBL at 0.5, 2, 6 and 24h after irradiation.

3.4. ANALYSIS OF DSB REPAIR BY PGFE ASSAY

To verify whether the disappearance of γ-H2AX foci correlated with the rejoining of double strand breaks [137], γ-irradiated PBL (10Gy) we subjected to PFGE assay. Firstly, the progression of DSBs repair was analyzed in earth condition (1g) by determining the fraction of DNA released (FR) in the gel at different times during a post-irradiation incubation of 6h. DSB rejoining activity showed a typical biphasic kinetics: FR quickly decreased during the first minutes (60% at 30min), followed by a slower rejoining rate that resulted in a further decrease to 17% of the initial damage (Fig. 16A).

With the same experimental protocol we analyzed the time course of DSB repair in PBL maintained for 2 and 6h in 1g or MMG after irradiation with 10Gy. Fig. 12B shows that, in PBL incubated in MMG, FR was higher than in 1g (77% vs. 33% at 2 h and 50% vs. 17% at 6 h, respectively, $p<0.05$, t-test). To further evaluate DNA rejoining activity in 1g and MMG, the FR was calculated through quantification of DNA remaining in the plug after PFGE with Quant-iTTM method; these FR values confirmed, with minor variations, the OD results: a lower rate of DSB rejoining in PBL incubated in MMG compared to those in 1g (Fig. 16B), in agreement with the kinetics of γ-H2AX foci.

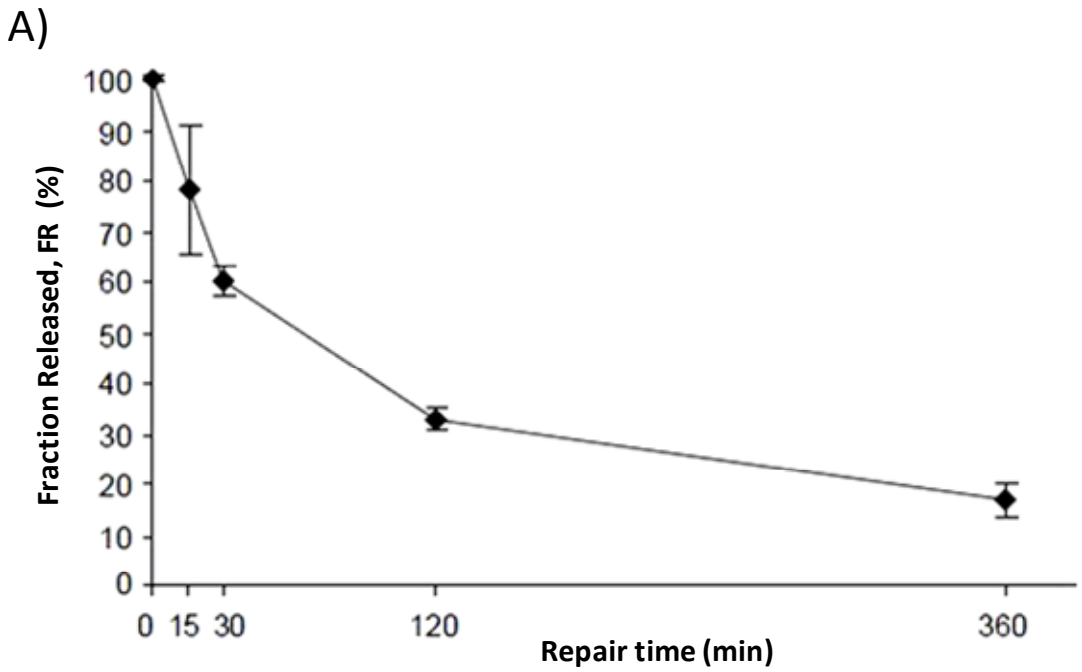

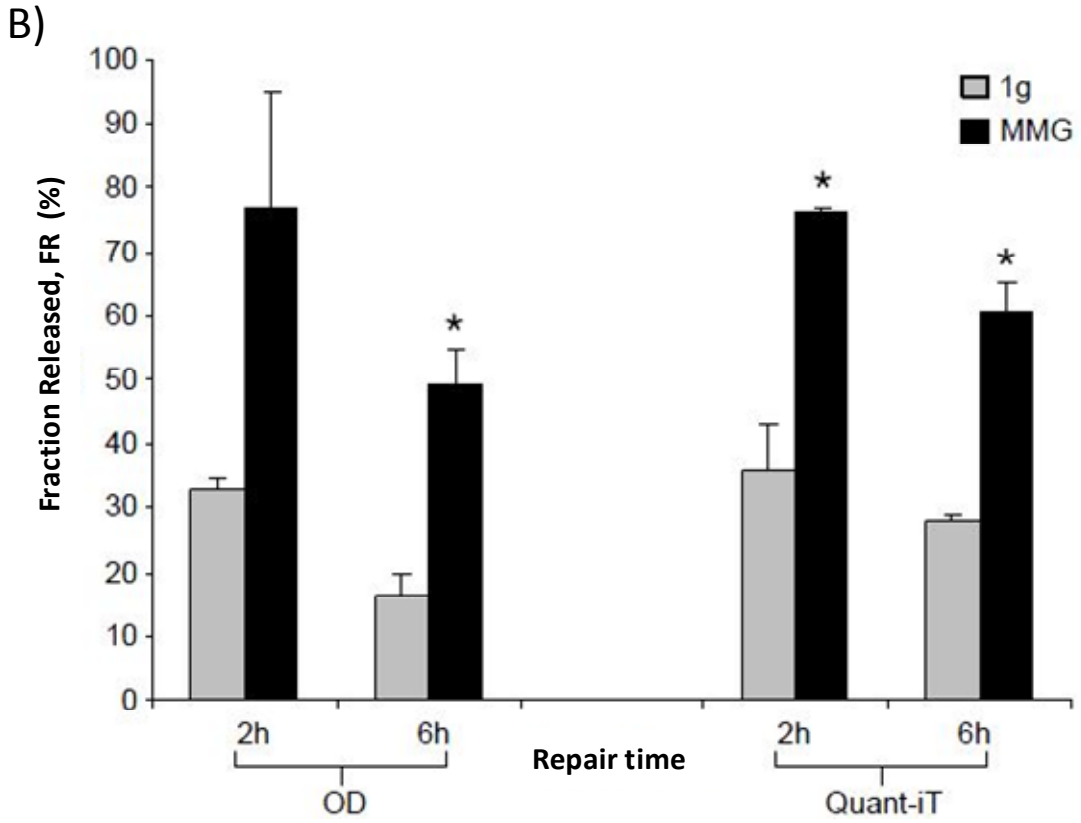

Fig. 16. Fraction of DNA released (FR) from the plugs after PFGE. FR was calculated from OD values of DNA migrating in the gel in PBL irradiated with 10Gy and incubated for 6 h in 1g (A). FR of PBL irradiated with 10Gy and incubated in 1g or MMG calculated from OD values of DNA migrating in the gel or determined by Quant-iT method (B). FR values were reported as percentage of initial damage (time 0). Data points represent means±S.E. of 3–4 determinations. Significant differences were observed between 1g and MMG samples (*$p<0.05$, t-test).

3.5. EXPRESSION OF SIGNALLING/REPAIR PROTEINS

The cellular levels of proteins involved in DSB repair and cell cycle checkpoints, such as p53, $p21^{Waf1}$, Ku70 and RAD51 were determined by western blotting approach in non-irradiated and irradiated PBL incubated for 2, 6 and 24h in 1g and MMG. As reported in Fig. 17A, the expression of both p53 and $p21^{Waf1}$ increased over control cells from 2 and 6h, respectively, after irradiation and persisted up to 24h, without differences between the two culture conditions. The investigation on key components of DSB repair pathways demonstrates that Ku70, of the NHEJ, was constitutively expressed in non-irradiated and irradiated cells at all times considered, whereas RAD51, component of the HR, was absent in G0 lymphocytes. To confirm this observations were performed experiments in non-irradiated and irradiated PBL stimulated to enter in cell cycle with phytohemaglutinin-M (PHA); results showed that RAD51 was always expressed, without differences and in both gravity conditions, in stimulated PBL compared to G0 PBL (Fig. 17B). Thus, in G0 PBL the NHEJ repair pathway is predominantly involved in double strand break repair.

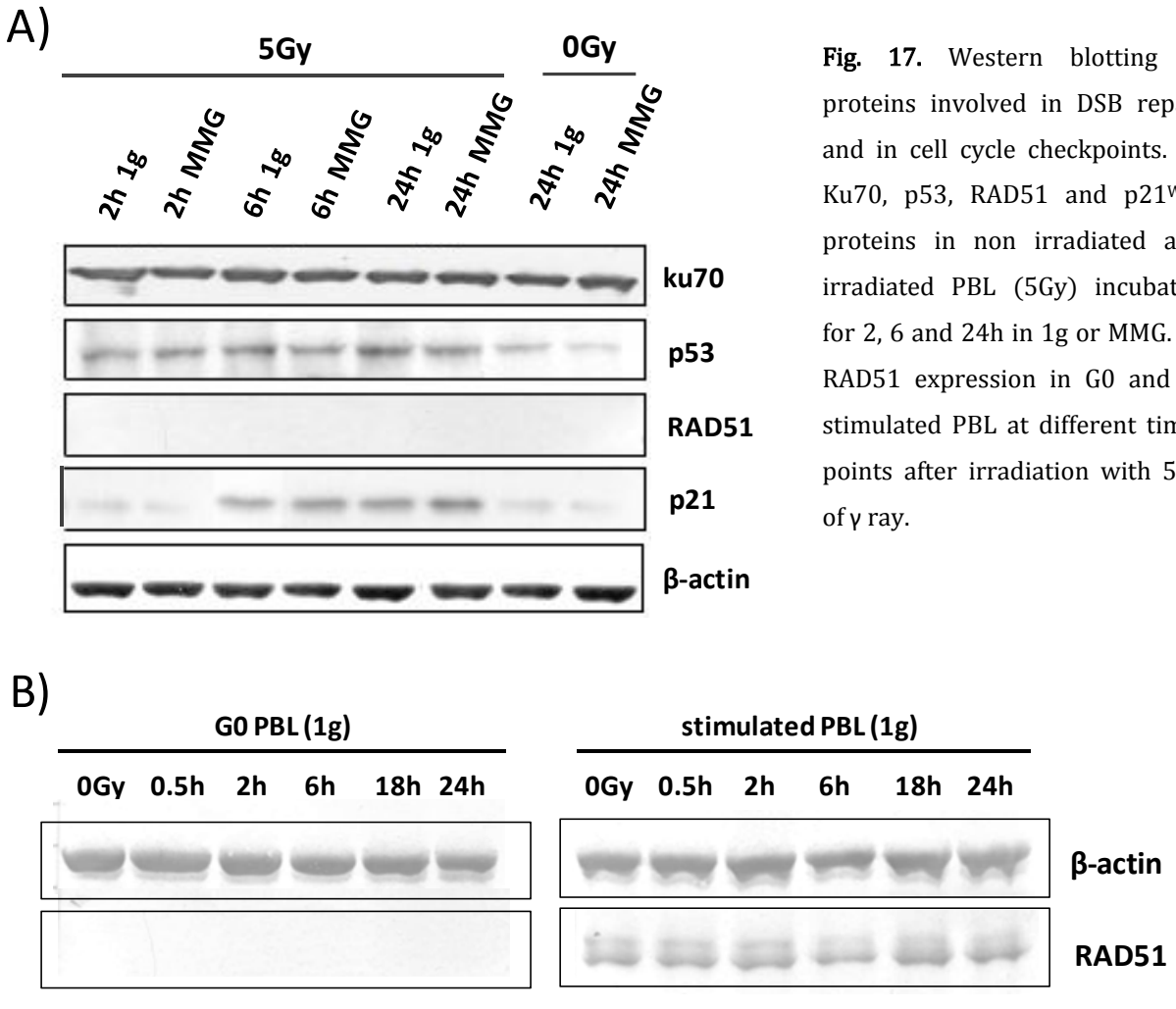

Fig. 17. Western blotting of proteins involved in DSB repair and in cell cycle checkpoints. A) Ku70, p53, RAD51 and $p21^{Waf1}$ proteins in non irradiated and irradiated PBL (5Gy) incubated for 2, 6 and 24h in 1g or MMG. B) RAD51 expression in G0 and in stimulated PBL at different time-points after irradiation with 5Gy of γ ray.

3.6 STUDY OF miRNA EXPRESSION PROFILES WITH MICROARRAY APPROACH

To investigate which miRNAs were de-regulated in response to IR stress, human lymphocytes were isolated from peripheral blood of 12 healthy donors, each donor representing an independent experiment. Peripheral Blood Lymphocytes (PBL) were irradiated with 0.2Gy and 2Gy of γ-rays (6 donors/dose) and, immediately after irradiation, cells were incubated for 4 and 24h in modeled microgravity (MMG) and in parallel ground condition (1g). Non-irradiated PBL were subjected to the same conditions as the irradiated cells. At the end of each incubation time, lymphocytes were collected and the RNA was extracted to perform microarray and RT-qPCR experiments. The miRNA expression profiles were analysed using "*Human miRNA Microarray Kit V2*" (Agilent) that allows the detection of 723 known human miRNA species deposited in the Sanger miRBase (miRBase v.10.1). At the end, significantly changed miRNAs were identified by Significance Analysis of Microarrays (SAM) algorithm using a stringent false discovery rate (FDR<3%). The expression levels of miRNAs were generally similar among PBL of most donors and slight differences were observed according to the inter-individual radio-sensitivity.

• Effects of γ-irradiation on miRNA expression profile of PBL incubated in ground gravity (1g)

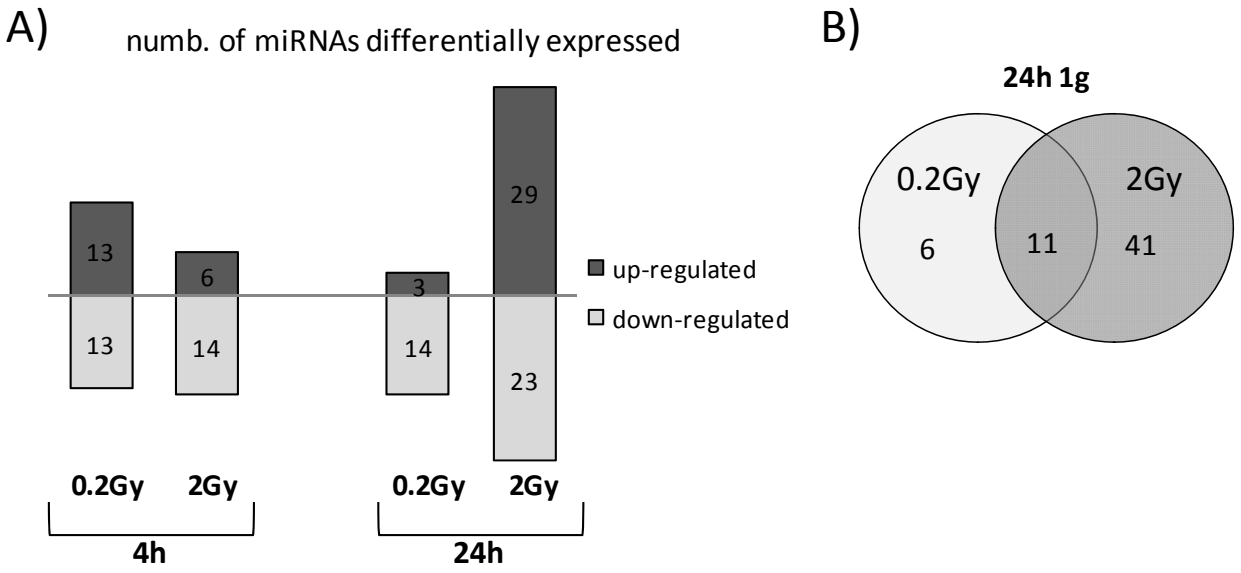

Fig. 18. Effect of ionizing radiation on miRNA expression profile in γ-irradiated PBL incubated in 1g condition. A) Number of miRNAs differentially expressed at 4h and 24h in response to 0.2 and 2Gy of γ-ray. B) Venn diagram showing the number of miRNAs deregulated at 24h after irradiation specific to 0.2 and 2Gy and common to both doses.

The one-class SAM analysis, performed on γ-irradiated PBL samples incubated 4h in 1g, revealed that IR alters the expression of 26 and 20 miRNAs species with 0.2Gy and 2Gy of γ-ray, respectively; at 24h after irradiation: 17 and 52 miRNAs were differentially expressed respectively in 0.2- and 2Gy-irradiated PBL (Fig. 18A), 11 of these were common to both IR doses (Fig. 18B).

Within the radio-responsive miRNAs identified in 0.2Gy- and 2Gy-irradiated PBL, respectively 24 and 44 showed a time-related expression pattern from 4h and 24h after IR, as emerged from the two-class SAM analysis(Fig. 19A and 19B). We noted that there was an evident opposite direction in the change of expression of miRNAs differentially expressed between 4 and 24h after irradiation.

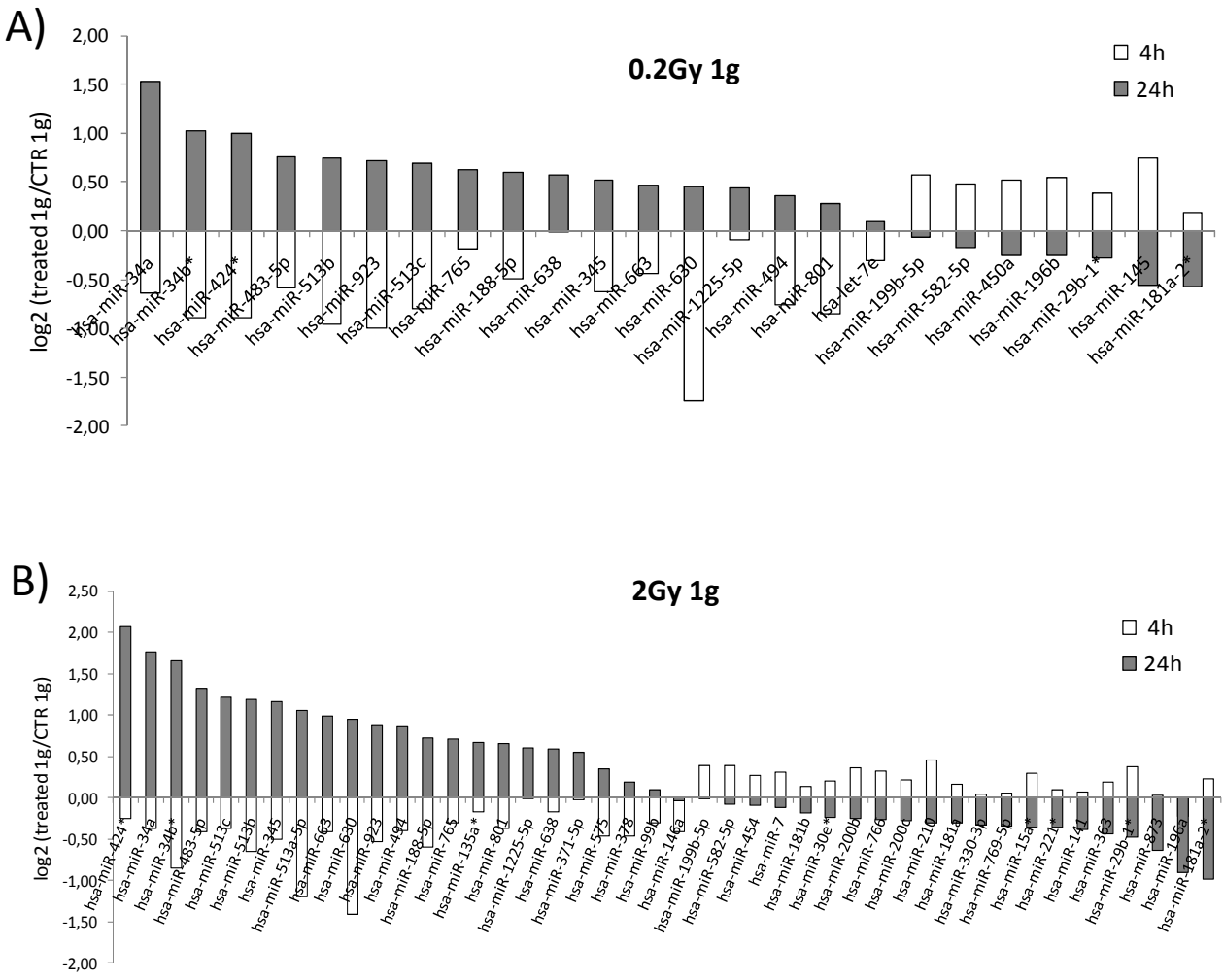

Fig. 19. miRNAs differentially expressed as a function of time after irradiation in 1g condition. *Two class*-SAM analysis of miRNA expression patterns at 4h and 24h shows: A) 24 miRNAs differentially expressed after 0.2Gy and B) 44 miRNAs differentially expres*s*ed after 2Gy. In the bar charts are reported mean values of miRNA expression levels (log_2(treated1g/CTR1g)).

By comparing of the results obtained with the two SAM analysis, 20 miRNA species were found commonly deregulated to both doses, with a substantial down-regulation at 4h and up-regulation at 24h after irradiation (Fig. 20A and 20B).

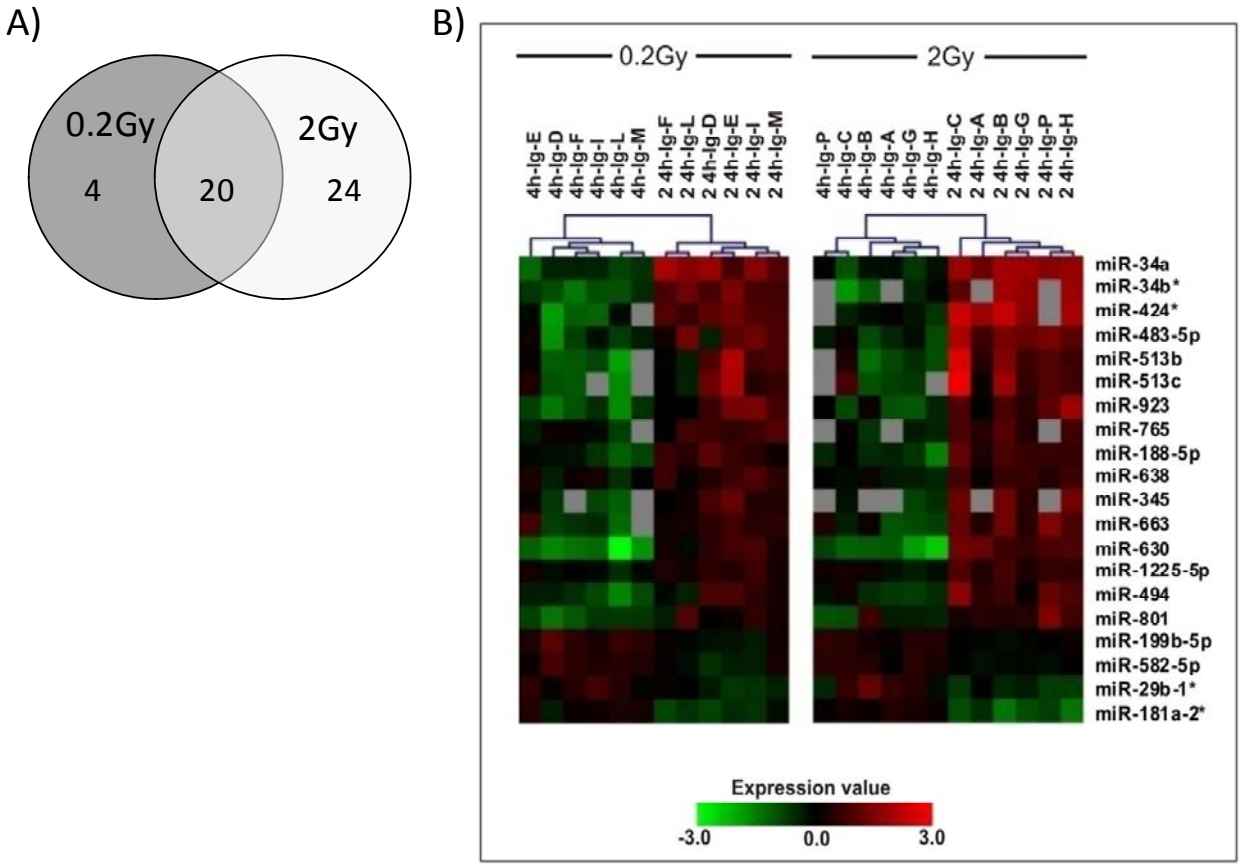

Fig. 20. Time-dependent effect on miRNA expression profile in ground gravity (1g). Two class SAM analysis of miRNAs modulated between 4h and 24h in response to 0.2 and 2Gy of IR. Within the miRNAs differentially expressed, 20 miRNA species were found commonly deregulated with both IR doses. A) Venn diagram showing the number of radio-responsive miRNAs. B) *Two class*-SAM analysis showing a temporal activation program for the 20 common miRNAs. The range of expression values is from -3.0 (green, down-regualtion) to 3.0 (red, up-regulation).

In addition we observed that, for long incubation time, the change in the miRNA expression levels was correlated with the radiation dose, suggesting a dose-dependent effect on miRNA expression profile (Fig. 21).

On the whole, our results showed that miRNA expression may be altered in response to ionizing radiation with a dose- and time-dependent effect; indeed, early after irradiation both doses induced consistent changes, whereas late after irradiation, the effects of the higher dose predominated, not only in terms of number but also in terms of expression levels.

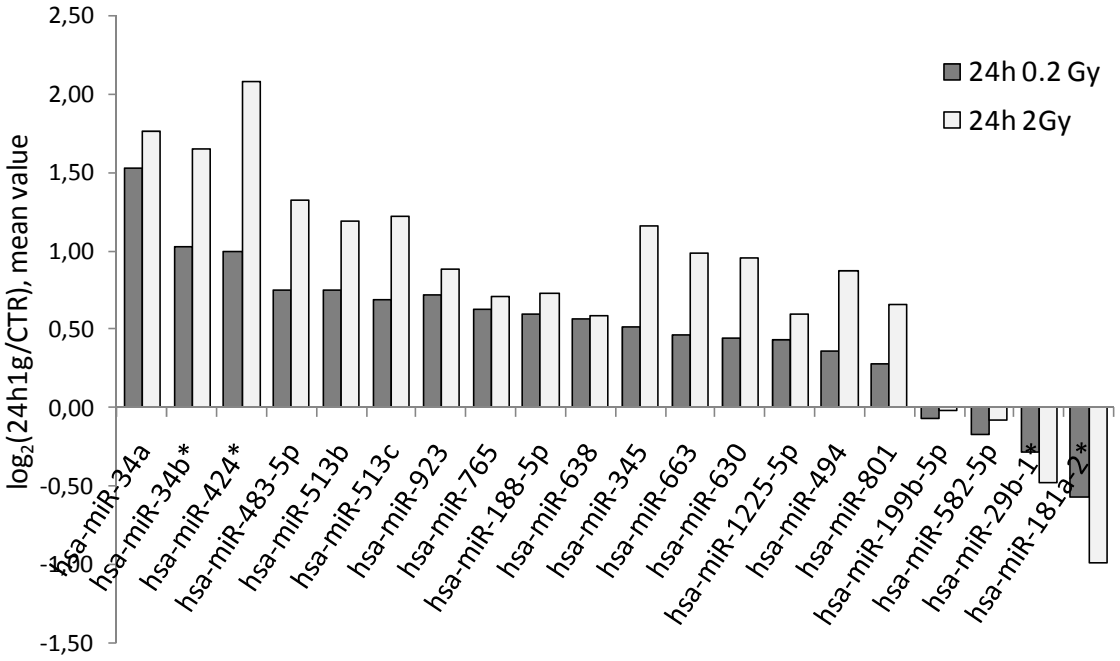

Fig. 21. Dose-dependent effect on miRNA expression profile. In the bar chart are reported the 20 common miRNAs and their expression levels (mean values) at 24h after irradiation.

• Effects of Modeled Microgravity (MMG) on miRNA expression profile in PBL irradiated and not

To investigate the role of MMG on miRNA expression profile in response to ionising radiation, first of all, we analysed the expression profiles of not-irradiated PBL incubated 24h in MMG (12 samples). With a *one class*-SAM analysis we identified 42 differentially expressed miRNAs in MMG respect to 1g condition: 25 up-regulated and 17 down-regulated; three of these miRNAs were deregulated with a > 2.4-fold change (miR-9, miR-9*, miR-155). Then, we analysed the expression profile of γ-irradiated PBL after MMG incubation. Performing *one class*-SAM analysis in 0.2Gy PBL we identified 16 and 4 differentially expressed miRNAs, respectively at 4 and 24h; at the same time points, 22 and 33 miRNAs resulted differentially expressed in 2Gy PBL. Our results showed that, in both gravity conditions the dose-effect was predominant at 24h after irradiation but, a general decrease of radio-responsive miRNAs was evident in MMG respect to 1g (Fig. 22A). With a Venn diagram (Fig. 22B) we summarized the number of miRNAs common and exclusively deregulated at 24h, as a consequence of: only irradiation with both doses in 1g, only MMG incubation, 0.2 and 2Gy irradiation combined with MMG. Only 16 of the 42 miRNAs

modulated by MMG were common to the radio-responsive miRNAs in 1g and MMG. There were no miRNAs altered by the combination of IR and MMG in 0.2Gy-irradiated PBL; in fact, miR-99b was equally modulated by 0Gy- and 0.2Gy-MMG. On the contrary, at a higher dose of IR, 5/9 miRNAs were found altered by the combination with MMG: miR-27a, miR-184, miR-598, miR-144, miR-650; the others appeared to be activated also in 0Gy-MMG PBL, with a >1.1-fold change and repressed in association with IR , with a ~1.4-fold change of down-regulation (let-7i*, miR-7, miR-200a, miR-7-1*). The lists of significantly deregulated miRNAs in each condition are reported in the Appendix 1 and 2.

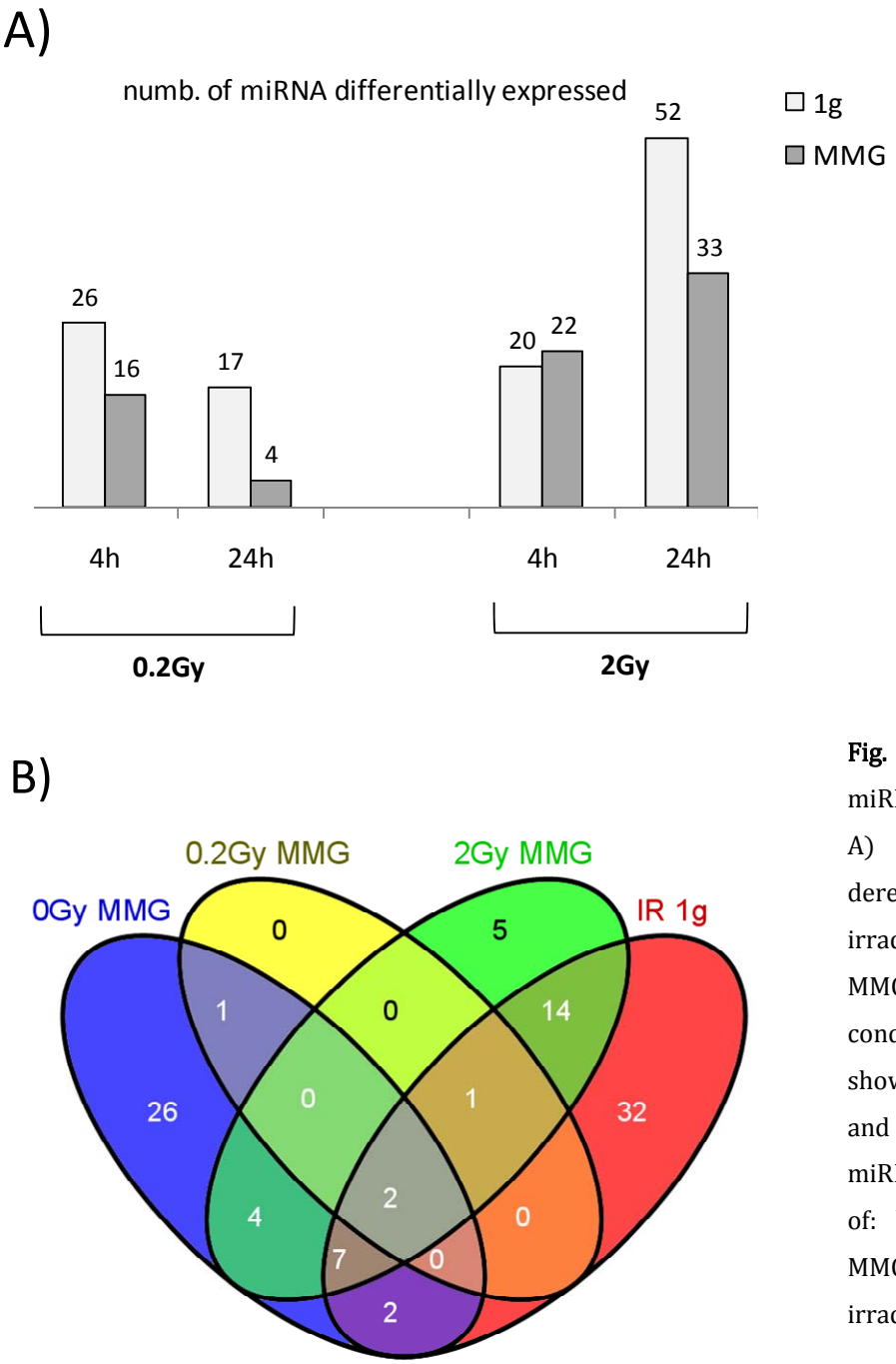

Fig. 22. Microgravity effect on miRNA expression profiles. A) Number of significantly deregulated miRNAs in γ-irradiated PBL at 4h and 24h in MMG compared with 1g condition. B) Venn diagram shows the number of common and exclusively deregulated miRNAs at 24h, as consequence of: both IR-doses in 1g, only MMG incubation, 0.2 and 2Gy irradiation combined with MMG.

3.7 VALIDATION OF miRNA EXPRESSION WITH RT-qPCR (TaqMan®)

To confirm the microarray-generated expression profiles of the radio-responsive miRNAs in 1g and MMG, we carried out real time-quantitative PCR (RT-qPCR) experiments for six miRNAs: miR-9, miR-27a, miR-34a, miR-181a-2*, miR378 and miR-424*. The microarray data indicated that miR-9 and miR-378 were respectively up- and down-regulated only in response to 24h-incubation in MMG, whereas miR-27a was specifically up-regulated in response to IR-treatment in MMG. miR-424* and miR-181a-2*, were respectively highly up- and down-regulated at 24h after irradiation in 1g and in 2Gy-MMG samples. We selected also miR-34a, which was up-regulated in response to IR with a >2.4-fold change in both gravity conditions; previous studies indicated that miR-34a is directly transactivated by p53 in response to stress signals, and increases its activity promoting apoptosis [107, 111]. The miRNA expression values were normalized to the U48 small nuclear RNA (RNU48) which was used as endogenous control, since it is both abundantly and stably expressed; then, we calculated the expression levels relative to the control (un-treated PBL) using the $2^{\Delta\Delta Ct}$ (RQ, relative quantification) method, implemented in the 7500 Real Time PCR System software [77, 78, 138, 139]. As reported in the bar charts (Fig. 23A and 23B), for each candidate miRNA, the RT-qPCR study revealed patterns of up- and down-regulation similar to those observed in the microarray analysis. In the Appendix 3 are reported the RT-qPCR data analysis and the box-plots obtained with the statistic program R.

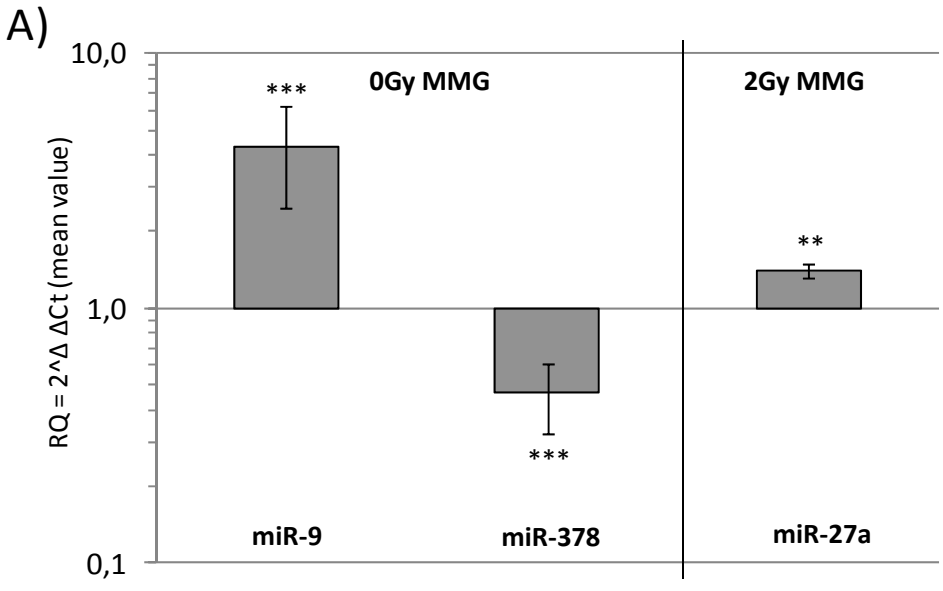

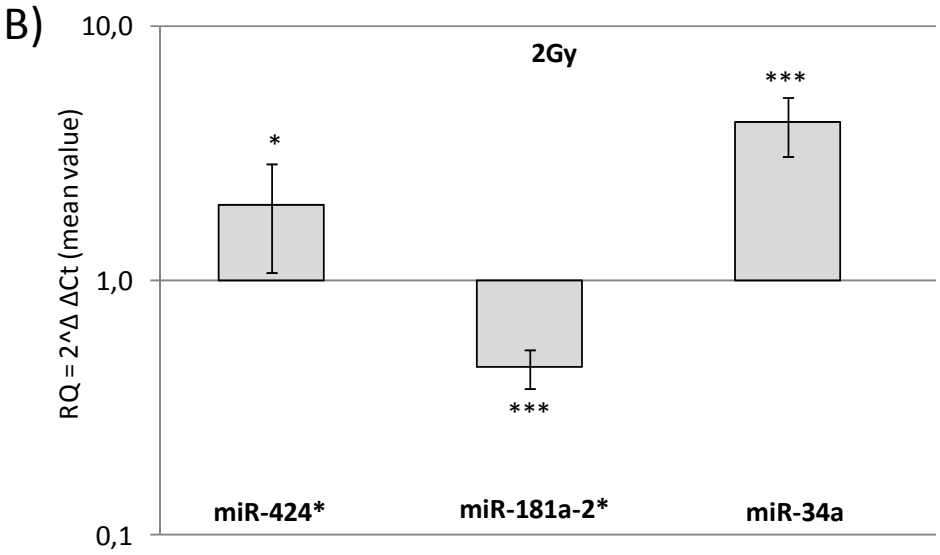

Fig. 23. RT-qPCR analysis of miRNA expression in human peripheral blood lymphocytes. In the bar charts are reported the expression levels relative to the control (un-treated PBL) calculated through the $2^{\Delta\Delta Ct}$ method. A) miR-9 (up-regulated) and miR-378 (down-regulated) in PBL incubated 24h in MMG condition; miR-27a (up-regulated) in 2Gy-MMG samples. B) miR-34a, miR-424* (up-regulated) and miR-181a-2* (down-regulated) in γ-irradiated PBL and maintained 24h in 1g or MMG conditions. Results represent $2^{\Delta\Delta Ct}$ mean values of 4–6 sample donors±S.D, each donor was analyzed with four replicates. All miRNAs are significant with ***$p<0.001$ or **$p<0.01$, only miR-424* is moderately significant (*$p<0.05$).

3.8 miRNA TARGETS PREDICTION

To identify target genes of the radio-responsive miRNAs in 1g and MMG, a preliminary computational analysis was performed to detect putative target mRNAs having functions related to: apoptosis, cell cycle control, DNA damage signaling and repair, immune cell differentiation and activation; since these pathways represent the main response observed in irradiated cells in ground gravity and microgravity.

PITA is the algorithm used in this study for identifying potential targets, it looks for the presence of miRNA "seed-region" binding sites in the 3'UTR of mRNAs, considering also the thermodynamic stability of the RNA-RNA duplex. Since molecular basis of miRNA-target interaction are still poorly understood, all target prediction methods suffer of large fraction of false positives (false discovery rate, FDR); for this reason, target identification requires extensive experimental validation. Based on the evidence that miRNAs tend to down-regulate target genes with a mechanism of mRNA degradation or translational repression, miRNA expression profiles and miRNA target predictions were integrated with gene target expression profiles. Therefore, the integrated analysis compared miRNA and mRNA target expression levels determined on the same PBL samples; miRNA-mRNA direct interactions were expected to be anti-correlated, that means opposite expression levels.

Gene expression profiles were studied in the PBL samples irradiated with 2Gy of γ-ray incubated 24h in 1g or MMG and in the respectively not-irradiated samples; since for this dose and time point miRNA deregulations were more consistent and thus useful to appreciate differences between 1g and MMG conditions. In addition, our previous results demonstrated that cell survival, DSB repair, mutant frequency and apoptosis were affected in γ-irradiated PBL incubated 24h in MMG [135, 140]. mRNA expression profiles were analyzed using "*Whole Human Genome Oligo Microarray*" (Agilent) consisting in oligonucleotide probes representing the human genome (~41.000 genes and transcripts); significantly altered mRNAs were identified by Significance Analysis of Microarrays (SAM) algorithm using a stringent false discovery rate (FDR<3%).

• Gene expression profiles of 2Gy-irradiated PBL incubated in 1g and MMG

The study was carried out on 0Gy- and 2Gy-PBL samples (6 donors) incubated 24h in 1g and MMG. For each gene, expression level alterations were calculated by comparing the ratio in irradiated samples with the corresponding un-irradiated; significant deregulated

mRNAs were identified performing a *one class*-SAM analysis (FDR<3%). As reported in the Venn diagram (Fig. 24) the expression of 488 and 550 transcripts was altered respectively in 2Gy 1g and 2Gy MMG samples, 164 of these were in common. With SAM analysis of un-irradiated PBL incubated in MMG were detected 543 mRNAs significantly altered, 48/543 were also radio-responsive in 1g and MMG.

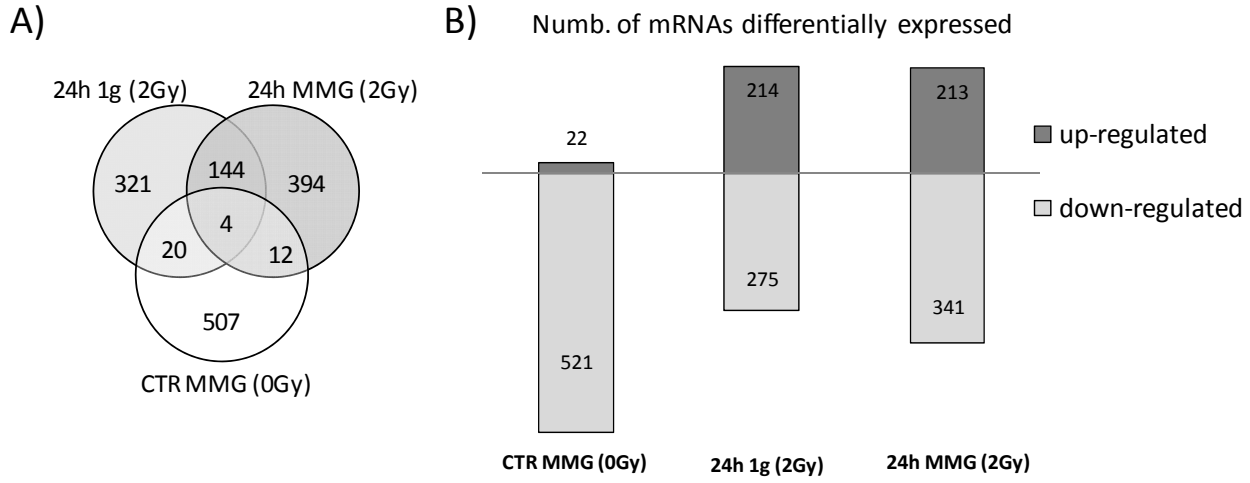

Fig. 24. Number of significant deregulated mRNAs obtained with a one class-SAM analysis (FDR<3%). A) Venn diagram representing the number of modulated genes, exclusively or common, in unirradiated PBL incubated 24h in MMG, 2Gy-irradiated PBL at 24h 1g and MMG. B) Bar chart showing the distribution of significant deregulated mRNAs in up- and down-regulated.

• Anti-correlation analysis of miRNA- and mRNA-expression data

In order to understand the mechanism through which radio-responsive miRNAs may modulate biological functions, in modeled microgravity respect to ground gravity, it was necessary to improve the detection of functional miRNA-mRNA relationships. MAGIA (MiRNA And Genes Integrated Analysis) web tool [141] was used to integrate miRNA expression profiles, PITA target predictions and mRNA expression profiles; to estimate the degree of anti-correlation between any putative pairs of miRNA and mRNA was used a Spearman correlation index <-0.775, that means opposite miRNA- and mRNA-expression levels. The complete lists of miRNA-mRNA anticorrelated in 2Gy 1g PBL and 2Gy MMG PBL are reported in the Appendix 3.

Finally, the anti-correlated transcripts were classified according to *DAVID* (Database for Annotation, Visualization and Integrated Discovery) web tool [142], to determine which Gene Ontology (GO) terms were significantly enriched in our set of genes in relation to the different stressor. Were selected only significantly enriched GO Biological Processes (level 3) with a p-value <0.05 (Fig. 25).

Gene Ontology functional categories significantly enriched (*DAVID*)		
0Gy, 24h in MMG	**2Gy, 24h in 1g**	**2Gy, 24h in MMG**
defense response		
lipid methabolic process	regulation of cell proliferation	
membrane invagination	regulation of cell cycle	
endocytosis	regulation of cell death	
cell morphogenesis	lymphocytes activation	
cellular component morphogenesis	programmed cell death	
macromolecular complex morphogenesis	regulation of biological process	
regulation of mediated vesicle tansport	cellular response to stress	regulation of immune system process
mediated vesicle-transport	response to wounding	regulation of cell activation
cellular transport	response to DNA damage stimulus	hemopoietic or lymphoid organ development
cell projection morphogenesis	cell cycle phase	regulation of leukocyte activation
phagocytosis, recognition	cell cycle arrest	regulation of cytokine production
regulation of developmental processes	G1/S transition of mitotic cell cicle	regulation of cell differentiation
carbohydrate metabolic process	G2/M transition of mitotic cell cicle	negative regulation of antigen-receptor mediated signaling
cell motility	mitotic metaphase progression	positive regulation of immune response
cell projection assembly	cell structure disassembly during apoptosis	positive regulation of response to stimulus
	chemotaxis	

Fig. 25. Gene Ontology analysis of anti-correlated mRNAs performed with DAVID database. Table reporting common and specific biological processes found enriched ($p<0.05$) in: unirradiated PBL incubated 24h in MMG, 2Gy-irradiated PBL incubated 24h in 1g and MMG.

Genes deregulated at 24h in 2Gy-irradiated PBL incubated either in 1g or MMG were commonly associated to: positive and negative regulation of biological process, cell proliferation, regulation of cell death and lymphocytes activation. The over-represented functional categories in irradiated PBL incubated in 1g were those of: response to DNA damage, response to stress and wounding, cell cycle, cell cycle check-points and chemotaxis. On the contrary, in irradiated PBL incubated in MMG were predominant immune system-related categories, such as: leukocyte activation, regulation of cell differentiation, regulation of cell activation, cytokine production, negative regulation of antigen-receptor mediated signaling pathway, hemopoietic and lymphoid organ development; all characterized by many under-expressed transcripts. Interestingly, categories of cellular

response to stress and response to DNA damage were not enriched, most likely because IR in MMG affects the miRNA-mediated gene regulation compared with 1g. With the same approach, were also analyzed the un-irradiated PBL incubated 24h in MMG to figure out the effect of weightlessness at cellular level; the GO functional categories found significantly enriched in these samples were associated to: cell metabolism (lipid metabolic process, carbohydrate metabolic process), transport (endocytosis, regulation of vesicle-mediated transport), cell mobility, cell morphogenesis and cell projection assembly.

At the end, to study the effect of simulated space environment on human cells, pathway-enrichments analysis was carried out on the anti-correlated mRNAs in irradiated PBL incubated in 1g and MMG. Using *KEGG* web tool, which is present in *DAVID* database [142], biological pathways mainly involved in the cell response were determined with a p-value <0.05.

Enriched biological pathways (KEGG, p<0.05)			
2Gy, 24h in 1g	*p*-value	**2Gy, 24h in MMG**	*p*-value
p53 signaling pathway	1.6E-11	Cell cycle	1.3E-5
		p53 signaling pathway	4.6E-5
Cell cycle	2.8E-5	Natural killer cell mediated cytotoxicity	1.2E-4
		Antigen processing and presentation	1.1E-3
Natural killer cell mediated cytotoxicity	4.3E-7	T cell receptor signaling pathway	5.8E-3
		Primary immunodeficiency	1.1E-2
Cytokine-cytokine receptor interaction	6.5E-4	B cell receptor signaling pathway	1.1E-2
		Apoptosis	2.2E-2
Pathways in cancer	1.5E-2	Pathways in cancer	3.7E-2
		Toll-like receptor signaling pathway	4.2E-2

Fig. 26. Pathway-enrichments analysis performed with KEGG-DAVID database ($p<0.05$). Table reporting biological pathways enriched for the mRNAs anti-correlated in 2Gy-irradiated PBL incubated 24h in 1g and in MMG. Pathways are showed on the base of their p-value.

As reported in the table (Fig. 26), ionizing radiation exposure induces expression profile changes of many genes belonging to p53-signaling pathway, cell cycle and cell mediated cytotoxiciy, in both gravity conditions; although, in irradiated PBL incubated in MMG were predominant biological pathways related to the immune system, such as: antigen processing and presentation, T and B cell receptor signaling, Toll-like receptor signaling and immunodeficiency. These observations are in agreement with studies reported in literature describing impaired immune system function in astronauts [116, 118].

3.9 PATHWAY-ENRICHMENTS ANALYSIS

The Pathway-enrichments analysis was carried out to investigate and compare the alterations occurring on cellular pathways in response to γ-irradiation in both gravity conditions; in particular, were studied two of the main biological pathways involved in radiation cell response: p53-signaling pathway and cell cycle pathway, which were found significantly modulated in our samples.

•p53-signaling pathway

The Tumor Protein p53 is a sequence-specific transcription factor. Various cellular stresses, such as DNA damage, hypoxia and nutrient deprivation can activate p53 function via effects on p53 stability, nuclear localization and its interactions with other proteins, resulting in p53-stimulated transcription of a hundred or more genes [143]. The p53-regulated genes encode proteins sharing functions in regulation of cell cycle progression, DNA repair, apoptosis, angiogenesis and in feedback regulation of p53 function [144]. Among the stress signals activating p53, ionizing radiation causes the DNA double-strand breaks (DSBs); these are followed by the phosphorylation and stabilization of p53 by activated Ataxia-Telangiectasia Mutated (ATM), a nuclear protein kinase main transducer of DSB signals [145]. The activated p53 selectively induces cell cycle arrest or apoptosis [146]. These serial processes are controlled by DNA damage checkpoint pathways which inhibit the cell cycle progression through G1 and G2 phases and delay the cell cycle in irradiated cells [147].

Performing the Pathway-enrichments analysis, p53-signaling pathway was found significantly enriched in response to γ-irradiation in both gravity conditions, although many genes differed between 1g and MMG for type and anti-correlated miRNAs (Fig. 27 and 28). Our results showed that, 13 and 10 transcripts belonging to p53-signaling pathways were significantly deregulated respectively in 1g and MMG; among these genes: CDKN1A (p21) and
CCNG1 (cyclin G1) transcripts, inducing cell cycle arrest respectively in G1 and G2 phases, were significantly anti-correlated only in 1g. Among miRNAs targeting these transcripts, miR-873, miR-181a-2* and miR-188-5p were similarly deregulated in MMG. miR-200b was differentially expressed only in 1g, where it targeted CDKN2A. SESN1, which is involved in cell cycle arrest, was induced (~2.57 fold change) only in 1g and targeted by miR-188-5p,

miR-34a, miR-483-5p, miR-513b, miR-19b; the first three miRNAs were differentially expressed also in MMG. The genes CCND2, CDC2, EI24 and MDM2 were found commonly altered in both gravity condition, although in some cases miRNAs associated were different.

Fig. 27. p53-signaling pathway found enrich in 2Gy-irradiated PBL in 1g. A) Table reporting the 13 mRNAs altered in p53-signaling pathway and the anti-correlated radio-responsive. B) Biological pathway scheme, significantly deregulated genes are indicated with a red star. Analysis performed with KEGG-DAVID

A)

2Gy 1g: modulated transcripts in p53-signaling pathway		
mRNA	**Description**	**miRNA**
BBC3	BCL2 binding component 3	hsa-miR-371-5p
		hsa-miR-877*
BCL2L11	BCL2-like 11 (apoptosis facilitator)	hsa-miR-345
CCNG1	cyclin G1	hsa-miR-188-5p
CCND2	cyclin D2	hsa-miR-371-5p
		hsa-miR-424*
		hsa-miR-574-5p
		hsa-miR-765
		hsa-miR-877*
CDC2	cell division cycle 2, G1 to S and G2 to M	hsa-miR-345
CDKN1A	cyclin-dependent kinase inhibitor 1A (p21, Cip1)	hsa-miR-17
		hsa-miR-873
CDKN2A	cyclin-dependent kinase inhibitor 2A	hsa-miR-200b
DDB2	damage-specific DNA binding protein 2	hsa-miR-877*
EI24	etoposide induced 2.4 mRNA	hsa-miR-100
GADD45A	growth arrest and DNA-damage-inducible, alpha	hsa-miR-200b
MDM2	transformed 3T3 cell double minute 2	hsa-miR-34a
PPM1D	protein phosphatase 1D magnesium-dependent	hsa-miR-371-5p
		hsa-miR-630
		hsa-miR-877*
SESN1	sestrin 1	hsa-miR-188-5p
		hsa-miR-34a
		hsa-miR-483-5p
		hsa-miR-513b
		hsa-miR-19b

B)

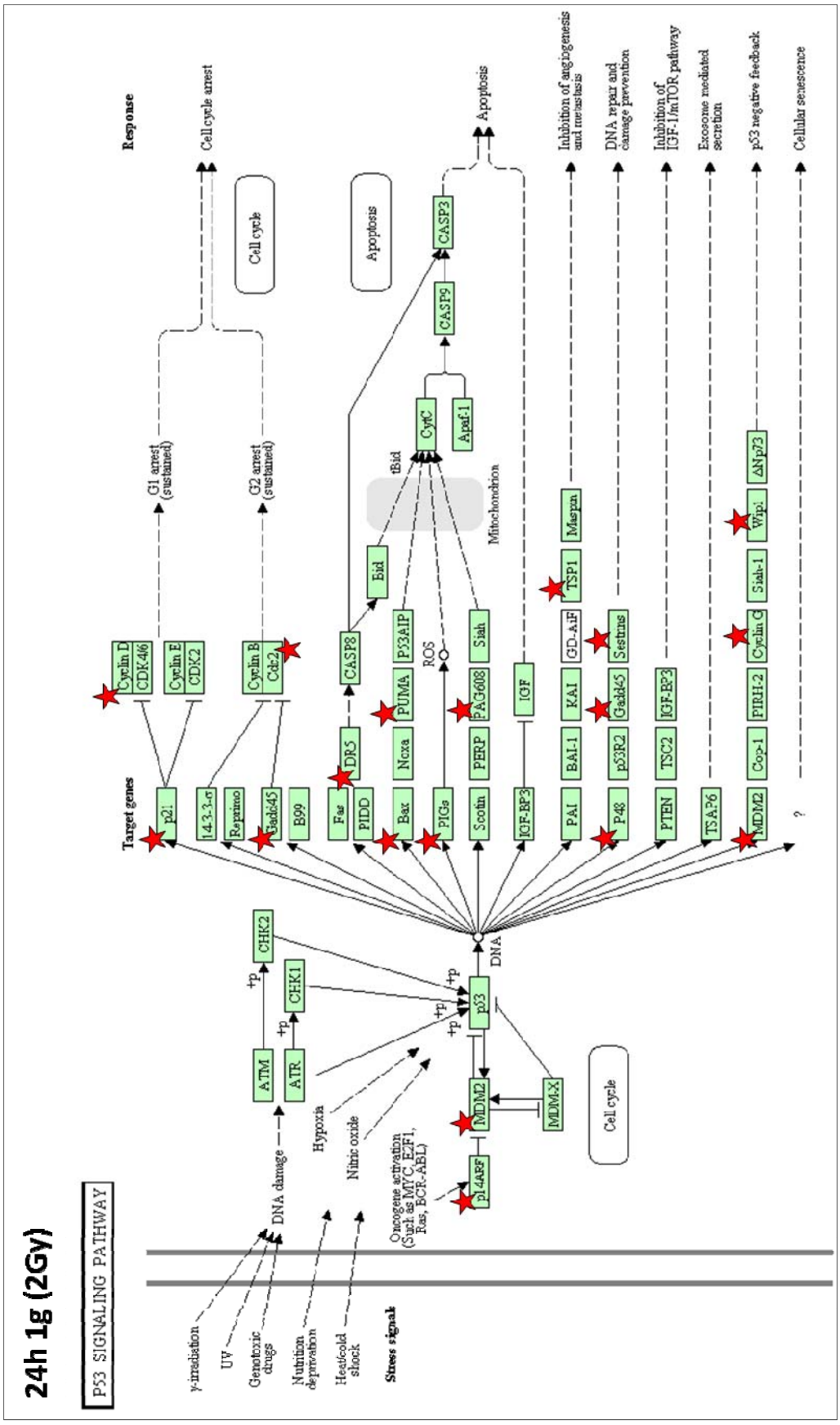
24h 1g (2Gy)
P53 SIGNALING PATHWAY
Response
Cell cycle arrest
Cell cycle
Apoptosis
Inhibition of angiogenesis and metastasis
DNA repair and damage prevention
Inhibition of IGF-1/mTOR pathway
Exosome mediated secretion
p53 negative feedback
Cellular senescence
G1 arrest (sustained)
G2 arrest (sustained)
Target genes
p21
14-3-3-σ
Reprimo
Gadd45
B99
Fas
PIDD
DR5
Bax
Noxa
PUMA
PIGs
Scotin
PERP
P53AIP
PAG608
Siah
IGF
IGF-BP3
PAI
BAI-1
P48
p53R2
KAI
Gadd45
GD-AIF
Sestrins
TSP1
Maspin
PTEN
TSC2
IGF-BP3
TSAP6
MDM2
Cop-1
PIRH-2
Cyclin G
Siah-1
Wip1
ΔNp73
?
Cyclin D
CDK4/6
Cyclin E
CDK2
Cyclin B
Cdc2
CASP8
Bid
tBid
CytC
Apaf-1
CASP9
CASP3
Mitochondrion
DNA
p53
MDM2
MDM-X
p14ARF
ATM
ATR
CHK2
CHK1
+p
DNA damage
Hypoxia
Nitric oxide
Oncogene activation (Such as MYC, E2F1, Ras, BCR-ABL)
Cell cycle
Stress signal
γ-irradiation
UV
Genotoxic drugs
Nutrition deprivation
Heat/cold shock
ROS

Fig. 28. p53-signaling pathway found enrich in 2Gy-irradiated PBL in MMG. A) Table reporting the 10 mRNAs altered in p53-signaling pathway and the anti-correlated radio-responsive miRNAs. B) Biological pathway scheme, significantly deregulated genes are indicated with a red star. Analysis performed with KEGG-DAVID database ($p<0.05$).

A)

2Gy MMG: modulated transcripts in p53-signaling pathway		
mRNA	**Description**	**miRNA**
ATM	ataxia telangiectasia mutated	hsa-miR-34b*
		hsa-miR-27a
BAX	BCL2-associated X protein	hsa-miR-144
		hsa-miR-200a
		hsa-miR-200a
		hsa-miR-650
		hsa-miR-598
		hsa-miR-144
CCND2	cyclin D2	hsa-miR-345
		hsa-miR-494
		hsa-miR-513c
		hsa-miR-135a*
		hsa-miR-923
		hsa-miR-424*
CDC2	cell division cycle 2, G1 to S and G2 to M	hsa-miR-345
		hsa-miR-494
EI24	etoposide induced 2.4 mRNA	hsa-miR-345
		hsa-miR-513c
		hsa-miR-940
		hsa-miR-873
GADD45B	growth arrest and DNA-damage-inducible	hsa-miR-34b*
		hsa-miR-135a*
		hsa-miR-923
		hsa-miR-494
MDM2	transformed 3T3 cell double minute 2	hsa-miR-34b*
		hsa-miR-663
		hsa-miR-494
RRM2B	ribonucleotide reductase M2 B (TP53 inducible)	hsa-miR-196b
		hsa-miR-940
TNFRSF10B	tumor necrosis factor receptor superfamily, member 10b	hsa-miR-650
		hsa-miR-7-1*
		hsa-miR-886-3p
		hsa-miR-7
		hsa-miR-144
		hsa-miR-363
TP53	tumor protein p53	hsa-miR-200a
		hsa-miR-95
		hsa-miR-181a-2*
		hsa-miR-598

B)

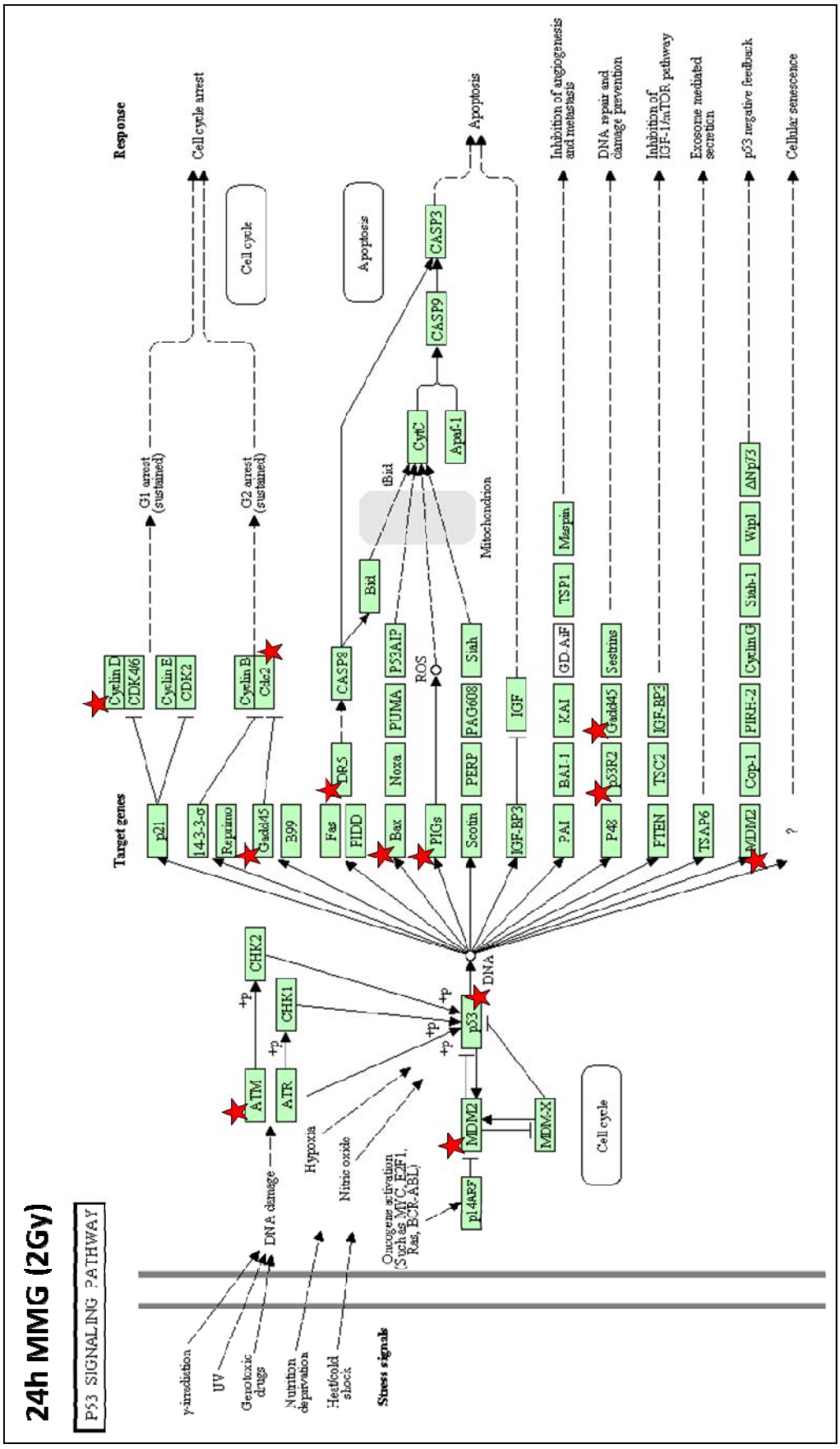
24h MMG (2Gy)
P53 SIGNALING PATHWAY
Response
Cell cycle arrest
Apoptosis
Inhibition of angiogenesis and metastasis
DNA repair and damage prevention
Inhibition of IGF-1/mTOR pathway
Exosome mediated secretion
p53 negative feedback
Cellular senescence
Cell cycle
Apoptosis
G1 arrest (sustained)
G2 arrest (sustained)
Target genes
p21
14-3-3-σ
Reprimo
Gadd45
14-3-3
Fas
FIDD
DR5
Bax
Noxa
PUMA
PIGs
P53AIP
PERP
PAG608
Scotin
Siah
IGF
IGF-BP3
BAI-1
PAI
KAI
GD-AF
TSP1
Maspin
P53R2
P48
Gadd45
Sestrins
TSC2
PTEN
IGF-BP3
TSAP6
Cop-1
PIRH-2
MDM2
Cyclin G
Siah-1
Wip1
ΔNp73
Cyclin D
CDK4/6
Cyclin E
CDK2
Cyclin B
Cdc2
CASP8
Bid
tBid
CytC
Apaf-1
CASP9
CASP3
Mitochondrion
ROS
DNA
p53
CHK2
CHK1
ATM
ATR
+p
MDM2
MDM-X
p14ARF
DNA damage
Hypoxia
Nitric oxide
Oncogene activation (Such as MYC, E2F1, Ras, BCR-ABL)
Stress signals
γ-irradiation
UV
Genotoxic drugs
Nutrition deprivation
Heat/cold shock

- **Cell cycle pathway**

Although chemical and physical agents may initiate cell damage or stress, the cellular proteins that are involved in control of cell cycle and apoptosis are the final regulators of cell fate. The biochemical pathways involved in cell cycle transition and/or inducing cell death after stress are known as cell cycle checkpoints. Cells can arrest at different checkpoints temporarily to allow: cellular damage repair, dissipation of exogenous cellular stress signal, availability of growth factors or nutrients [148]. The G1/S checkpoint consists in the negative regulation of G1 phase cyclin/Cdk complexes. Cdks are negatively regulated by a group of functionally-related proteins called Cdk inhibitors which fall in two groups: INK4 inhibitors (p16, p15, p19, p18) and the Cip/Kip inhibitors (p21, p27, p57), when they bind to cyclin/Cdk complexes the progression of cells from G1 to S phase is blocked [149, 150]. The G2 checkpoint consists in biochemical pathways involved in the DNA damage-induced G2 arrest that converge to inhibit the activation of Cdc2. During S and G2 phases cells accumulate cyclin B1/Cdc2 in an inactive form due to inhibitory phosphorylations, mitotic events are stimulated by the conversion of inactive Cdc2 to the active form mediated by Cdc25C phosphatase. After DNA damage, members of PI-3K family (DNA-PK, ATM, ATR) become activated and can directly phosphorylate p53 resulting in a protein stabilization/activation. The p53-dependent G2 arrest involves in an initial inhibition of cyclin B1/Cdc2 activity directly or through p21 [151]. The Cell cycle pathway altered in 2Gy-irradiated PBL was found enriched in 13 and 14 transcripts significantly deregulated in 1g and MMG, respectively (Fig. 29 and 30). As reported for p53-signaling pathway, also in this case many genes differed between 1g and MMG for type and anti-correlated miRNAs; indeed, in 2Gy MMG PBL were exclusively deregulated: ATM, TP53, CD45L, GADD45B, WEE1 and RBL2, although their predicted miRNAs were responsive in both gravity conditions. Finally, by comparing radio-responsive mRNAs in 1g and MMG, 8 transcripts were found commonly modulated: CDC2, CCND2, CDKN1C, E2F1, E2F5, MDM2, MYC, PCNA; as observed in the p53-signaling pathway they were anti-correlated to different miRNAs species. The positive regulators of cell cycle progression CCND2 and CDC2 were repressed in both gravity conditions, with different fold change values between 1g and MMG. 9 miRNAs were predicted to interact with CCND2 in 1g and 6 in MMG: miR-513c, miR-494, and miR-424* were commonly anti-correlated.

Fig. 29. Cell cycle pathway found enrich in 2Gy-irradiated PBL in 1g. A) Biological pathway scheme indicating significantly deregulated genes with a red star. B) Table reporting the 13 mRNAs altered in Cell cycle pathway and the anti-correlated radio-responsive miRNAs in ground gravity. Analysis performed with KEGG-DAVID database ($p<0.05$).

A)

2Gy 1g: modulated transcripts in Cell cycle pathway		
mRNA	**Description**	**miRNA**
BUB1B	BUB1 budding uninhibited by benzimidazoles 1	hsa-miR-200b
		hsa-miR-513a-5p
CDC2	cell division cycle 2, G1 to S and G2 to M	hsa-miR-345
CCND2	cyclin D2	hsa-miR-371-5p
		hsa-miR-424*
		hsa-miR-574-5p
		hsa-miR-765
		hsa-miR-877*
		hsa-miR-1225-5p
		hsa-miR-494
		hsa-miR-663
		hsa-miR-513c
CDKN1A	cyclin-dependent kinase inhibitor 1A (p21, Cip1)	hsa-miR-17
		hsa-miR-873
		hsa-miR-181a-2*
		hsa-miR-335
CDKN1C	cyclin-dependent kinase inhibitor 1C (p57, Kip2)	hsa-miR-181a-2*
		hsa-miR-505*
		hsa-miR-17
		hsa-miR-363
		hsa-miR-873
CDKN2A	cyclin-dependent kinase inhibitor 2A	hsa-miR-200b
E2F1	E2F transcription factor 1	hsa-miR-345
		hsa-miR-30e*
E2F5	E2F transcription factor 5, p130-binding	hsa-miR-34a
		hsa-miR-19b
MAD2L1	MAD2 mitotic arrest deficient-like 1	hsa-miR-135a*
		hsa-miR-371-5p
		hsa-miR-424*
		hsa-miR-1225-5p
		hsa-miR-494
		hsa-miR-18b
MDM2	Mdm2, transformed 3T3 cell double minute 2	hsa-miR-34a
MYC	v-myc myelocytomatosis viral oncogene homolog	hsa-miR-513a-5p
PCNA	proliferating cell nuclear antigen	hsa-miR-19b
		hsa-miR-18b
RB1	retinoblastoma 1	hsa-miR-877*
		hsa-miR-630

B)

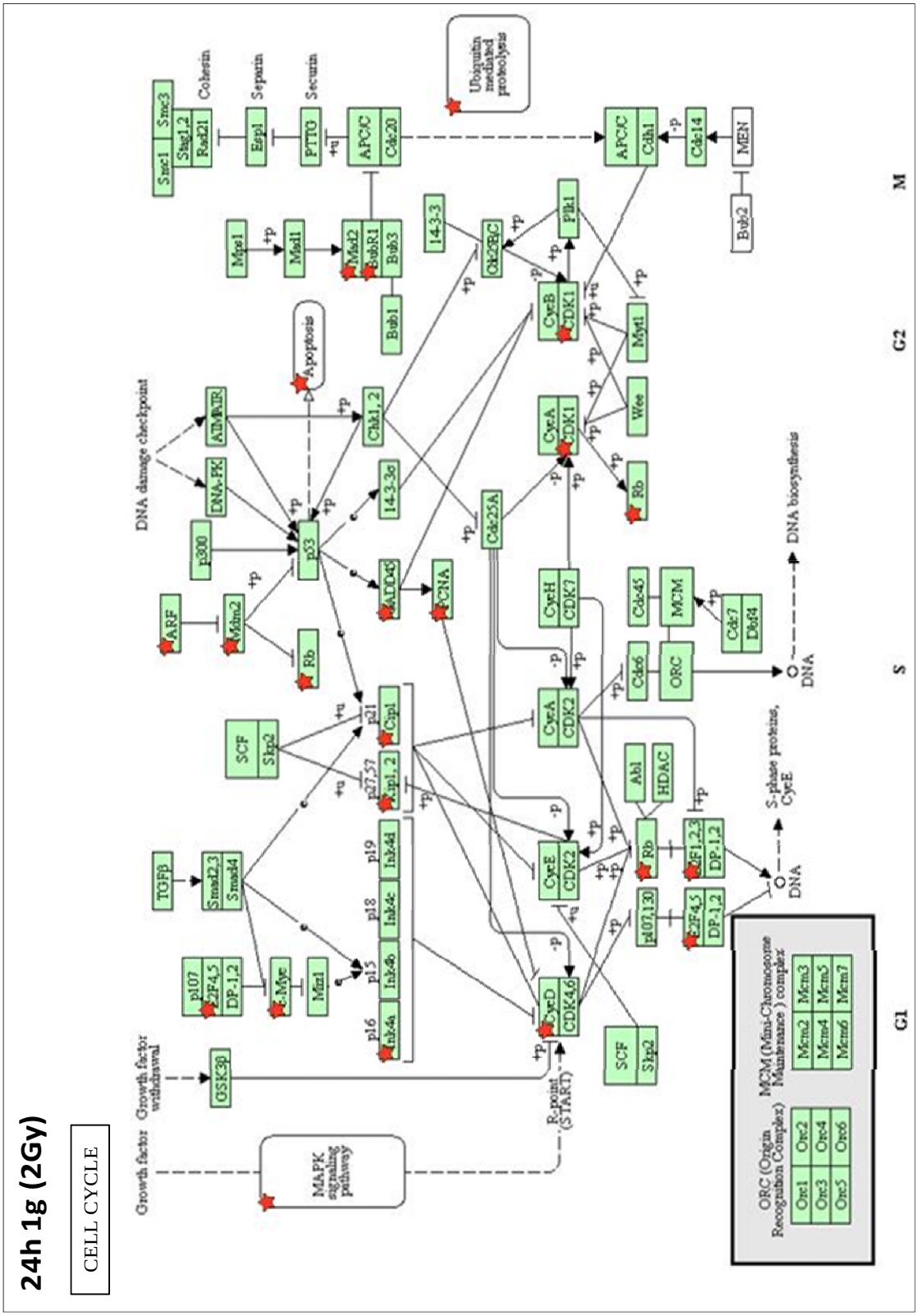
24h 1g (2Gy)
CELL CYCLE
G1
S
G2
M
DNA damage checkpoint
Growth factor
Growth factor withdrawal
MAPK signaling pathway
R-point (START)
Apoptosis
Ubiquitin mediated proteolysis
DNA biosynthesis
S-phase proteins, CycE
ORC (Origin Recognition Complex)
MCM (Mini-Chromosome Maintenance) complex

Fig. 30. Cell cycle pathway found enrich in 2Gy-irradiated PBL in MMG. A) Table reporting the 14 mRNAs altered in Cell cycle pathway and the anti-correlated radio-responsive miRNAs. B) Biological pathway scheme, significantly deregulated genes are indicated with a red star. Analysis performed with KEGG-DAVID database ($p<0.05$).

A)

2Gy MMG: modulated transcripts in Cell cycle		
mRNA	**Description**	**miRNA**
ATM	ataxia telangiectasia mutated	hsa-miR-34b*
		hsa-miR-27a
CDC2	cell division cycle 2, G1 to S and G2 to M	hsa-miR-345
		hsa-miR-494
CDC45L	CDC45 cell division cycle 45-like	hsa-miR-135a*
		hsa-miR-513c
		hsa-miR-424*
CDKN1C	cyclin-dependent kinase inhibitor 1C (p57, Kip2)	hsa-miR-940
CCND2	cyclin D2	hsa-miR-345
		hsa-miR-494
		hsa-miR-513c
		hsa-miR-135a*
		hsa-miR-923
		hsa-miR-424*
E2F1	E2F transcription factor 1	hsa-miR-34b*
		hsa-miR-923
E2F5	E2F transcription factor 5, p130-binding	hsa-miR-135a*
		hsa-miR-494
		hsa-miR-424*
		hsa-miR-923
GADD45B	growth arrest and DNA-damage-inducible, beta	hsa-miR-34b*
		hsa-miR-135a*
		hsa-miR-923
		hsa-miR-494
MDM2	Mdm2, transformed 3T3 cell double minute 2	hsa-miR-34b*
		hsa-miR-663
		hsa-miR-494
MYC	v-myc myelocytomatosis viral oncogene homolog	hsa-miR-424*
PCNA	proliferating cell nuclear antigen	hsa-miR-34b*
RBL2	retinoblastoma-like 2 (p130)	hsa-miR-196b
TP53	tumor protein p53	hsa-miR-200a
		hsa-miR-95
		hsa-miR-181a-2*
		hsa-miR-598
WEE1	WEE1 homolog	hsa-miR-34b*
		hsa-miR-923

B)

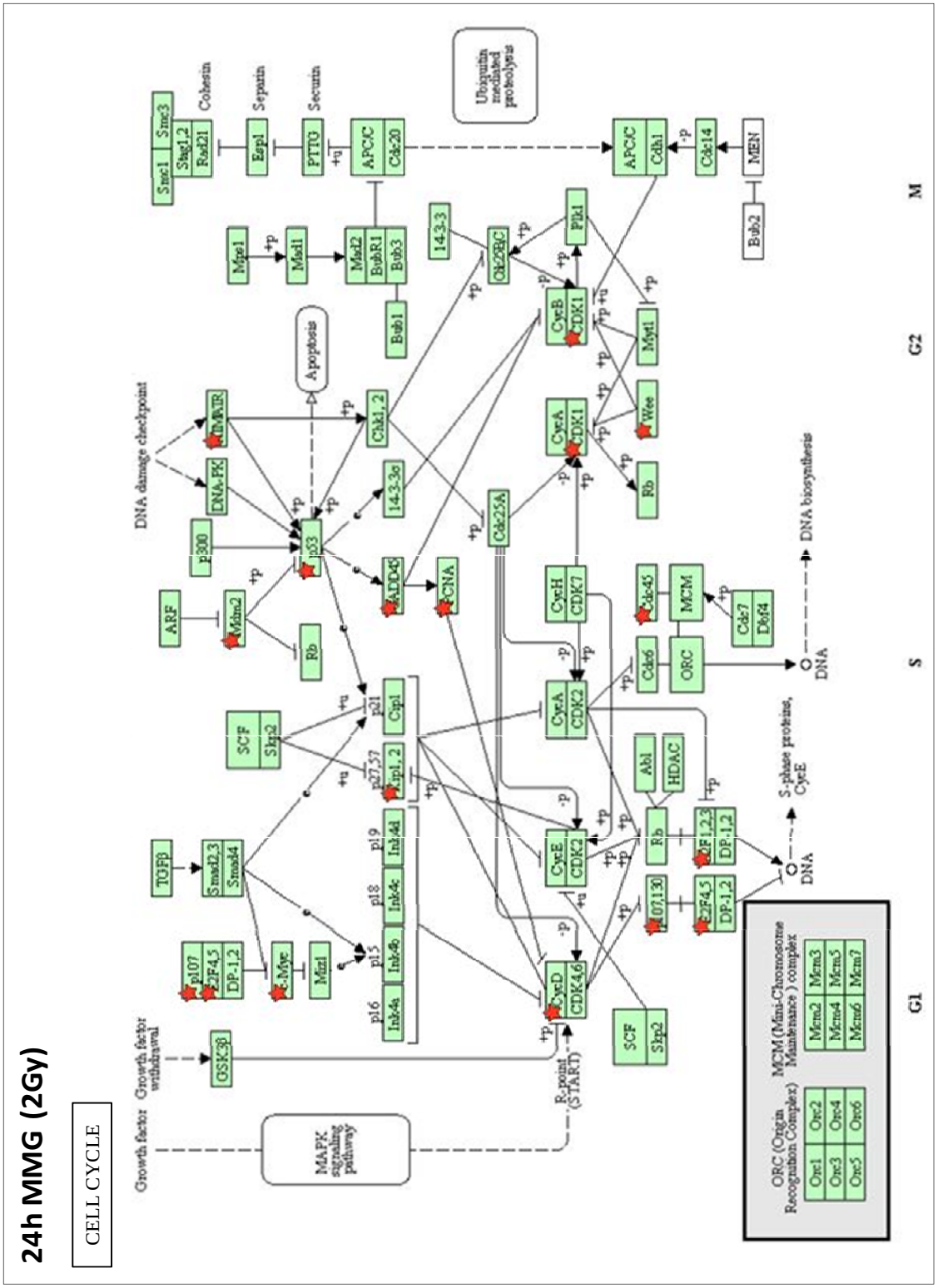
24h MMG (2Gy)
CELL CYCLE
G1
S
G2
M
DNA damage checkpoint
Growth factor
Growth factor withdrawal
MAPK signaling pathway
R-point (START)
Apoptosis
Ubiquitin mediated proteolysis
DNA biosynthesis
S-phase proteins, CycE
DNA
ORC (Origin Recognition Complex)
MCM (Mini-Chromosome Maintenance) complex
Orc1
Orc2
Orc3
Orc4
Orc5
Orc6
Mcm2
Mcm3
Mcm4
Mcm5
Mcm6
Mcm7

- **mRNAs commonly modulated in both gravity condition**

			2Gy 1g		2Gy MMG	
	Gene		fold change	miRNA	fold change	miRNA
p53-signaling pathway	CCND2	cyclin D2	-1,82	miR-371-5p	-1,59	miR-345
				miR-424*		miR-494
				miR-574-5p		miR-513c
				miR-765		miR-135a*
				miR-877*		miR-923
						miR-424*
	CDC2	cell division cycle 2, G1 to S and G2 to M	-1,95	miR-345	-2,48	miR-345
						miR-494
	EI24	etoposide induced 2.4 mRNA	1,46	miR-100	1,41	miR-345
						miR-513c
						miR-940
						miR-873
	MDM2	p53 binding protein	3,76	miR-34a	2,87	miR-34b*
						miR-663
						miR-494
cell cycle	CDKN1C	cyclin-dependent kinase inhibitor 1C	2,12	miR-181a-2*	4,24	miR-940
				miR-505*		
				miR-17		
				miR-363		
				miR-873		
	E2F1	E2F transcription factor 1	-1,57	miR-345	-2,04	miR-34b*
				miR-30e*		miR-923
	E2F5	E2F transcription factor 5	-1,93	miR-34a	-2,81	miR-135a*
						miR-494
				miR-19b		miR-424*
						miR-923
	MYC	myelocytomatosis viral oncogene	-2,48	miR-513a-5p	-2,89	miR-424*
	PCNA	proliferating cell nuclear antigen	2,41	miR-19b	2,61	miR-34b*
				miR-18b		

Fig. 31. Transcripts of cell cycle and p53-signaling pathways commonly modulated after irradiation in 1g and MMG. Analysis performed with KEGG-DAVID database ($p<0.05$) in 2Gy-irradiated PBL incubated 24h in 1g and MMG.

Finally, to investigate the possibility that ionizing radiation and modeled microgravity have a synergistic action on human cells, the study was focused on radio-responsive transcripts modulated in both gravity conditions. Predicted miRNA-mRNA target interactions, belonging to Cell cycle and p53-signaling pathways, were compared to identify alterations occurring on cellular pathways in response to γ-irradiation in MMG respect to 1g. Results showed that within significantly deregulated genes: CCND2, CDC2, CDKN1C, EI24, E2F1, E2F5, MDM2, MYC and PCNA were commonly altered in both gravity conditions, although they were correlated to different miRNAs in terms of number and specie. In addition, 6/9 mRNAs presented a higher deregulation level in MMG than in 1g

(Fig. 31). Two positive regulators of cell cycle progression were repressed in both gravity conditions, with different fold change values: CCND2 ~1.8 in 1g and ~1.6 in MMG, CCD2 ~1.9 in 1g and ~2.47 in MMG; they were anti-correlated to several miRNAs common to 1g and MMG: miR-345, miR-513c, miR-494, and miR-424*. Also the members of E2F transcription factor family, E2F1 and E2F5, were repressed in both gravity conditions. They play a crucial role in the control of cell cycle and act as tumor suppressor proteins; thus, it was interesting to observe that their down-regulation levels were ~1.9- and ~1.5-fold change in 1g, ~2.0- and ~2.8- fold change in MMG, respectively. Among the significantly anti-correlated transcripts involved in DNA-damage response, the oncogene MYC and the repair gene PCNA were similarly induced in both gravities and anti-correlated to different miRNA species; miR-424* and miR-34b*, targeting respectively MYC and PCNA in MMG, were differentially expressed also in 1g.

On the whole, these observations could probably demonstrate that radiation associated with MMG reduces the radio-responsiveness of miRNAs compared to ground gravity, altering the DNA-damage response in simulated space environment.

3.10 miRNA-mRNA PREDICTED INTERACTIONS MODULATED IN MMG

Since previous experiments demonstrated a lower rate of DSB rejoining in irradiated PBL incubated in MMG, miRNA-mRNA integrated analysis was performed to figure out the function of some radio-responsive miRNAs and to elucidate the mechanism of IR-cell response in modeled microgravity. By using the Cytoscape software package [152] it is possible visualize miRNA-mRNA predicted interaction and in figure 32 are showed some examples of the most significant. Interestingly, ATM gene was found down-regulated (~1.4 fold change) in 2Gy MMG samples and was anti-correlated to miR-34b* and miR-27a, the latter activated by the possible combined action of IR and MMG. Also the stress-responsive TP53 was specifically deregulated (~1.7 fold change) in 2Gy MMG PBL and associated to: miR-95, miR-181a-2* (radio-responsive miRNAs), miR-200a (MMG-responsive miRNA) and miR-598 activated only by the combination of IR and MMG. The Growth Arrest and DNA-Damage-inducible (GADD45B) gene and the Ribonucleotide Reductase (RRM2B) gene, which are involved respectively in growth arrest/apoptosis and DNA repair, were found significantly deregulated in the p53-signaling pathway of 2Gy MMG samples; although they were regulated by miRNAs differentially expressed also in 1g. Another gene specifically

deregulated in 2Gy MMG PBL was CARD11, member of Caspase-Associated Recruitment Domain protein family, which is involved in the apoptosis pathway regulation; through miRNA-mRNA integrated analysis it was anti-correlated to miR-10a, which was significantly modulated also in 1g. The Signal Transducer and Activator of Transcription STAT5A is an anti-apoptotic factor which was under-expressed only in MMG (~1.5 fold change) and anti-correlated to: miR-424*, miR-494 (radio-responsive miRNAs), miR-27a (radio-responsive in MMG) and miR-135a* modulated in irradiated and not-irradiated cells in both gravity conditions. Among the significantly anti-correlated transcripts regulating apoptosis, the pro-apoptotic factor TNFRSF10B (TNF-receptor superfamily member) was more induced in MMG than in 1g (3.6- vs 2.6-fold change) and resulted anti-correlated to different miRNAs according to the gravity condition; in particular, miR-7, miR-7-1*, miR-144 and miR-650 were activated only in 2Gy-MMG lymphocytes. Also the apoptotic activator BAX (BCL2 protein family member) was targeted by different miRNA species in 1g and MMG; notably, miR-144, miR-200a, miR-598 and miR-650 were all activated exclusively in MMG PBL.

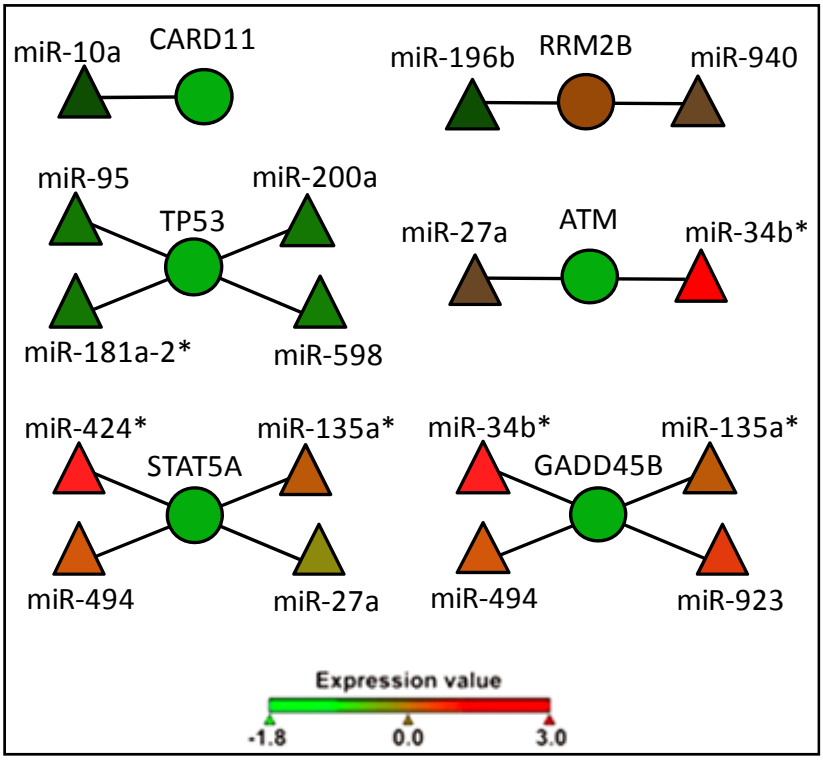

Fig. 32. miRNA-mRNA predicted interactions specifically modulated in γ-irradiated PBL (2Gy) incubated 24h in MMG. miRNA-mRNA integrated analysis was performed with computational approach (MAGIA bioinformatics tool) and the interactions were showed through Cytoscape web tool.

From these data emerged that ionizing radiation and MMG incubation specifically affect the expression level of key genes involved in DNA-damage response and cell cycle checkpoints, with a general down-regulation. The hypothesis that miRNAs may regulate this process was tested through mRNA-miRNA anti-correlation analysis; results provided only evidences that simulated microgravity impairs miRNA expression profiles, because several radio-responsive miRNAs were found differentially expressed in both gravity conditions. Since the anti-correlation analysis was performed integrating miRNA and mRNA expression profiles with computational predictions (PITA algorithm), the resulting miRNA-mRNA interactions were affected by a large fraction of false positives. Therefore, to better understand the role of miRNAs in IR-human cell response in ground gravity and simulated microgravity, the target identification requires an extensive experimental validation through 3'UTR Report-Assay and functional studies in cell lines (i.e Jurkat, TK6, IM9).

3.11 VALIDATION OF miRNA-mRNA PREDICTED INTERACTIONS

This PhD program was carried out for seven months in the laboratory of Prof. Riccardo Dalla-Favera at "*Institute for Cancer Genetics*", Columbia University (New York, USA), to acquire some expertise in molecular biology techniques and their applications to the study of microRNAs useful to carry on the research work on IR-human cell response. During the learning process I contributed to a few projects with the common aim to study miRNAs found to be involved in normal mature B cell differentiation (naïve, centroblasts, centrocytes and memory cells) and in B cell tumors.

• Investigation of a small tRNA-derived fragment (tRF) and its biological functions in human B cells

MiRNAs expressed in the human mature B-cell compartment (naive, germinal center, memory B cells and a Burkitt lymphoma cell line) have been studied by short RNA libraries. Short RNA sequences were mapped to the human genome and upon computational analysis were identified 178 miRNAs representing the mature B-cell miRNome which included 75 not previously reported miRNAs [153]. A fraction of these novel miRNAs displayed similarity to the 3'-end of post-trascriptionally modified tRNAs, suggesting that

even a larger set of tRNA derived fragments (tRF) are likely not to be random degradation products but stabilized fragments with a biological function [154]. This project aims to the investigation of a candidate tRF including the biogenesis, its miRNA-like functions and the role in normal and malignant B cells.

In order to identify the origin of the predicted novel miRNA and candidate tRF, the genomic region predicted to host the precursor miRNA and the tRNA genomic region were sub-cloned in expression vectors. Transient transfection in 293T cells, followed by Northern Blot detection showed that the tRNA-encoding locus, but not the predicted miRNA precursor, was competent in producing the mature small RNA fragment. These results confirmed that the analyzed small RNA is a bona fide tRF. In order to investigate the role of this tRF in B cells, were generated inducible expression vectors carrying the tRNA encoding locus or an artificial miRNA-like gene engineered to express the tRF of interest. The functionality of the generated expression vectors has been tested by transient transfection in 293T cells followed by Northern Blot detection. The tRF miRNA-like repression on the 3-UTR of potential targets has been initially tested using an artificial construct in which fully or partially complementary sites were introduced in the 3'UTR region downstream to a luciferase reporter. Luciferase-reporter assay performed with the tRF expressing plasmid and the 3'UTR reporter plasmids showed a reduction in luciferase activity when the 3'end of the targeted site was maintained, but not in mutants abrogating recognition by the tRF "seed" sequence. These in vitro results show that the tRF recognizes target regions in the 3'UTR of candidate targets with a behavior similar to miRNAs.
My contribution to this project ranged from the expression plasmids generation to the validation of their proper expression by Northern Blot.

- **Experimental validation for a novel miRNA predicted precursor**

Genome-wide copy number alteration studies suggested that loss of a region in chromosome 1q42.12 may be associated with lymphoma. This region includes the predicted precursor of a novel miRNA [153]. The goal of this project was to experimentally verify if the predicted precursor was able to code for the identified miRNA. To test if the predicted precursor mapped on chromosome 1q42.12 was competent to produce the novel miRNA of interest, the genomic region has been sub-cloned in an expressing plasmid and transiently-transfected in 293T cells. Transcription of the genomic region inserted in the

plasmid was confirmed by RT-PCR upon transfection in 293T cells. Northern Blot has been performed to detect the miRNA precursor and its mature form.
As contribution to this project I performed transient transfections of the expression plasmid in 293T cells, purified RNA, performed RT-PCR and preliminary Northern Blot analyses.

- **Experimental validation of BCL6 as miR-150 predicted target**

miR-150 has been found to be a lymphopoietic-specific miRNA that is is mainly expressed in the lymphnodes and spleen and is highly up-regulated during the development of mature T and B cells [155]. This miRNA as been predicted by computational analysis to bind the 3'UTR of BCL6. BCL6 has been predicted by computational analysis as target gene of miR-150. BCL6 3'UTR reporter assay was performed to verify the predicted direct interaction. Toward this goal BCL6-3'UTR has been sub-cloned in the pmirGLO vector (luciferase reporter vector) and this has been co-trasfected in 293T cells with a miR-150-expressing plasmid. Transient transfections have been followed by reporter Luc-Assays to test the effects of miR-150 on BCL6 3'UTR.
My contribution to this project included transient transfections and luciferase assays to consolidate data previously generated.

.

4. CONCLUSIONS

This study demonstrates that, in PBL irradiated with γ-rays, the DSB rejoining process is impaired in modeled microgravity, since it was almost completed in few hours in ground gravity whereas it took more time in simulating microgravity. Moreover, the higher apoptotic activity observed in MMG cells could be due to the persistence of the DNA damage in modeled microgravity respect to normal cultured cells (1g). The modality by which MMG incubation increased IR-induced apoptosis appeared unclear; indeed, p53 and $p21^{Waf1}$ increased in PBL after irradiation, but their amount was very similar in 1g or MMG. Most likely, in irradiated PBL DNA damage activates the intrinsic pathway of apoptosis, which is regulated through p53-signaling pathway; in addition, MMG incubation during repair time could activate some signals increasing the IR-induced apoptosis, independently to p53 level.

To better investigate the mechanism of radiation cell response, miRNA- and mRNA-expression profiles of γ-irradiated human PBL incubated in 1g and MMG were analyzed and compared. From Significance Analysis of Microarrays arose that radiation associated with MMG reduces the number of radio-responsive miRNAs respect to ground condition; although, the number of differentially expressed mRNA was higher in MMG than in 1g. According to previous studies, this work confirms the involvement in IR-cell response of genes such as, CDKN1A, XPC, DDB2, PCNA, CCNG1, MCM2, XRCC4, MDM2, TNFSF9, CD69, PLK, ISG20L1, DNA-PK, LIG4, which have key role in cell cycle, proliferation, stress-response and apoptosis [29, 33, 36, 41-43]. Among the significantly deregulated miRNAs found in this study, several are already considered as radio-responsive or involved in carcinogenesis: let-7, miR-34a, -16-2*, -202, -221, -345, -363, -638, -630 and miR-663 [93, 99, 100, 101, 103, 110]. Pathway enriched analysis showed that biological categories of the DNA-damage response were little enriched in MMG, but genes mainly involved in p53-signaling pathway, cell cycle and others DDR genes, such as ATM, TP53, GADD45B, RRM2B were specifically affected. Interestingly, in irradiated PBL incubated in MMG were found altered biological functions related to the immune system, such as: regulation of immune system process, leukocyte activation, regulation of cytokine production; this observation is in agreement with studies reported in literature describing impaired immune system function in astronauts [116, 118]. From anti-correlation analysis emerged that the same mRNA could be targeted by different miRNA, in terms of number and specie, according to the gravity condition; in addition, radio-responsive miRNAs commonly deregulated in both

gravities not always targeted the same mRNA. Our results cannot explain the reason why the same mRNA could be anti-correlated to different miRNA species in relation to the gravity condition or, radio-responsive miRNAs common to both gravity conditions may be anti-correlated to different mRNAs. We hypothesize that the smaller number of radio-responsive miRNAs in MMG can operate an unscheduled regulation of the expression level of transcripts usually not targeted. The scenario proposed in this work is that modeled microgravity incubation, following ionizing radiation exposure (simulated space environment), could affect the appropriate radiation cell response of human lymphocytes reducing the efficiency of DNA repair. As a matter of fact, our results provide evidence that MMG impairs the chromatin structure modulation after DSB formation, the radio-responsiveness of miRNAs and the expression of mRNAs involved in DNA damage response, cell cycle and apoptosis.

Since the presence of unrepaired DSBs increases the risk of gene mutations, chromosomal aberrations and cell death, these results support the tesis that less DNA repair efficiency in modeled microgravity could represent a further risk factor for subjects exposed to IR in conditions of reduced gravity force.

5. MATERIALS AND METHODS

5.1 LYMPHOCYTE ISOLATION

Peripheral blood lymphocytes (PBLs) were isolated by separation on Biocoll (Biochrom KG, Seromed) density gradient from freshly collected buffy coats from anonymous healthy donors provided by the Blood Centre of Padova's Hospital, under the ethical rules of the Transfusion Medicine Committee. After isolation, cells were preincubated overnight at a concentration of 3×10^6/ml in RPMI 1640medium containing GlutaMAX-I (Gibco, Invitrogen), 124U/ml penicillin, 63µg/ml streptomycin and 10% fetal bovine serum (FBS, Biochrom KG, Seromed) to remove of adherent monocytes. After incubation, the lymphocyte suspension was collected and the cell number determined. For PFGE experiments, lymphocytes were stimulated entering G1 phase of cell cycle with phytohemaglutinin M (PHA-M, Biochrom) 20–22h before irradiation. In the other experiments PBLs were irradiated in G0 phase.

5.2 CELL IRRADIATION AND MICROGRAVITY SIMULATION

Irradiation with γ-rays was performed at the Department of Oncological and Surgical Sciences of Padua's University with a ^{137}Cs source (dose-rate: 5.155cGy/s). PBL were kept on ice before and after irradiation, then suspended in fresh medium at the concentration of 1×10^6/ml and incubated in MMG and in 1g for different times up to 24 h. Non-irradiated PBLs were subjected to the same conditions of irradiated cells.

Microgravity was simulated by culturing PBL in the Rotating Wall Vessel (RWV) bioreactor (Synthecon, Cellon). Briefly, 50 or 10ml vessels, filled with a suspension of 1×10^6/ml of γ-irradiated PBLs, were positioned in the bioreactor vertically rotating at 23rpm. Non-irradiated PBL were also subjected to modeled microgravity. 1g PBL cultures, both irradiated and non-irradiated, were kept in 75cm^2 flasks at the same density.

5.3 IMMUNOFLUORESCENCE STAINING

At 0.5, 2, 6 and 24h from irradiation, aliquots of PBL incubated in the two gravity conditions were cytospun on glass slides, air-dried and fixed in 4% formaldehyde (Invitrogen) in PBS. Glass slides were washed three times for 5 min in PBS, permeabilized in 0.2% Triton X-100–PBS and blocked in 10% goat serum–PBS for 1h at room

temperature; then, they were incubated 2h at room temperature with primary antibodies anti-γH2AX (Upstate, 1:200), anti-NBS1-p343 (Novus Biologicals, 1:200), anti-53BP1 (Bethyl laboratories, 1:100) and anti-ATM-p1981 (Rockland, 1:100). The cells were washed twice with PBS and incubated with secondary antibodies Alexa Fluor® 488 goat anti-mouse and Alexa Fluor® 594 donkey anti-rabbit (Molecular Probes, 1:250) for 1h at room temperature. At the end, cells were washed, counterstained with 2μg/ml DAPI (4,6-diamidino-2-fenilindole) in antifade solution (Vectashield, Vector Laboratories, CA) and cover glass slides were mounted. The immunofluorescence images were captured with a MRC-1024 Laser Scanning Confocal Imaging System (BIO-RAD) and with an epifluorescence microscope (Leica 5000, Wetzlar, Germany) equipped with a CCD imaging system. Images were processed by Adobe PhotoShop 8.0 software (Adobe, San José, CA). For each experimental point, 300–500 nuclei were captured at a constant exposure time and scored for foci by eye. The percentages of positive cells for γ-H2AX, NBS1-p353, 53BP1 and ATM-p1981 foci (at least 1focus/nucleus) were determined on 3–4 independent experiments.

5.4. APOPTOSIS INDUCTION

Apoptotic index was determined in non-irradiated and irradiated (5Gy) PBL incubated for 2, 6 and 24h in MMG or 1g. For detection of apoptotic morphology, PBL were washed once in Hank's solution and fixed with an ice-cold ethanol:acetic acid (9:1) solution, following standard procedure. Lastly, fixed cells were dropped on clean slides and stained with 2μg/ml 4,6-diamino-2-phenylindol (DAPI, Roche), in an antifade solution (Vectashield, Vector Lab). At least 2000 cells were scored for each time-point by fluorescence microscopy (1000× magnification). The activation of caspase-3 was measured at by the Caspase-3 fluorescent assay Kit (Clontech, BD Biosciences), at 2, 6 and 24h after irradiation and incubation in 1g or MMG. The fluorescent emission at 505nm (excitation at 400 nm) of cleaved 7-amino-4-trifluoromethyl coumarin (AFC) was measured with a PerkinElmer LS-50 B spectrofluorimeter. The data of fluorescence intensities of irradiated cells incubated in 1g or MMG were presented as fold increase over their relative controls (non irradiated cells maintained in 1g or MMG for the indicated times).

5.5 PULSED-FIELD GEL ELECTROPHORESIS

Approximately 5×10^5 of non-irradiated and irradiated G1-lymphocytes were processed for PFGE (according to [156]). Immediately after γ-irradiation (time 0) and after 15min, 30min, 2h and 6h in MMG or 1g, the cells were collected, centrifuged and washed twice with ice-cold PBS. Plugs were prepared by resuspending 5×10^4 in 35µl of cell suspension buffer (10mM Tris–HCl, pH 7.2, 20mM NaCl, 50mM EDTA). The cell suspensions were then mixed with equal volume of 2% clean-cut agarose (Biorad) at 50˚C and pipetted into plastic moulds on ice. Plugs were stored at 4 ◦C for gelling. After solidification the agarose blocks were incubated for 20h at 0˚C with 0.5–1 ml/plug of ESP buffer (1mg/ml proteinase K (Promega), 2% N-lauroylsarcosine and 0.5M EDTA, pH 8.0). Proteinase-K was added just before use; then, ESP buffer was replaced with 0.5–1 ml/plug of HS buffer (1.85M NaCl, 0.15M KCl, 5mM MgCl2, 2mM EDTA, 4mM Tris, 0.5% Triton X-100, added just before use, pH 7.5) and incubated at 0˚C for 20–40h. Ultimately, blocks were washed four times in washing buffer (10mM Tris/HCl and 1mM EDTA, pH 7.5), 1h each at room temperature with gentle agitation. Plugs were stored at 4˚C and used within few days. The agarose blocks were subjected to electrophoresis or used for the DNA content estimation. For PFGE analysis, agarose plugs were placed into the wells of a 1% NuSieve GTG low melting agarose gel (FMC BioProducts) and plugs containing *S. pombe* artificial chromosomes (BioRad) were added as DNA size standards. The gel was placed into a PFGE unit (CHEF-DR II, BioRad) with 120˚ reorientation angle and the electrophoresis was performed in 1× TAE buffer, at 14˚C and 1.7 V/cm, using three 31h blocks: 50–200, 200–600, and 2000–2200s, respectively. After electrophoresis, the wells containing agarose plugs were detached by cutting across the gel about 2cm to the cathode side; each well was stored at 4˚C for DNA content estimation.

5.6. QUANTIFICATION OF DNA RELEASED TO THE GEL

The fraction of DNA released (FR) from the plug after PFGE was calculated either by measuring optical density (OD) of DNA migrating in the gel and by ng of DNA retained in the plug. After PFGE the gels were transferred to 3mm paper, dried, stained with SYBR-Gold (Molecular Probes) for 40min and visualized under a 312nm UV transilluminator. Images were captured with a CCD camera and analyzed with Quantity-one software (BioRad). OD values were assigned to selected areas of the gel images. OD values depend on the pixel values (i.e. fluorescence intensity) within the selected area and were

considered a measure of the DNA amount. FR was reported in percentage of initial damage (FR at time 0=100). For estimation of DNA content we analyzed a pair of equally sized plugs for each sample: one subjected and one non-subjected to PFGE. At the end, the plugs were washed twice with TE 1× for 2h and melted by heating at 50–65°C for 15min. Samples were equilibrated at 42°C for 15min; then molted agarose were incubated with 1U/200ml of β-Agarase (BioLabs) at 42°C for 1.5–2h. Estimation of DNA content of samples subjected to PFGE and samples non-subjected to PFGE was performed following the instructions of Quant-iTTM dsDNA Broad-Range Assay Kit (Molecular Probes, Invitrogen). DNA standard solutions (Sigma) in the range of 0–300ng/ml were used to set the standard curve. Fluorescence was read with a spectrofluorophotometer (FluoSkan Ascent, Lab System) at 485nm excitation and 527nm emission wavelengths. DNA concentrations in the samples were determined from standard curve and DNA content per one plug was measured. FR was expressed as the ratio of DNA released from the plug to total DNA loaded, and reported in percentage.

5.7 WESTERN BLOTTING

Cellular extracts were prepared from non-irradiated and irradiated PBL at 0.5, 2, 6 and 24h after irradiation and incubation in the two gravity conditions. Briefly, cells (10×10^6) were permeabilized for 5min on ice in cytosolic extraction buffer containing 200μg/ml digitonin. Cellular plasma membrane permeabilization was confirmed by trypan blue staining. Cells were centrifuged 5min at 1000×g at 4°C and the supernatans (cytosolic fraction) were recovered. Pellets were then resuspended in mitochondrial lysis buffer [157] for 15min on ice and then centrifuged at 10000×g for 10min at 4°C. Supernatants were recovered and pellets were incubated in HCl 0.5M on ice for 20min to exctract histones. Samples were centrifuged 10 min at 16000×g, the three fractions (cytosolic, mitochondrial, and nuclear) were pooled and protein concentrations determined. 20μg of total proteins were separated on 12% SDS-polyacrylamide gels and transferred to nitrocellulose membranes Hybond-C Extra (Amersham, GE Healthcare). Membranes were probed with primary monoclonal antibodies anti-γ-H2AX (Upstate, 1:100), anti-$p21^{Waf1}$ (Calbiochem, 1:200), anti-p53 (Santa Cruz Biotechnology, 1:300), anti-Ku70, anti-RAD51 (Santa Cruz Biotechnology, 1:200), anti-β-actin (clone AC-74, Sigma, 1:5000) and subsequently incubated with Amersham ECL horseradish peroxidase-conjugated secondary antibodies

(GE Healthcare, 1:40000). The resulting immunoreactive bands were detected by the enhanced chemioluminescent HRP substrate (Millipore).

5.8. FLOW CYTOMETRY FOR γ-H2AX

PBL were fixed in 1ml of 70% ethanol, additioned with 1ml of PBS 1×, centrifuged. According to MacPhail et al. [158], pellets were resuspended in 1 ml of cold PBS plus 4% FBS and 0.1% Triton X-100 (TST) and incubated 10 min on ice. PBL were centrifuged and resuspended in 200 ml of TST containing anti-H2AX (Upstate) 1:500. Tubes were incubated 2 h, rinsed with cold 2% FBS in TBS and resuspended in 200ml secondary antibody Alexa Fluor® 488 goat anti-mouse (Molecular Probes), diluted 1:200 in TST and incubated 1h at room temperature. Cells were centrifuged, rinsed with cold 2% FBS in TBS, resuspended in PBS 1× and analyzed in a FACScan (Becton Dickinson) by using the CellQuest software program. The mean values of γ-H2AX fluorescence were estimated by gating analyses to exclude debris (low forward scatter and low side scatter) and late apoptotic cells (low forward scatter and high side scatter).

5.9 TOTAL RNA ISOLATION

At the end of incubation time (4 and 24h) in 1g and MMG, total RNA was isolated from 10^7 irradiated and non-irradiated PBL, by using Trizol® Reagent (Invitrogen, CA), according to the manufacturer's protocol. Total RNA was quantified using the ND-1000 spectrophotometer and the integrity of miRNA and total RNA was confirmed by Agilent Bioanalyzer 2100 (Agilent Small RNA kit and Nano kit, Agilent Technologies, Palo Alto, CA). Only total RNA samples with RNA Integrity Number (RIN) values ≥ 6 and with miRNA $<$ 20% were used for microarray analysis.

5.10 miRNA AND GENE EXPRESSION PROFILING

The miRNA expression profiling was carried out in 12 donors' lymphocytes at 4h and 24h after irradiation (0.2 and 2Gy, 6donors/dose) incubated in 1g and MMG, and in their corresponding controls. The *"Human miRNA Microarray kit (V2)"* (Agilent Technologies) was used according to the Agilent miRNA one-color Microarray protocol (www.Agilent.com); slides contain eight individual microarrays. Every single array is representative of 723 human miRNAs and 76 human viral miRNAs sourced from the Sanger miRBASE public database (http://microrna.sanger.ac.uk.; miRBase v.10.1). There

are ~15.000 features each, including 48 negative control features used to estimate fluorescence background and background variance. Each miRNA is targeted by 2-12 probes replicated 20-40 each. Total RNA (200ng) was labeled with pCp-Cy3, according to the Agilent protocol and unincorporated dyes were removed with MicroBioSpin6 columns (BioRad). Probes were hybridized at 55°C for 22h using the Agilent's Hybridization Oven that is suited for bubble mixing and microarray hybridization processes. Then, slides were washed by Agilent Gene expression wash buffer 1 and 2 and scanned using an Agilent microarray scanner (model G2565CA) at 100% and 5% sensitivity settings. Agilent Feature Extraction software version 10.5.1.1 was used for image analysis. Raw data are available on the National Center for Biotechnology Information Gene Expression Omnibus (GEO) website (http://www.ncbi.nlm.nih.gov/geo/) using accession number GSE20120.

The mRNA gene expression profiling was carried out in the same PBL analyzed for miRNA profiling: 5 donors' lymphocytes at 24h after irradiation (2Gy) in normal gravity and microgravity and their corresponding controls. We used the "*Whole Human Genome Oligo Microarray"* (Agilent), consisting of ~41.000 (60-mer) oligonucleotide probes, which span conserved exons across the transcripts of the targeted full-length genes. Each slide contains four individual microarrays, each with about 44.000 features. 800ng of total RNA were labeled with "Agilent One-Color Microarray-Based Gene Expression protocol" according to the manufacturer's instructions. The method uses T7 RNA polymerase, which simultaneously amplifies target material and incorporates cyanine 3-labeled CTP. Labeled cRNA was purified through Qiagen's RNeasy mini spin columns (Qiagen, Valecia, CA), the sample quality and the total yield were determined with NanoDrop ND-1000 spectrophotometer measurement (NanoDrop Technologies). 1.65 micrograms of labeled cRNA were used to prepare the hybridization samples and the hybridization was carried out at 65°C for 17h in a hybridization oven rotator (Agilent). The arrays were washed by Agilent Gene expression wash buffers and Stabilization and Drying Solution as suggest by the supplier. Slides were scanned on an Agilent microarray scanner (model G2565CA) and Agilent Feature Extraction software version 10.5.1.1 was used for image analysis. Raw data are available on GEO database using accession number GSE20173.

5.11 STATISTICAL ANALYSIS OF miRNA AND mRNA EXPRESSION DATA

Inter-array normalization of expression levels was performed with cyclic Lowess for miRNA experiments and with quantile for gene expression profiling to correct possible

experimental distorsions. Normalization function was applied to expression data of all experiments and then values of spot replicates within arrays were averaged. Furthermore, Feature Extraction Software provides spot quality measures in order to evaluate the goodness and the reliability of hybridization. In particular flag "glsFound" (set to 1 if the spot has an intensity value significantly different from the local background, 0 otherwise) was used to filter out unreliable probes: flag equal to 0 will be noted as "not available (NA)". In order to make more robust and unbiased the statistical analysis, probes with a high proportion of “NA” values were removed from the dataset. We decided to use the 40% of NA as threshold in the filtering process obtaining a total of 270 available human miRNAs. Principal component analysis, cluster analysis and profile similarity searching were performed with tMev that is part of the TM4 Microarray Software Suite. In particular, hierarchical cluster analysis was performed with Pearson correlation or Euclidean distance coefficient as distance measure with complete linkage. Identification of differentially expressed genes and miRNAs was performed with one and two class Significance Analysis of Microarray (SAM) program with default settings. SAM uses a permutation-based multiple testing algorithm and identifies significant genes and miRNA with variable false-discovery rates (FDR). This can be manually adjusted to include a reasonable number of candidate genes with acceptable and well defined error probabilities. The level of each miRNA was calculated as the $\log_2$ (irradiated sample/non-irradiated sample).

5.12 VALIDATION OF miRNA EXPRESSION LEVELS WITH TaqMan® RT-qPCR

To confirm the microarray results, we used the TaqMan® MicroRNA Assay kit (Applied Biosystems, Foster City, CA) that incorporate a target-specific stem-loop reverse transcription primer. The stem-loop structure provides specificity for only the mature miRNA target and forms a RT primer/mature miRNA-chimera that extends the 5’ end of the miRNA. The resulting longer RT amplicon presents a template amenable to standard real-time PCR using TaqMan Assays. In brief, each RT reaction (15µl) contained 10ng of total purified RNA, 5X stem-loop RT primer, 1X RT buffer, 0.25mM each of dNTPs, 50U MultiScribe™ reverse transcriptase and 3.8U RNase inhibitor. The reactions were incubated in a Mastercycler EP gradient S (Eppendorf) in 0.2 ml PCR tubes for 30min at 16°C, 30min at 42°C, followed by 5min at 85°C and then held at 4°C. The resulting cDNA was semiquantitatively amplified in 45 cycles on an ABI 7500 Real-Time PCR System, using TaqMan Universal PCR Master Mix and Taqman MicroRNA Assays (for hsa-miR-9, hsa-miR-

27a, hsa-miR-34a, hsa-miR-181a-2*, hsa-miR-378, hsa-miR-424*). To calculate the relative expression ratio was used the $2^{-\Delta\Delta Ct}$ (RQ, relative quantification) method, implemented in the 7500 Real Time PCR System software. To evaluate differences in miRNA expression we used a relative quantification method, where the expression of the miRNA target is standardized by a non–regulated small non-coding RNA used as reference; U48 small nuclear (RNU48) was used as an endogenous control, since its level remains essentially constant from sample to sample. For each real-time PCR reaction four replicates of each sample (2Gy-irradiated and non-irradiated cells) and of the endogenous control were amplified. For each tested miRNA we analyzed 4-6 donors.

5.13 miRNA TARGETS PREDICTION: mRNA EXPRESSION DATA AND ANTI-CORRELATION ANALYSIS

To predict miRNA targets we have performed a computational analyses using PITA algorithm based on thermodynamic stability of the RNA-RNA duplex, considering free energy minimization. PITA algorithm was applied over up-to-date version 38 of RefSeq transcript sequences and it used miRNAs sequences downloaded from mirBase version 14. Based on known transcript to gene correspondences, gene-centered predictions were then derived combining transcript-based results into a single group for each gene. In this way a gene was considered a predicted target of a given miRNA if at least one of its transcripts carries predicted target site(s). However all available software for target prediction are characterized by a large fraction of false positives, thus to identify the most likely targets, we have integrated mRNA and miRNA expression data, obtained on the same biological samples, using MAGIA web tool. We used a non-parametric index (Spearman correlation coefficient), the most indicated statistical coefficient for a small number of measures, to estimate the degree of anti-correlation (i.e up-regulated miRNA and corresponding down-regulated mRNA target) between any putative pairs of miRNA and mRNA and we have selected as functional only those anti-correlated less than -0.775. To identify biological processes most involved in the biological phenomena under study we have performed a GO analysis, using DAVID tool, on significant anti-correlated target genes identifying biological pathways significantly enriched ($P<0.05$). Pathway enrichment analysis was carried out by KEGG web tool whereas miRNA-mRNA anti-correlations were visualized by Cytoscape software package.

5.14 TRANSIENT TRASFECTION

This technique has been applied in the study of miRNA expression/processing or to validate the predicted miRNA-target interaction by 3'UTR report assay. The transfection based on the chemical method (Hepes-NaP+$CaCl_2$ 2M) has been used to obtain a suspension of DNA precipitates that is added directly to the cells; by endocytosis the cells uptake the salt crystals with the DNA (Graham and van der Eb, Virology 1973).

For each DNA sample to transfect was prepared a solution of DNA/water in 438 µl and 62 µl of $CaCl_2$ 2M were added (final volume 500 µl). 500 µl of DNA- $CaCl_2$ sample were added, making bubbles by pipetting air inside the tube, in a 15ml falcon tube containing 500µl of a mix Hepes-NaP (49:1) prepared as reported: 490 µl solution (50mM Hepes - 200mM NaCl) + 10µl NaP (35mM NaP). In dish plates containing 293T (cultured for 24h) was added drop by drop a 1/10 of the plate volume of transfection preparation (10ml plate →1ml; 3ml plate →300 µl). Transfected plates were moved to distribute well the crystal preparation and incubated at 37 °C. After 16h, plates were washed with PBS and fresh complete medium was added. If the experiment provides an induction the fresh change media was additioned with a Doxocyclin*dilution [1µg/ml]. 40-46 hours upon transfection, cells were collected and subject to the assay of interest.

Transient transfections was performed in 293T cells, a variant of the 293 cell line (human embryonic kidney) which contains the SV40 large T-antigen that allows replication of transfected plasmids with a SV40 replication origin. 2 x10^6/ml 293T cells were cultured in 10 ml or 3ml plates in complete media (500ml DMEM + 50ml FBS(10%) + 5.6 ml Antibiotics).

5.15 NORTHERN BLOT FOR miRNA DETECTION

This technique has been applied to study the expression/processing of small RNAs of interest. 20 mg of goodquality total RNA was loaded on a 12% polyacrilamide denaturing gel (Sequagel, National Diagnostic), and after electrophoresis transferred to a Nylon membrane (Duralon UV, Stratagene). Membrane was cross-linked using ultraviolet light for 30s at 1200 mJ/cm2. Hybridization with specific 20mer-probes end- labeled with (dATP)^{32}P was performed at 50 °C O/N. Upon washing the radioactive signal was detected exposing the membrane to a photographic Kodak film. For most miRNAs the results showed two bands: the precursor miRNA (60-70 nt) and the mature miRNA (20-25nt).

5.16 CLONING STRATEGY

Genomic regions corresponding to miRNA coding sequences, 3'UTR of protein coding genes or promoter/regulatory regions have been sub-cloned in multiple types of expression vectors. Primers have been designed to contain specific restriction sites. The restriction sites are selected on the basis of the vector that will be used in the cloning strategy. The target sequence has been subject to PCR reaction to obtain a product corresponding to the genomic sequence flanked by the restriction sites. Restriction enzymes specific to the introduced sites have been used to digest the PCR product and the vector. After purification and dephosphorylation of the vector, the PCR-derived insert and the vector have been ligated using the T4-DNA ligase enzyme and the ligation product has been used to transform bacteria. The bacteria colonies obtained from the transformation have been picked and the presence of the insert in the plasmid DNA has been investigate performing colony-PCR using one primer that recognizes the vector and another specific for the insert. The colonies that showed positive PCR results have been selected, expanded in culture and the plasmid DNA has been extracted and purified from genomic bacteria DNA by CsCl gradient-maxiprep.

Following this approach, miRNA coding sequences have been introduced both in constitutive and doxocyclin inducible expression vectors. 3'UTR sequences have been sub-cloned downstream of a luciferase reporter gene in order to obtain a fusion transcript coding for the luciferase but carrying the 3'UTR of interest. These expression vectors have been used for testing the responsiveness of target 3'UTRs to the repression activity of miRNAs. Promoter and other transcriptional regulatory regions have been sub-cloned in promoter-luciferase reporter vectors, in which the genomic region under investigation is inserted upfront the reporter gene. Upon co-expression with transcription factor(s) of interest, changes in luciferase activity are monitored to identify regions of relevance for transcriptional regulation.

5.17 REPORTER ASSAY

Genetic reporter systems are used to study eukaryotic gene expression and cellular physiology, including the study of the activity of transcription factors and miRNA translational repression. In particular, the "Dual-Luciferase® Reporter Assay" system (Promega) has been used in the assays described here. The term "dual reporter" refers to the simultaneous expression and measurement of two individual reporter enzymes within

a single system, *Luciferase* and *Renilla*. Typically, Luciferase activity is correlated with the effect of specific experimental conditions (experimental reporter), while the activity of Renilla (co-transfected or encoded by the same plasmid of luciferase) provides an internal control that serves to normalize the activity of the experimental reporter minimizing the experimental variability caused by differences in cell viability, transfection efficiency, pipetting volumes or cell lysis efficiency.

Firefly luciferase is a 61kDa monomeric protein that does not require post-translational processing for enzymatic activity (de Wet, J.R. et al. *Proc. Natl. Acad. Sci.* 1985), thus it functions as a genetic reporter immediately upon translation. Photon emission is achieved through oxidation of luciferin in a reaction that requires ATP, Mg^{2+} and O_2.

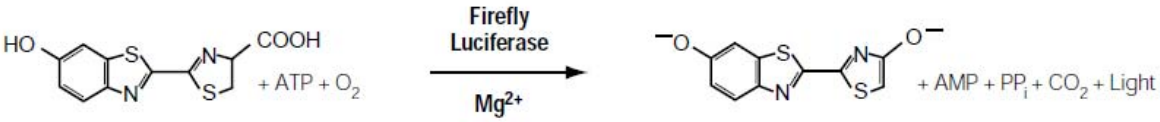

Beetle Luciferin **Oxyluciferin**

Renilla luciferase is a 36kDa monomeric protein and like firefly luciferase, post-translational modifications are not required for its activity. The luminescent reaction catalyzed by Renilla luciferase utilizes O_2 and coelenterateluciferin (coelenterazine).

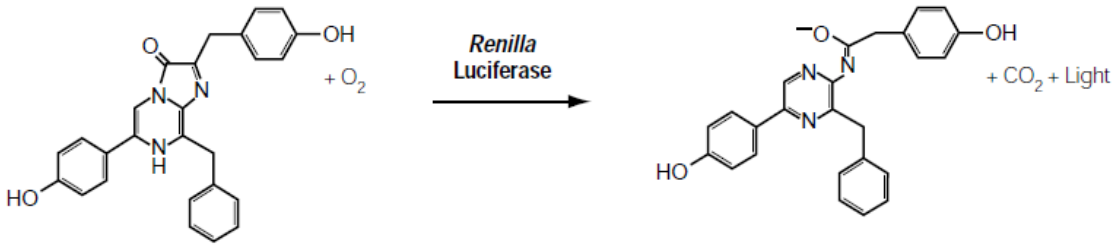

Coelenterazine **Coelenteramide**

The firefly luciferase reporter assay is initiated by mixing cell lysate with a buffer containing luciferin and co-factors according to Promega protocol and luminometer user manual. The luciferase activity is measured by a luminometer and after, the emission is quenched and the Renilla luciferase is activated by adding a reagent containing Coelenterazine to the sample tube. Light emission is measured by a luminometer.

Luciferase reporter assays have been used to investigate the direct effects of miRNAs on their predicted targets (3'UTR reporter assay) and to test the activity of a transcription factor on the promoter/regulatory regions of a target gene.

REFERENCES

1) Zdzienicka M.Z.: Mammalian mutants defective in the response to ionizing radiation-induced DNA damage. *Mutat Res*, 336, 203-213, 1995.

2) Mills K.D., Ferguson D.O., Alt F.W.: The role of DNA breaks in genomic instability and tumorigenesis. *Immunol Rev*, 194, 77–95, 2003.

3) Ambros V.: The functions of animal microRNA. *Nature* , 431, 350-355, 2004.

4) Cember H., Johnson T.E.: Introduction to Health Physics, Fourth Edition. *McGraw Hill Companies, Inc., New York, NY,* 2008.

5) Shea M.A., Smart D.F.: Cosmic ray implications for human health. *Space Sci Rev*, 93, 187–205, 2000.

6) Zhang Y., Zhou J., Lim C.: The role of NBS1 in DNA double strand break repair, telomere stability, and cell cycle checkpoint control. *Cell Res*, 16, 45-54, 2006.

7) Cadet J., Douki T., Gasparutto D., Ravanat J.L.: Oxidative damage to DNA: formation, measurement and biochemical features. *Mutat Res*, 531, 5-23, 2003.

8) Lengauer C., Kinzler K.W., Vogelstein B.: Genetic instabilities in human cancer. *Nature*, 396, 643-649, 1998.

9) Burma S., Chen B.P. C., Chen D.J.: Role of non-homologous end joining (NHEJ) in maintaining genomic integrity. *DNA Repair*, 5, 1042-1048, 2006.

10) Sancar A., Lindsey-Boltz L.A., Unsal-Kaccmaz K., Linn S.: Molecular mechanisms of mammalian DNA repair and the DNA damage checkpoints. *Annu Rev Biochem*, 73, 39-85, 2004.

11) Jowsey P., Morrice N.A., Hastie C.J., McLauchlan H., Toth R., Rouse J.: Characterisation of the sites of DNA damage-induced 53BP1 phosphorylation catalysed by ATM and ATR. *DNA Repair (Amst)*, 6, 1536-1544, 2007.

12) Gatei M., Young D., Cerosaletti K.M., Desai-Mehta A., Spring K., et al.: ATM-dependent phosphorylation of nibrin in response to radiation exposure. *Nat Gen*, 25, 115-119, 2000.

13) Chen G., Yuan S.F., Liu W., Xui Y., Trujillo K., Song B.,et al.: Radiation-induced assembly of Rad51 and Rad52 recombination complex requires ATM and c-Abl. *Int J Biol Chem*, 274, 12748-12752, 1999.

14) Fernandez-Capetillo O., Chen H., Celeste A., Ward I., Romanienko P.J., Morales J.C., et al.: DNA damage–induced G2-M checkpoint activation by histone H2AX and 53BP1. *Nat Cell Biol*, 4, 993-997, 2002.

15) Abraham R.: Cell cycle checkpoint signaling through the ATM and ATR kinases. *Genes Dev*, 15, 2177-2196, 2001.

16) Lee H.J., Paull T.T.: ATM Activation by DNA Double-Strand Breaks Through the Mre11-Rad50-Nbs1 Complex. *Science*, 308, 551, 2005.

17) Stucki M., Jackson S.P.: MDC1/NFBD1: a key regulator of the DNA damage response in higher eukaryotes. *DNA Repair (Amst)*, 3, 953-957, 2004.

18) West A.G., van Attikum H.: Chromatin at the crossroads. *EMBO Rep*, 7, 1206–1210, 2006.

19) Groth A., Rocha W., Verreault A., Almouzni G.: Chromatin challenges during DNA replication and repair. *Cell*, 128, 721–733, 2007.

20) Zweidler A.: Complexity and variability of the histone complement. *Life Sci Res Rep*, 4, 187–196, 1976.

21) Rogakou E., Pich D., Orr A., Ivanova V., Bonner W.: DNA double stranded breaks induce histone H2AX phosphorylation on serine 139. *J Biol Chem*, 273, 5858-5868, 1998.

22) Paull T.T, Rogakou E.P., Yamazaki V., Kirchgessner C.U., Gellert M., Bonner W.M.: A critical role for histone H2AX in recruitment of repair factors to nuclear foci after DNA damage. *Curr Biol*, 10, 886-895, 2000.

23) Wu Y., Xiao S., Zhu X.D.: MRE11-RAD50-NBS1 and ATM function as co-mediators of TRF-1 in telomere length control. *Nat Struct Mol Biol*, 14, 832-840, 2007.

24) D'Amours D., Jackson S.P.: The Mre11 complex: at the cross-roads of DNA repair and checkpoint signaling. *Nat Rev Mol Cell Biol*, 3, 317-327, 2002.

25) Berkovich E., Monnat R.J. Jr and Kastan M.B.: Roles of ATM and NBS1 in chromatin structure modulation and DNA double-strand break repair. *Nat Cell Biol*, 9, 683-690, 2007.

26) Löbrich M., Jeggo P.A.: The impact of a negligent G2/M checkpoint on genomic instability and cancer induction. *Nat Rev*, 7, 861-869, 2007.

27) Katsura Y., Sasaky S., Sato M., Yamaoka K., Suzukawa K., Nagasawa T., et al.: Involvement of Ku80 in microhomology-mediated end joining for DNA double-strand breaks *in vivo*. *DNA Repair*, 6, 639-648, 2007.

28) Matsuura S., Kobayashi J., Tauchi H., Komatsu K.: Nijmegen breakage syndrome and DNA double strand break repair by NBS1 complex. *Adv Biophys*, 38, 65-80, 2004.

29) Amudson S.A., Do K.T., Shahab S., Bittner M., Meltzer P., Trent J.: Identification of potential mRNA biomarkers in peripheral blood lymphocytes for human exposure to ionizing radiation. *Radiat Res*, 154, 342-346, 2000.

30) Fält S., Holmberg K., Lambert B., Wennborg A.: Long-term global gene expression patterns in irradiated human lymphocytes. *Carcinogenesis*, 24(11), 1837-1845, 2003.

31) Sakamoto-Hojo E.T., Mello S.S., Pereira E., Fachin A.L., Cardoso R.S., Moraes Junta C.: Gene expression profiles in human cells submitted to genotoxic stress. *Mutat Res*, 544, 403-413, 2003.

32) Fachin A.L., Mello S.S., Sandrin-Garcia P., Moraes Junta C., Donadi E.A., et al.: Gene expression profiles in human Lymphocytes irradiated in vitro with low doses of gamma rays. *Radiat Res,* 168, 650-665, 2007.

33) Turtoi A., Brown I., Oskamp D., Schneeweiss F.H.A.: Early gene expression in human lymphocytes after γ-irradiation–a genetic pattern with potential for biodosimetry. *Int J Radiat Bio*, 84(5), 375-387, 2008.

34) Coleman M.A., Yin E., Peterson L.E., Nelson D., Sorensen K., Tucker J.D.: Low-dose irradiation alters the transcript profiles of human lymphoblastoid cells including genes associated with cytogenetic radioadaptive response. *Radiat Res*, 164, 369-382, 2005.

35) Wang H.P., Long X.H., Sun Z.Z., Rigaud O., Xu Q.Z., Huang Y.C.: Identification of differentially transcribed genes in human lymphoblastoid cells irradiated with 0.5Gy of γ-ray and the involvement of low dose radiation inducibile CHD6 gene in cell proliferation and radiosensitivity. *Int J Radiat Bio*, 82(3), 181-190, 2006.

36) Kis E., Szatmari T., Keszei M., Farkas R., Ésik O., Lumniczky K..: Microarray analysis of radiation response genes in primary human fibroblasts. *Int J Radiation Oncology Biol Phys*, 66(5), 1506-1514, 2006.

37) Boerma M., van der Wees C.G., Vrieling H., et al.: Microarray analysis of gene expression profiles of cardiac myocytes and fibroblasts after mechanical stress, ionizing radiation or ultraviolet radiation. *BMC Genomics*, 6, 6, 2005.

38) Burns T.F., El Deiry W.S.: Microarray analysis of p53 target gene expression patterns in the spleen and thymus in response to ionizing radiation. *Cancer Biol Ther*, 2, 431-443, 2003.

39) Amundson S.A, Grace M.B., McLeland C.B., Eppely M.W., Yeager A., Zhan Q., et al.: Human in vivo radiation-induced biomarkers: gene expression changes in radiotherapy patients. *Cancer Res*, 64, 6368-6371, 2004.

40) Amundson S. A, Do K. T., Shahab S., Bittner M., Meltzer P., Trent J., et al.: Identification of potential mRNA biomarkers in peripheral blood lymphocytes for human exposure to ionizing radiation. *Radiat Res*, 154, 342-346, 2006.

41) Bahassi E.M., Conn C.W, Myer D.L., et al.: Mammalian Polo-like kinase 3 (Plk3) is a multifunctional protein involved in stress response pathways. *Oncogene*, 21, 6633-6640, 2002.

42) RØdningen O.K., Overgaard J., Alsner J., Hastie T, BØrresen-Dale A.: Microarray analysis of the transcriptional response to single or multiple doses of ionizing radiation in human subcutaneous fibroblasts. *Radiother Oncol*, 77, 231-240, 2002.

43) Tomasini R., Samir A.A., Carrier A., et al.: TP53INP1s and homeodomain-interacting protein kinase-2 (HIPK2) are partners in regulating p53 activity. *J Biol Chem*, 278, 37722-37729, 2003.

44) Bartel D.P.: MicroRNAs: Genomics, Biogenesis, Mechanism and Function. *Cell*, 116, 281-297, 2004.

45) Kim V.N: MicroRNA biogenesis: coordinated cropping and dicing. *Nat Rev Mol Cell Biol*, 6, 376-385, 2005.

46) Rodriguez A., Griffiths-Jones S., Ashurst J.L., Bradley A.: Identification of mammalian microRNA host genes and transcription units. *Genome Res*, 14, 1902-1910, 2004.

47) Lagos-Quintana M., Rauhut R., Lendeckel W., Tuschl T.: Identification of novel genes coding for small expressed RNAs. *Science*, 294, 853-858, 2001.

48) Lau N.C., Lim L.P., Weinstein E.G., Bartel D.P.: An abundant class of tiny RNAs with probable regulatory roles in Caenorhabditis elegans. *Science*, 294, 858-862, 2001.

49) Lee Y., Jeon K., Lee J.T., Kim S., Kim V.N.: MicroRNA maturation: stepwise processing and subcellular localization. *EMBO J*, 21, 4663-4670, 2002.

50) Reinhart B.J., Weinstein E.G., Rhoades M.W., Bartel B., Bartel D.P.: MicroRNAs in plants. *Genes Dev*, 16, 1616-1626, 2002.

51) Bentwich I., Avniel A., Karov Y., et al.: Identification of hundreds of conserved and nonconserved human microRNAs. *Nat Genet*, 37, 766–70, 2005.

52) Lee Y., Kim M., Han J., Yeom K.H., Lee S., Baek S.H., Kim V.N.: MicroRNA genes are transcribed by RNA polymerase II. *EMBO J*, 23, 4051-4060, 2004.

53) Lee Y., Ahn C., Han J., Choi H., Kim J., et al.: The nuclear RNase III Drosha initiates microRNA processing. *Nature*, 425, 415-419, 2003.

54) Yi R., Qin Y., Macara I.G., Cullen B.R.: Exportin-5 mediates the nuclear export of pre-microRNAs and short hairpin RNAs. *Genes Dev*, 17, 3011-3016, 2003.

55) Esquela-Kerscher A., Slack F.J.: Oncomirs-microRNAs with a role in cancer. *Nat Rev*, 6, 259-269, 2006

56) Schwarz D.S., Hutvagner G., Du T., Xu Z., Aronin N., Zamore P.D: Asymmetry in the assembly of the RNAi enzyme complex. *Cell*, 115, 199-208, 2003.

57) Zeng Y., Yi R., Cullen B.R.: microRNAs and small interfering RNAs can inhibit mRNA expression by similar mechanisms. *PNAS*, 100, 9779-9784, 2003.

58) Farh K.K, Grimson A., Jan C., Lewis B.P., Johnston W.K., Lim L.P., et al.: The widespread impact of mammalian microRNAs on mRNA repression and evolution. *Science*, 310, 1817-1821, 2005.

59) Lewis B.P, Burge C.B., Bartel D.P.: Conserved seed pairing, often flanked by adenosines, indicates that thousands of human genes are microRNA targets. *Cell*, 120, 15-20, 2005

60) Lim L.P., Lau N.C., Garret-Engele P., Grimson A., Schelter J.M., et al.: Microarray analysis shows that some microRNAs downregulate large numbers of target mRNAs.*Nature*, 433, 769-773, 2005.

61) Song J.J., Liu J., Tolia N.H., Schneiderman J., Smith S.K., et al.: The crystal structure of the Argonaute2 PAZ domain reveals an RNA binding motif in RNAi effector complexes. *Nat Struct Biol*, 10, 1026-1032, 2003.

62) Yan K.S., Yan S., Farooq A., Han A., Zeng L., Zhou M.M.: Structure and conserved RNA binding of the PAZ domain. *Nature*, 426, 468-474, 2003.

63) Parker J.S., Roe S.M., Barford D.: Structural insights into mRNA recognition from a PIWI domain-siRNA guide complex. *Nature*, 434, 663-666, 2005.

64) Song J.J., Smith S.K., Hannon G.J., Joshua-Tor L.: Crystal structure of Argonaute and its implications for RISC slicer activity. *Science*, 305, 1434-1437, 2004.

65) Nowotny M., Gaidamakov S.A., Crouch R.J., Yang W.: Crystal structures of RNase H Bound to an RNA/DNA hybrid: substrate specificity and metal-dependent catalysis. *Cell*, 121, 1005-1016, 2005.

66) Lewis B.P., Shih I.H., Jones-Rhoades M.W., Bartel D.P., Burge C.B.: Prediction of mammalian microRNA targets. *Cell*, 115, 787-798, 2003.

67) Brennecke J., Stark A., Russell R.B., Cohen S.M.: Principles of microRNA-target recognition. *PLoS Biol*, 3, E85, 2005.

68) Xie Z., Kasschau K.D., Carrington J.C.: Negative feedback regulation of Dicer-Like1 in Arabidopsis by microRNA-guided mRNA degradation. *Curr Biol*, 13, 784-789, 2003.

69) Hwang H.W., Mendell J.T.: microRNAs in cell proliferation, cell death and tumorigenesis. *Br J Cancer*, 94, 776-780, 2006.

70) Griffiths-Jones S., Grocock R.J., van Dongen S., Bateman A., Enright A.J.: miRBase: microRNA sequences, targets and gene nomenclature. *Nucleic Acids Res*, 34, 140-144, 2006.

71) Griffiths-Jones S., Saini H.K., van Dongen S., Enright A.J.: miRBase: tools for microRNA genomics. *Nucleic Acids Res*, 36, 154-158, 2008.

72) Ambros V., Bartel B., Bartel D.P., Burge C.B., Carrington J.C., Chen X., et al.: A uniform system for microRNA annotation. *RNA*, 9(3), 277-279, 2003.

73) Griffiths-Jones S.: The microRNA registry. *Nucleic Acids Res*, 32, 109-111, 2004.

74) Sun Y., Koo S., White N., Peralta E., Esau C., et al.: Development of a micro-array to detect human and mouse microRNAs and characterization of expression in human organs. *Nucleic Acids Res*, 32, e188, 2004.

75) Barad O., Meiri E., Avniel A., Aharonov R., Barzilai A., Bentwich I., et al.: MicroRNA expression detected by oligonucleotide microarrays: System establishment and expression profiling in human tissues. *Genome Res*, 14, 2486-2494, 2004.

76) Agilent Human, Mouse, and Rat miRNA microarrays, Product note, Agilent Technologies (www. Agilent.com/chem /miRNA).

77) Schmittgen T.D., Lee E.J., Jiang J., Sarkar A., Yang L., Elton T.S., Chen C.: Real-time PCR quantification of precursor and mature microRNA. *Methods*, 44, 31-38, 2008.

78) Chen Y., Gelfond J., McManus L.M., Shireman P.K.: Reproducibility of quantitative RT-PCR array in miRNA expression profiling and comparison with microarray analysis. *BMC Genomics*, 10, 407-416, 2009.

79) Davoren P.A., McNeill R.E., Lowery A.J., Kerin M.J., Miller N.: Identification of suitable endogenous control genes for microRNA gene expression analysis in human breast cancer. *BMC Mol Biol*, 9, 76-86, 2008.

80) Rhoades M.W., Reinhart B.J., Lim L.P., Burge C.B., Bartel B., Bartel, D.P.: Prediction of plant microRNA targets. *Cell*, 110, 513–520, 2002.

81) Grimson A., Farh K.K., Johnston W.K., Garrett-Engele P., Lim L.P., Bartel D.P.: MicroRNA targeting specificity in mammals: determinants beyond seed pairing. *Mol Cell*, 27(1), 91-105, 2007.

82) Gaidatzis D., van Nimwegen E., Hausser J., Zavolan M.: Inference of miRNA targets using evolutionary conservation and pathway analysis. *BMC Bioinformatics*, 8, 69, 2007.

83) Kertesz M., Iovino N., Unnerstall U., Gaul U., Segal E.: The role of site accessibility in microRNA target recognition. *Nat Genet*, 39 (10), 1278-1284, 2007.

84) Long D., Lee R., Williams P., Chan C.Y., Ambros V., Ding Y.: Potent effect of target structure on microRNA function. *Nat Struct Mol Biol*, 4 (4), 287-294, 2007.

85) Robinson H., Li Y., Padgett R.W.: Incorporating structures to predict microRNA targets. *PNAS*, 102, 4006-4009, 2005.

86) Yang M., Li Y., Padgett R.W.: MicroRNAs: Small regulators with a big impact. *Cytokine & Growth F R*, 16, 387-393, 2005.

87) Little J. B.: Radiation carcinogenesis. *Carcinogenesis*, 21, 397-404, 2000.

88) Gluzman D., Imamura N., Sklyarenko L., Nadgornaya V., Zavelevich M., Machilo V.: Malignant diseases of hematopoietic and lymphoid tissues in Chernobyl clean-up workers. *Hematol J*, 5, 565-571, 2005.

89) Yoshinaga S., Mabuchi K., Sigurdson A.J., Morin Doody M., Ron E.: Cancer risks among radiologists and radiologic technologists: review of epidemiologic studies. *Radiology*, 233, 313-321, 2004.

90) Egger G., Liang G., Aparicio A., Jones P.A.: Epigenetics in human disease and prospects for epigenetic therapy. *Nature*, 429, 457-463, 2004.

91) Plass C., Oakes C., Blum W., Marcucci G.: Epigenetics in acute myeloid leukemia. *Semin Oncol*, 35, 378-387, 2008.

92) Ilnytskyy Y., Zemp F.J., Koturbash I., Kovalchuk O.: Altered microRNA expression patterns in irradiated hematopoietic tissues suggest a sex-specific protective mechanism. *Biochem Bioph Res Com*, 377, 41-45, 2008.

93) Johnson S.M., Grosshans H., Shingara J., Byrom M., Jarvis R., Cheng A., et al.: RAS is regulated by the let-7 microRNA family. *Cell*, 120, 635-647, 2005.

94) Cimmino A., Calin G.A., Fabbri M., Iorio M.V., Ferracin M., Shimizu M. et al.: miR-15 and miR-16 induce apoptosis by targeting BCL2. *PNAS*, 102(39), 13944-13949, 2005.

95) Chan J.A., Krichevsky A.M., Kosik K.S.: MicroRNA-21 is an antiapoptotic factor in human glioblastoma cells. *Cancer Res*, 65, 6029-6033, 2005.

96) Roldo C., Missiaglia E., Hagan J.P., Falconi M., Capelli P., et al.: MicroRNA expression abnormalities in pancreatic endocrine and acinar tumors are associated with distinctive pathologic features and clinical behavior. *J Clin Oncol*, 24, 4677-4684, 2006.

97) Si M.L., Zhu S., Wu H., Lu Z., Wu F., Mo Y.Y.: miR-21-mediated tumor growth. *Oncogene*, 26, 2799-2803, 2007.

98) Lu Z., Liu M., Stribinskis V., Klinge C.M., Ramos K.S., Colburn N.H., Li Y.: MicroRNA-21 promotes cell transformation by targeting the programmed cell death 4 gene. *Oncogene*, 27, 4373-4379, 2008.

99) Ivanovska I., Ball A.S., Diaz R.L., Magnus J.F., Kibukawa M., Schelter J.M.: MicroRNAs in the miR-106b family regulate p21/CDKN1a and promote cell cycle progression. *Mol Cell Biol*, 28(7), 2167-2174, 2008.

100) Gillies J.K., Lorimer I.A.: regulation of p27Kip1 by miRNA 221/222 in glioblastoma. *Cell Cycle*, 6, 2005-2009, 2007.

101) Sage I., Nagel R., Egan D.A., Schrier M., Mesman E., et al.: regulation of the p27(Kip1) tumor suppressor by miR-221 and miR-222 promotes cancer cell proliferation. *EMBO J,* 26, 3699-3708, 2007.

102) Cha H. J, Shin S., Yoo H., Lee E., Bae S. Yang K., et al.: Identification of ionizing radiation-responsive microRNAs in the IM9 human B lymphoblastic cell line. *Int J Oncol*, 34, 1661-1668, 2009.

103) Shin S., Cha H.J., Lee E., Lee S., Seo S., Jin H., Park I., et al.: Alteration of miRNA profiles by ionizing radiation in A459 human non-small cell lung cancer cells. *Int J Oncol*, 35, 81-86, 2009.

104) Yamakuchi M., Ferlito M. and Lowenstein C.J.: miR-34a repression of SIRT1 regulates apoptosis. *PNAS*, 105 (36), 13421-13426, 2008.

105) Chang T., Wentzel E.A., Kent O.A., Ramachandran K., Mullendore M., Lee K.H.: Transactivation of miR-34a by p53 broadly influences gene expression and promotes apoptosis. *Mol Cell*, 26, 745-752, 2007.

106) Rokhlin W., Scheinker V.S., Taghiyev A.F., et al.: MicroRNA-34a mediates AR-dependent p53-induced apoptosis in prostate cancer. *Cancer Biol Ther*, 7, 1288-1296, 2008.

107) Sun F., Fu H., Liu Q., et al.: Downregulation of CCND1 and CDK6 by miR-34a induces cell cycle arrest. *FEBS Lett*, 582, 1564-1568, 2008.

108) Tazawa H., Tsuchiya N., Izumiya M., Nakagama H.: Tumor-suppressive miR-34a induces senescence-like growth arrest through modulation of the E2F pathway in human colon cancer cells. *PNAS*, 104, 15472-15477, 2008.

109) Raver-Shapira N., Marciano E., Meiri E., Spector Y., Rosenfeld N., et al.: Transcriptional activation of miR-34a contributes to p53-madiated apoptosis. *Mol Cell*, 26, 731-743, 2007.

110) Shin S., Cha H.J., Lee E., Lee S., Jung J.H., Lee S., Park I., et al.: MicroRNAs are significantly influenced by p53 and radiation in HCT116 human colon carcinoma cells. *Int J Oncol*, 34, 1645-1642, 2009.

111) Yamakuchi M., Lowenstein C.J.: MiR-34, SIRT1 and p53. The feedback loop. *Cell Cycle*, 8, 1-4, 2009.

112) Swenberg C., Horneck G., Stassinopoulos E.G.: Biological Effects and Physics of Solar and Galactic Cosmic Radiation _ Part B, *Plenum, New York,* 1993.

113) Badhwar, G.D.: Radiation Dose Rates in Space Shuttle as a Function of Atmospheric *Density Rad Meas*, 30, 401–414, 1999.

114) Rastegar N., Eckart P., Mertz M.: Radiation-induced cataract in astronauts and cosmonauts. *Graefes Arch Clin Exp Ophthalmol*, 240(7), 543-547, 2002.

115) Jones J.A., McCarten M., Manuel K., Djojonegoro B., Murray J., et al.: Cataract formation mechanisms and risk in aviation and space crews. *Aviat Space Environ Med*, 78, A56-66, 2007.

116) Crucian B.E., Stowe R.P., Pierson D.L., Sams C.F.: Immune system dysregulation following short- vs long-duration spaceflight. *Aviat Space Environ Med*, 79, 835-843, 2008.

117) Sibonga J.D., Evans H.J., Sung H.G., Spector E.R., Lang T.F., et al.: Recovery of spaceflight-induced bone loss: bone mineral density after long-duration missions as fitted with an exponential function. *Bone*, 41, 973-978, 2007.

118) Lewis M.L., Reynolds J.L., Cubano L.A., Hatton J.P., Lawless B.D., Piepmeier E.H.: Spaceflight alters microtubules and increases apoptosis in human lymphocytes (Jurkat). *FASEB J*, 12, 1007–1018, 1998.

119) Fitts R.H., Riley D.R., Widrick J.J.: Functional and structural adaptations of skeletal muscle to microgravity. *J Exp Biol*, 204, 3201-3208, 2001.

120) Baevsky R.M., Baranov V.M., Funtova I.I., Diedrich A., Pashenko A.V., et al.: Autonomic cardiovascular and respiratory control during prolonged spaceflights aboard the International Space Station. *J Appl Physiol*, 103, 156-161, 2007.

121) Ullrich O., Huber K., Lang K.: Signal transduction in cells of the immune system in microgravity. *Cell Commun Signal*, 6, 9, 2008.

122) Sytkowski A.J., Davis K.L.: Erythroid cell growth and differentiation in vitro in the simulated microgravity environment of the Nasa Rotating Wall Vessel Bioreactor. *In Vitro Cell Dev Biol Anim*, 37, 79–83, 2001.

123) Mosesso P., Schuber M., Seibt D., Schmitz C., Fiore M., Schinoppi A., Penna S., Palitti F.: X-ray-induced aberrations in human lymphocytes in vitro are potentiated under simulated microgravity conditions (Clinostat). *Phys Med XVII, Supplement 1*, 2001.

124) Longnecker D.E., Manning F.J., Worth M.H. Jr.: Review of Nasa's Longitudinal Study of Astronaut Health. *National Academies Press, Washington, DC*, 2004.

125) Durante M., Snigiryova G., Akaeva E., Bogomazova A., Druzhinin S., Fedorenko B., et al.: Chromosome aberration dosimetry in cosmonauts after single or multiple space flights. *Cytogenet Genome Res*, 103, 40-46, 2003.

126) NASA website: www.quest.nasa.gov

127) Borchers A.T., Keen C.L., Gershwin M.E.: Microgravity and immune responsiveness: implications for space travel. *Nutrition*, 18, 889-898, 2002.

128) Unsworth B.R., Lelkes P.I.: Growing tissues in microgravity. *Nat Med*, 4(8), 901-907, 1998.

129) Pellis N., Goodwin T.J., Risin D., et al.: Changes in gravity inhibit lymphocyte locomotion through type I collagen. *In Vitro Cell Dev Biol*, 33A, 398-405, 1997.

130) Risin D., Pellis N.R.: Modeled microgravity inhibits apoptosis in peripheral blood lymphocytes. *In Vitro Cell Dev Biol*, 37, 66-72, 2001.

131) Plett P.A., Abonour R., Frankovitz S.M., Orschell C.M.: Impact of modeled microgravity on migration, differentiation, and cell cycle control of primitive human hematopoietic progenitors cells. *Exp Hematol*, 32, 773-781, 2004.

132) Arase Y., Nomura J., Sugaya S., Sugita K., Kita K, Suzuki N.: Effects of 3-D clino-rotation on gene expression in human fibroblast cells. *Cell Biol Int*, 26, 225-233, 2002.

133) Sambandam Y., Blanchard J. J., Daughtridge G., Kolb R.J., Shanmugarajan S., Pandruvada S.N. et al.: Microarray profile of gene expression during osteoclast differentiation in modelled microgravity. *J Cell Biochem*, 111(5), 1179-1187, 2010.

134) Horneck G.: Impact of microgravity on radiobiological processes and efficiency of DNA repair. *Mut Res*, 430, 221–228,1999.

135) Mognato M., Celotti L.: Modeled microgravity affects cell survival and *HPRT* mutant frequency, but not the expression of DNA repair genes in human lymphocytes irradiated with ionising radiation. *Mutat Res*, 578*,* 417-429, 2005.

136) Canova S., Fiorasi F., Mognato M., Grifalconi M., Reddi E., Russo A., Celotti L.: "Modeled microgravity" affects cell response to ionizing radiation and increases genomic damage. *Radiat Res*, 163, 191-199, 2005.

137) Ager D.D., Phillips J.W., Columna E.A., et al: Analysis of restriction enzyme-induced DNA double-strand breaks in Chinese hamster ovary cells by pulsed-field gel electrophoresis: implications for chromosome damage. *Radiat Res,* 128, 150–156, 1991.

138) Livak K.J., Schmittgen T.D.: Analysis of Relative Gene Expression Data using Real-Time Quantitative PCR and the $2^{-\Delta\Delta Ct}$ Method. *Methods*, 25, 402-408, 2001.

139) Chen C., Ridzon D. A., Broomer A. J., Zhou Z., Lee D. H., Nguyen J. T., et al.: Real-time quantification of microRNAs by stem-loop RT-PCR. *Nucleic Acids Res*, 33, e179, 2005.

140) Mognato M., Girardi C., Fabris S., Celotti L.: DNA repair in modeled microgravity: Double strand break rejoining activity in human lymphocytes irradiated with γ-rays. *Mutat Res*, 663, 32–39, 2009.

141) Sales G., Coppe A., Bisognin A., Biasiolo M, Bortoluzzi S., Romualdi C.: MAGIA, a web-based tool for MiRNA and Genes Integrated Analysis. *Nucleic Acid Res*, in press.

142) Huang D.W., Sherman B.T., Lempicki R.: Systematic and integrative analysis of large gene lists using DAVID bioinformatics resources. *Nature Protocols* 4, 44-57, 2009.

143) Levine A. J., Hu W., Feng Z.: The P53 pathway: What questions remain to be explored?. *Cell Death Differ*, 13, 1027-1036, 2006.

144) Harris S. L., Levine A. J.: The P53 pathway: Positive and negative feedback loops. *Oncogene* 24, 2899-2908, 2005.

145) Canman C.E., Lim D.S., Cimprich K.A., et al: Activation of the ATM kinase by ionizing radiation and phosphorylation of p53. *Science*, 281, 1677-1679, 1998.

146) Barlow C., Brown K.D., Deng C.X., et al: ATM selectively regulates distinct p53-dependent cell-cycle checkpoint and apoptotic pathways. *Nat Genet*, 17, 453-456, 1997.

147) Iliakis G., Wang Y., Guan J., Wang H.: DNA damage checkpoint control in cells exposed to ionizing radiation. *Oncogene*, 22, 5834-5847, 2003.

148) Pietenpol J.A., Stewart Z.A.: Cell cycle checkpoint signaling: Cell cycle arrest versus apoptosis. *Toxicology*, 181-182, 475-476, 2002.

149) Xiong Y.: Why are there so many CDK inhibitors? *Biochim Biophys Acta Rev Cancer* , 1288, 1-5, 1996

150) Sherr C.J., Roberts J.M.: Inhibitors of mammalian G1 cyclin-dependent kinases. *Genes Dev*, 9, 1149-1163, 1995.

151) Canman C.E., Lim D.S.: The role of ATM in DNA damage response and cancer. *Oncogene*, 17, 3301-3308, 1998.

152) Cline M.S., Smoot M., Cerami E., Kuchinsky A., Landys N., Workman C., et al: Integration of biological networks and gene expression data using Cytoscape. *Nat Protoc*, 2, 2366-2382, 2007.

153) Basso K., Sumazin P., et al.: Identification of the human mature B cell miRNome. *Immunity*, 30(5), 744-752, 2009.

154) Lee Y.S., Shibata Y., et al.: A novel class of small RNAs: tRNA-derived RNA fragments (tRFs). *Genes Dev*, 23(22), 2639-2649, 2009.

155) Zhou B., Wang S., et al.: miR-150, a microRNA expressed in mature B and T cells, blocks early B cell development when expressed prematurely. *PNAS*, 104(17), 7080-7085, 2007.

156) Gradzka I., Iwanenko T.: A non-radioactive, PFGE-based assay for low levels of DNA double-strand breaks in mammalian cells. *DNA Repair*, 4, 1129–1139, 2005.

157) Adrain C., Creagh E.M., Martin S.J.: Apoptosis-associated release of Smac/DIABLO from mitochondria requires active caspases and is blocked by Bcl-2. *EMBO J*, 20, 6627–6636, 2001.

158) MacPhail S.H., Bànath J.P., Yu T.Y., Chu E.H., Olive P.L.: Cell cycle-dependent expression of phosphorylated histone H2AX: reduced expression in unirradiated but not X-irradiated G1-phase cells. *Radiat Res*, 159, 759–767, 2003.